universität wien

MASTERARBEIT

Titel der Masterarbeit

„The role of the EGFR in intestinal stem cells“

verfasst von

Vasfiye Bilge Göçen (BSc)

angestrebter akademischer Grad

Master of Science (MSc)

Wien, 2014

Studienkennzahl lt. Studienblatt:	A 066 834
Studienrichtung lt. Studienblatt:	Molekulare Biologie
Betreut von:	Univ. Prof. Dr. Maria Sibilia

Abstract

The mammalian intestine is a multitasking tissue that is not only responsible for the absorption of nutrients but also has important immune functions, while being home to a multitude of commensal microorganisms. The intestinal epithelium is the most rapidly self-renewing tissue of the mammalian body, with a complete turnover every five days in the mouse.

The small intestine can be divided in two parts: finger-like structures called villi cover the surface of the lumen and villi are surrounded by underlying pockets termed crypts. Both structures are covered with a columnar epithelium.

The crypt base harbors LGR5^{+} stem cells and Paneth cells. Paneth cells are playing a very important role for stem cell function by secreting essential factors like Wnt, EGF and Notch ligands, and are also involved in the antimicrobial response. It has been shown that EGF is an essential survival factor for *in vitro* intestinal organoid cultures. However, its precise role for *in vivo* stem cell function has not yet been elucidated.

EGF exerts its function by binding to the EGFR, a receptor tyrosine kinase, belonging to the ErbB family, which plays key roles in cell proliferation and cell differentiation, which is facilitated by its downstream signaling via the MAPK/ERK and the Akt-PI3K pathways, respectively. Moreover, crosstalk with other signaling pathways, e.g. the Hedgehog or Notch pathway have been described.

The aim of my master thesis is to investigate the role of EGFR in intestinal stem cells. To this end, I employed mice lacking the EGFR in different cell types of the intestine namely Lgr5^{+}:

(1) EGFR$^{fl/fl}$ LGR5Cre^{ERT2}EGFP mice lack the EGFR in LGR5^{+} stem cells following Tamoxifen injection. The LGR5Cre^{ERT2}EGFP knock-in allele shows mosaic expression, therefore the EGFR is not deleted in every crypt.

(2) EGFR$^{fl/fl}$ Villin Cre mice lack the EGFR in all epithelial cells of the intestine, including crypt LGR5^{+} stem cells.

By using these two mouse models I was able to show that the lack of EGFR does not affect the differentiation of the intestinal epithelium but it impairs the proliferation in the crypt compartment as well as organoid formation *in vitro*.

Zusammenfassung

Der Darm der Säugetiere ist ein multifunktionales Gewebe, das nicht nur für Verdauung und Absorption von Nährstoffen verantwortlich ist sondern auch eine wichtige Immunfunktion besitzt. Gleichzeitig bietet der Darm Millionen von Bakterien, sogenannten symbiotischen Mikroorganismen, eine Unterkunft. Der Dünndarm besteht aus zwei Einheiten, nämlich aus fingerähnlichen Strukturen, den Zotten (Villi), und darunter liegenden Gruften (Crypten). Beide Strukturen besitzen an der Oberfläche ein kontinuierliches säulenartiges Epithel.

Das Dünndarm-Epithel ist das schnellste selbsterneuernde Gewebe bei den Säugetieren. Ein Maus Dünndarmepithel erneuert sich selbst innerhalb von 5 Tagen.

An der Basis der Crypten befinden sich LGR5 positive Stammzellen. Vermischt zwischen den Stammzellen sind die Paneth-Zellen zu finden, welche eine Doppelfunktion erfüllen, da sie essentielle Wachstumsfaktoren wie Wnt, Epidermal Growth Factor (EGF) und Notch Liganden sekretieren um die Aufrechterhaltung der Stammzell-Nische zu gewährleisten, während sie aber auch durch die Produktion und das Absondern von antimikrobiellen Substanzen dem angeborenen Immunsystem dienen. Es wurde mehrmals gezeigt, dass EGF ein sehr essentielles Wachstumsfaktor für *in vitro* Experimente mit Dünndarm-Stammzellen ist, das sogenannte “Organoid“. Seine genaue Funktion *in vivo* ist allerdings noch unklar.

Der EGF Rezeptor gehört zu der ErbB Familie der Rezeptor Tyrosin Kinasen und spielt eine Schlüsselrolle für Zellproliferation und Differenzierung, was unter anderem durch Aktivierung von MAPK/ERK und Akt-PI3K Signaltransduktionswegen erreicht wird. Der EGFR kann allerdings auch andere Signalwege wie Notch oder Hedgehog aktivieren.

Das Ziel meiner Masterarbeit ist, die Rolle des EGFR in den Stammzellen des Dünndarms zu zeigen. Dafür habe ich mit zwei Mausmodellen gearbeitet, mit denen ich den EGFR auf unterschiedliche Weise deletiert habe.

1) $EGFR^{fl/fl}$LGR5Cre^{ERT2}EGFP Mäusen fehlt der EGFR in $Lgr5^{+}$ Zellen nachdem Tamoxifen injiziert wird. Da das LGR5Cre^{ERT2}EGFP knock-in Allel eine Mosaik-

Expression hat, ist der EGFR wahrscheinlich nicht in allen Crypten des Darms deletiert.

2) $EGFR^{fl/fl}$ Villin Cre Mäuse besitzen keinen EGFR auf den gesamten Epithelzellen des Darms

Mit diesen zwei Mausmodellen konnte ich zeigen, dass die Deletion von EGFR die Differenzierung des Dünndarmepithels nicht beeinflusst. Allerdings wird die die Proliferation in den Crypten sowie die *in vitro* Organoid Formation beeinträchtigt.

Acknowledgments

First I want to thank Univ. Prof. Dr. Maria Sibilia for giving me this opportunity as a master position in her research group at the Medical University of Vienna.

Furthermore I would like to express my gratitude to my supervisor Mag. Nicole Amberg for teaching me as much as everything about research with an always nice attitude through the learning process. I also cannot forget the supports of my colleagues Dr. Elisabeth Glitzner and Mag. Karin Komposch. I thank to Lisi for helping me while finding solutions or creating new tools and I thank to Karin for supporting me and being on my left as a good friend.

Special thanks find place for Dr. Martin Holcmann, Alexsandra Bogusch as well as my colleagues Mag. Sriram Srivatsa, Mag. Markus Linder, Mag. Philip Novoszel, Dr. Jonathan Robson, Mag. Jörg Klufa and Mag. Gabriel Stulnig.

I would like to thank my family being always there for me and educating me in this way. Without them I could not be the same person. I own as much as everything to my family, that's why I want to dedicate my master thesis to my lovely father and mother.

Moreover I would like to thank to my teachers and especially Mr. Franz Kangler for believing in me and supporting me with a scholarship during my whole study, which makes the dream comes true.

Table of Contents

1 Introduction ____ *11*

1.1 The small intestine, small bowel ____ **11**

1.1.1 Differentiation zone ____ 14

1.1.2 Transit Amplifying (TA) Compartment ____ 16

1.1.3 Stem cell compartment and stem cell niche ____ 17

1.2 The large intestine; colon ____ **24**

1.2.1 Intestinal stem cell and cancer ____ 25

1.3 Epidermal Growth Factor Receptor (EGFR) ____ **26**

1.3.1 EGFR and cancer ____ 28

1.4 Mouse models ____ **30**

1.5 The Aim ____ **32**

2 Results ____ *33*

2.1 Establishment of a EGFR deletion protocol in $EGFR^{fl/fl}$ $LGR5Cre^{ERT2}EGFP$ mice ____ **33**

2.2 Analysis of EGFR mutant Gastrointestinaltract ____ **35**

2.2.1 The morphology of small intestine from control and $EGFR^{\Delta LGR5}$ ____ 35

2.2.2 The effect of the EGFR deletion on the differentiation of $EGFR^{\Delta LGR5}$ intestines ____ 36

2.2.3 The effect of the EGFR on the proliferation of ΔLGR5 mice ____ 38

2.2.4 Constitutive deletion of EGFR; $EGFR^{fl/fl}$ VillinCre ____ 41

2.2.5 The effect of the EGFR deletion on the differentiation of $EGFR^{\Delta IEC}$ intestine ____ 43

2.2.6 The effect of EGFR on the proliferation of ΔIEC mice ____ 46

3 Discussion ____ *59*

4 Materials and Methods ____ *62*

4.1 Materials ____ **62**

4.1.1 Buffers ____ 62

4.1.2 Reagents and solutions 65

4.2 Methods 69

4.2.1 Optimization of sample embedding for histology 69

4.2.2 PCR 69

4.2.3 Histological stainings 72

4.2.4 qRT-PCR 77

4.2.5 Western Blot 79

4.2.6 In vitro culture 80

4.2.7 Tamoxifen preparation 82

5 List of Abbreviations 83

6 References 85

1 Introduction

1.1 The small intestine, small bowel

The mammalian intestinal tract is subdivided into two compartments; the small intestine and the colon. The small intestine is a major member of the gastrointestinal tract, which is placed after the stomach and followed and surrounded by the large intestine (colon). In humans the length of the small intestine differs in gender. The average length for an adult human male is 6.9 m and for an adult female 7.1 m (Helander HF 2014).

The small intestine has several jobs, which make it a multitasking tissue. Together with the bile juice and pancreatic juice it is responsible for most of the digestion of food and absorption of nutrients and water (Leuschacke M. 2012). Besides this, the small intestine also shows an immune response in protection against pathogenic microorganisms, while it is containing trillions of microbiota or also called commensals (Lucia M. Kato 2014) ***Figure1***.

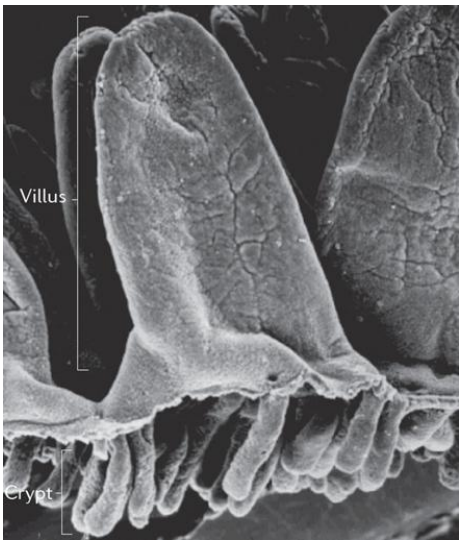

Figure 1: The electron microscopy image of small intestine. (Adapted from Barker 2013)

To maximize the absorptive surface area, the small intestine is folded into millions of finger like structures, protrusion called villus. At the base of the villi, multiple associated pockets can be found, called crypts, named after the discoverer Jonathan Nathanael Lieberkühn. Each villus is surrounded by multiple crypts.

This villus-crypt junction is like a border between proliferation and differentiation considering that the crypts harbor self-renewing and proliferative stem cells and the villi contain differentiated cells types. Since up to 6-8 crypts supply new cells for one single villus, the villi are polyclonal (François Gerbe 2012) ***Figure1***. Both structures, villi and crypts, are covered with a columnar epithelium (Clevers H. 2013) ***Figure2***.

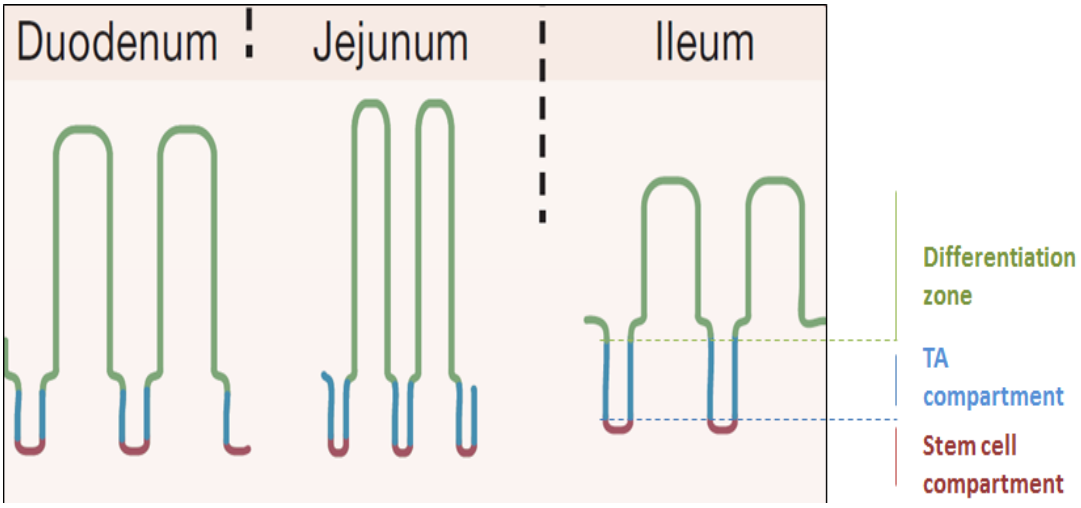

Figure 2: The scheme of small intestinal morphology and the different compartments. (Modified from Clevers H. and Batlle E. 2013)

The small intestine consists of three histologically different parts. The first part right after the stomach is called “duodenum”, second part is termed “jejenum”, where the villi have the maximum length and are thinner than in the duodenum, and the last part before the colon is the “ileum”, which contains the thickest and smallest villi. Each of these three parts can be subdivided into three different compartments: Since the stem cells are localized at the crypt base, this compartment is called after the stem cells the “stem cell compartment”. The middle part of the crypts above the stem cells is named after the located

progenitor cells “the transit-amplifying (TA) compartment”. The area from the top of the crypt to the tip of the villus is the “differentiation zone” (Clevers H. 2013) ***Figure2.***

This epithelial surface harbors six different differentiated cell types, which provide unique functions (Clevers H. 2009). These cells are the enterocytes, goblet cells, tuft cells, M cells, enteroendocrine cells, which are placed at the villi and another differentiated cell type are the Paneth cells at the crypt bottom, intermingled between the stem cells. Together with the stem cells, Paneth cells can also be referred to as crypt base columnar cells (CBCs) (Barker 2012) ***Figure3.***

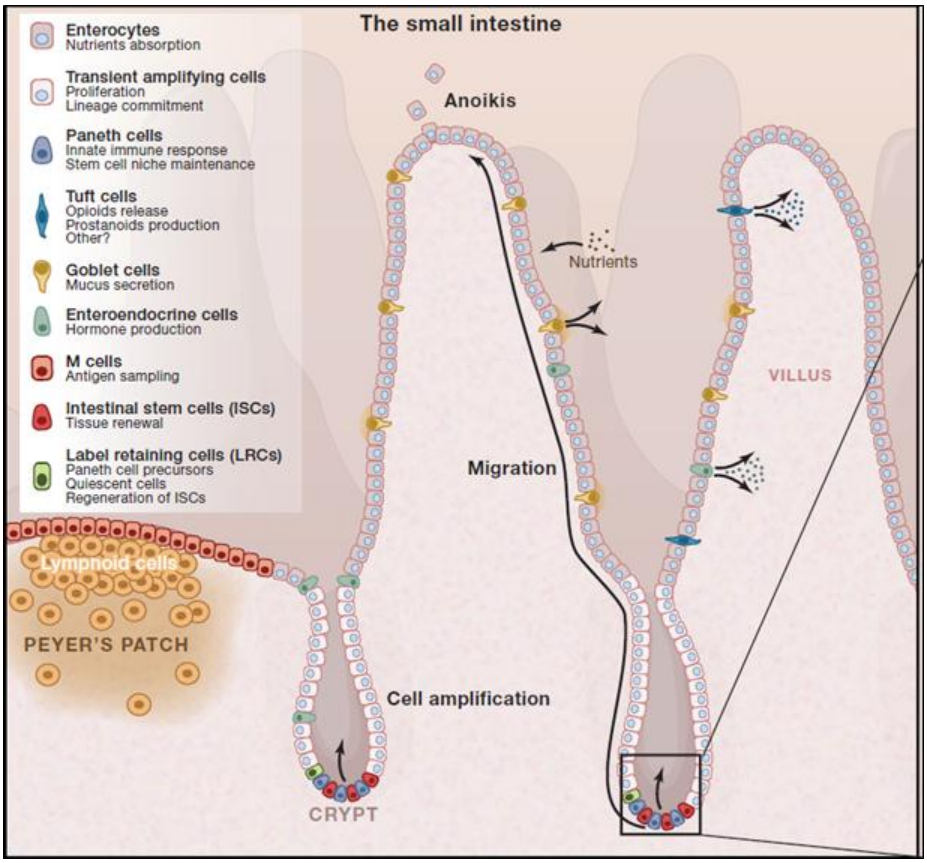

Figure 3: The scheme of the different cell types and the stem cell niche in small intestine. (Modified from Clevers H. and Batlle E. 2013)

1.1.1 Differentiation zone

1.1.1.1 The Enterocytes

The Enterocytes are the mostly present cell type along the villi and are responsible for the absorption of nutrients and water. The Enterocytes are columnar epithelial cells and highly polarized. They can synthetize hydrolytic enzymes in order to enable the absorption (Toshiro Sato 2011). During this procedure the epithelium is confronted with many invading microorganisms and different antigens from food. Therefore, the Enterocytes can react as an immune system element in two different pathways: In the first and the major pathway, they take up antigens by endocytosis and degrade them in the lysosomal compartment. In the second pathway there is no lysosomal degradation instead of this they were up taken by lymphatic vessels from the interstitial space. The Enterocytes exhibit class I and class II MHC molecules in order to present the antigens to the T cells (M. W. Smith 1985; Veerle Snoeck 2005).

1.1.1.2 The Goblet Cells

Goblet cells are the mucosa secreting gastrointestinal tract elements. The surface area of the human small intestinal mucosa is reaching approximately 30 m^2 (Helander HF 2014). The goblet cells are providing a protection of the villus epithelium by the production of mucins, which are made from high molecular weight glycoproteins. Mucins are the main components of the mucosa layer. To achieve viscous and protective charactesristics, mucins are oligomerized and glycosylated. Mucins are rich and filled with MUC2 that are hold in the granules of the goblet cells. In many studies it has been shown that loss of the mucus layer in MUC2 deficient mice causes spontaneous colitis, induced by pathogenic and commensal flora (Grootjans J. 2013). The goblet cells are belonging to the innate immunity by organizing a mucosa layer as a physical and a chemical barrier against the pathogenic bacteria, viruses and parasites. Furthermore the mucus blanket facilitates a protection from dehydration and mechanical damage (Janice J. Kim 2013). The goblet cells are not homogeneously distributed along the mouse small intestine. Their density is increasing from the duodenum to the ileum (Specian R.D. 1991). Goblet cells can be stained by using a PAS staining ***Figure4***.

1.1.1.3 M Cells

Microfold or membranous cells, known as M cells, are follicle associated-epithelial cells of the lymphoid tissue overlying on the Peyer's patches (PP). The murine M cells contain microvilli on the surface (T.Kucharzik 2000). They are antigen presenting cells and their main function is uptake and the transport of the antigens from the lumen to the underlying immune cells of lymphoid tissue. In order to facilitate rapid antigen delivery, M cells have some unique properties. On the basolateral side they are harboring invaginations like pockets, where the lymphocytes are stored. With this pocket formation the minimal transport distance is achieved. (Miller H. 2007). Another characteristic feature of M cells is a reduced glycocalix to allow the internalization of microorganisms and macromolecules (C Nicoletti 2000). The antigen uptake and the transport is mediated through phagocytosis and transcytosis (Mabbott 2013).

1.1.1.4 Tuft Cells

Tuft cells are also known as brush cells and can be found in many different organs of the digestive tract and the respiratory system. They can differ in shape, depending on the plane of the section, but they are mainly pear-shaped, barrel-shaped or goblet-shaped (Luciano 1990). Tuft cells can be recognized by their long and blunt microvilli and granular vesicles along the microvilli in the apical cytoplasm (Sato 1996). While the exact function of Tuft cells is unknown, it has been believed that the tuft cells have a role on the inflammation response by secreting prostaglandins, which are a subclass of eicosanoids and serve as mediators of inflammatory reactions (C. Benedikt Westphalen 2014). Moreover, it has been described, that with their unique shape and cytoskeletal components Tuft cells are important for the tolerance of mechanical stress (Sato A. 2007). DCAMKL-1 (double cortin calcium / calmodulin kinase-like 1) can be used as a Tuft cell marker (C. Benedikt Westphalen 2014) ***Figure4.***

1.1.1.5 The Enteroendocrine cells

The Enteroendocrine cells are hormone producing secretory cells. Although the enteroendocrine cells make up only 1% of the entire intestinal population, they determine the largest endocrine organ of the human body (Gordon W. 2008). They synthetize a variety of hormones or signaling molecules, including gastrin (G cells), ghrelin (P or X cells), somatostatin (D cells), cholecystokinin (CCK) (I

cells), serotonin (enterochromaffin cells), glucose-dependent insulinotropic peptide (GIP) (K cells), glucagon-like peptides (GLPs) and peptide YY (PYY) (L cells) (Catia Sternini 2008). The enteroendocrine cell can be visualized by a chromogranin A or synaptophysin staining (Sato 2009) ***Figure4***.

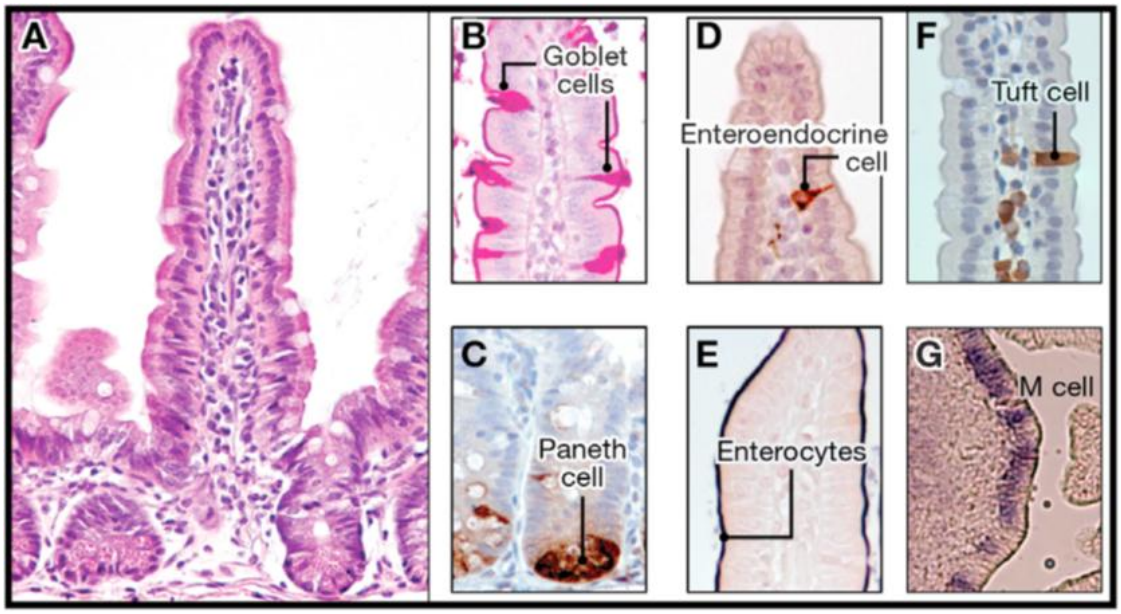

Figure 4: The epithelial cell types of small intestine. (A) Hematoxylin and eosin staining of the intestinal epithelium. (B) Periodic acid-Schiff-stained (purple) goblet cells on villus. (C) Lysozyme (brown)-stained Paneth cells at crypt bottoms. (D) Chromogranin-stained (brown) enteroendocrine cell. (E) Alkaline phosphatase-stained (blue) enterocytes. (F) DCAMKL1-stained tuft cell. (G) Spi-B expression in microfold (M) cells. (Adapted from Clevers 2013)

1.1.2 Transit Amplifying (TA) Compartment

Other than the terminally differentiated cells among of the villi, the cell population of transit amplifying compartment consists of proliferating progenitors. These progenitor cells are located in the crypt above the crypt base columnar cells. Progeny born at the crypt base moves upwards in direction to the villus tip and start to differentiate during this migratory process. Within 2 days they leave the crypt-villus junction and continue their migration to the villus tip, where they die (Anoikis) and are shed into the intestinal lumen. (Barker 2012)

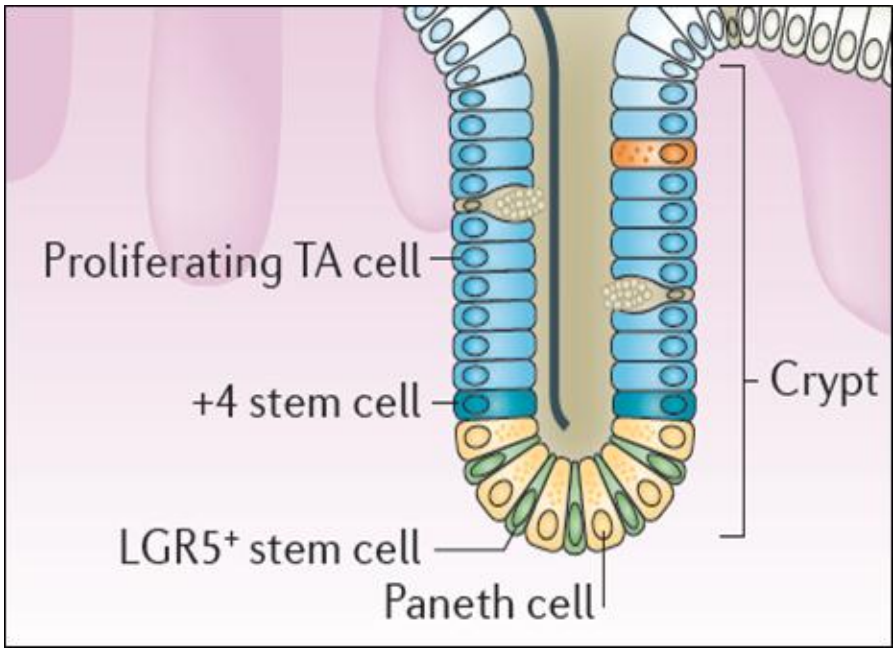

Figure 5: Scheme of the stem cell and transit amplifying (TA) compartment; crypt. (Adapted from Barker 2013)

1.1.3 Stem cell compartment and stem cell niche

1.1.3.1 Paneth cells

In contrast to the other differentiated cell types, Paneth cells are residing at the crypt base, intermingled between the stem cells, and constitute the stem cell niche (Clevers H. 2013) ***Figure5***. Together with the stem cell they are called crypt base columnar cells; CBCs. Paneth cells have a unique way of differentiation: after the passing the TA compartment - instead of moving upwards along the villus like other cell types - they migrate down from the crypt-villus junction into the base of the crypt, where they live about 6-8 weeks (Ireland 2005). Like many cell types of the intestine, Paneth cells are playing a dual function. They produce and secrete antimicrobial substances such as cyrptdins / defensins and hydrolytic enzymes like lysozymes in form of granules, which can be also seen under the light microscope by performing a simple H&E staining (Porter E. M. 2002). Besides of providing an innate immune defense, Paneth cells synthetize EGF, TGF-α, Wnt3 and the Notch ligand Dll4, which are believed to be required as essential factors for the maintenance and the proliferation of the stem cells

(Sato T. 2011). Paneth cells express CD24 and Lysozyme, which can be used as a marker for histological stainings (Sato 2009, Limberger 2013).

1.1.3.2 Adult Stem cells

Almost a century later in 1974 after the discovery of postmitotic Paneth cells by Austrian physician Joseph Paneth in 1887, another cycling cell type is proposed from Leblond at the crypt base, which are the crypt base columnar (CBC) stem cells. (Clevers 2013). Stem cells are defined by two important characteristics; longevity and multipotency. This means, that while the stem cells can renew themselves during the whole lifespan of the organism, they also have the capacity to produce all other cell types of the small intestine (Barker 2012, Clevers 2013).

The small intestine is one of the most rapid self-renewing tissues of the mammalian body. 10^{11} cells (approximately 200 g.) are daily dying on the surface epithelium of a human being, which requires a high rate of self-renewal. A mouse small intestine can renew itself almost completely every five days, and more than 300 million epithelial cells are generating daily (Barker 2013). This high turnover rate is facilitated by highly mitotic stem cells. Wnt target gene LGR5 (leucine-rich-repeat-containing G-protein-coupled receptor 5) marks these cycling columnar stem cells and gave them the name $LGR5^+$ stem cells (Barker 2007). LGR5 belongs to the seven pass transmembrane receptor protein family, whose task is to serve as a co-receptor for Wnt, which is an R-spondin-1 agonist (Carmon 2011, de Lau 2011). Every crypt contains about 15 LGR5 expressing cells (Barker 2012, Bjerknes 1999). However not all 15 cells are working as functional stem cells. The basal LGR5 stem cells are responsible for the crypt homeostasis, which are called workhorse stem cells. This central region of the crypt base constitutes the “Goldilocks zone”. The Goldilocks spot describes the center of this region, which is believed to harbor the highly mitotic, actively proliferating and irreplaceable stem cells (Walther 2014).

$LGR5^+$ stem cells also have some other markers like the transcription factor Achaete-Scute homologue 2 (Ascl2), Olfactomedin 4 (Olfm4), the RNA-binding protein Musashi-1, or the cell surface glycoprotein Prominin1 / CD133 (van der Flier 2009, He 2007, Zhu 2009). Recently, also the E3 ligases Rnf34 and Znrf3

were shown to be important for CBC homeostasis, as they are responsible for the release of Frizzleds from the cell surface, therefore controlling the crypt niche size (Hao 2012, Clevers 2013).

1.1.3.3 +4 cells

The second stem cell type besides the LGR5$^+$ stem cells is the quiescent +4 cell. Approximately 10 % of the stem cell population become a +4 cell (Barker 2007, Barker 2012). Due to their relative position within the crypt they have been called +4 cells, (Cairnie 1965) since they are mostly located at the fourth position above the Paneth cells from the crypt bottom ***Figure5***. However, their position is ranging from +2 to +7 position, the average being +4 position (Potten 1977, Potten 2002, Muñoz 2012). They are label retaining (LRCs) reserve stem cells (Li 2010). These damage responsive reserve stem cells have the capacity to regenerate the LGR5$^+$ CBC stem cell compartment in case of an injury (Barker 2013). Although they were first described as radiation sensitive cells by Potten, they lately have been postulated to be radiation resistant cells (Barker 2012).

Although many markers for the +4 cells were proposed, none of them is distinct specific for this reserve stem cells. Phospho-PTEN, Wip1 phosphatase, bone morphogenic protein inhibitor (Bmi1), Hopx, DCAMKL-1, Leucine rich repeats and immunoglobin like domain 1 (Lrig1), and mTert are known +4 cell markers. However, Phosho-PTEN can also label the enteroendocrine cells (Bjerknes 2005), Wip1 can mark CBCs (van der Flier 2007), DCAMKL-1 can also define the Tuft cells (Bezençon 2008, Gerbe 2012), Bmi1 is widely expressed in other LGR5 stem cells (Itkovitz 2012), mTert is generally found very rarely in cells (only 1 from the 150 crypts) (Barker 2012), Hopx is present abundantly in LGR5$^+$ stem cells (Powell 2012), and Lrig1 (a negative regulator of ErbB) can be found at the crypt base and in 25% of Ki67 positive TA cells (Barker 2012). Nevertheless, a transgenic mouse model of LGR5-DTR mice and lineage tracing of Bmi$^+$ cells has demonstrated, that LGR5$^+$ stem cells can be regenerated from the Bmi1$^+$ cells (Tian 2011), indicating that there are indeed 2 distinct stem cell populations existing, which have overlapping marking expression.

1.1.3.3.1 Homeostasis and the Development of small intestine

1.1.3.3.1.1 Intestinal stem cell homeostasis and signaling pathways

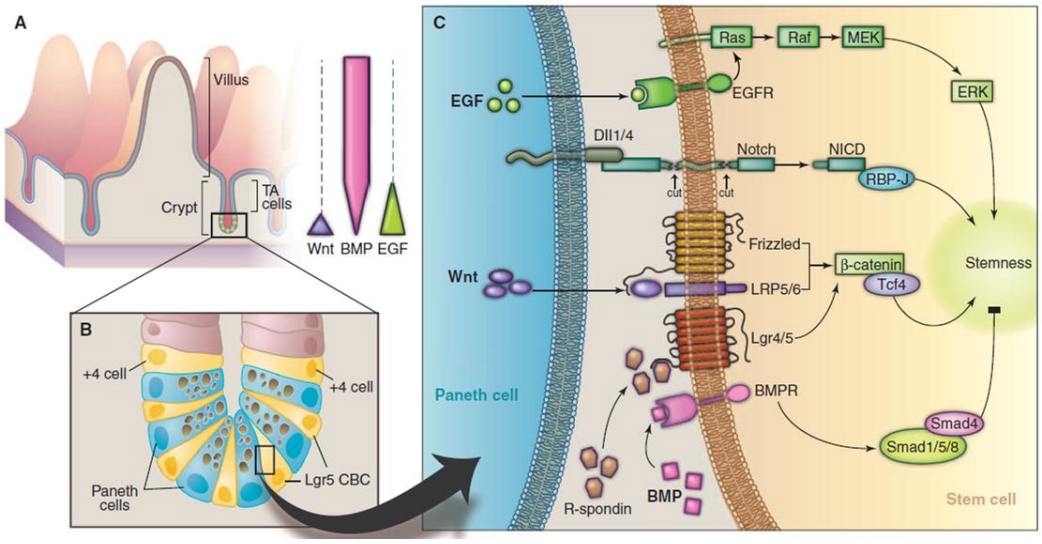

Figure 6: The scheme of the epithelial surface and the gradients of Wnt, BMP and EGF (A); the stem cell compartment (B) and the scheme of the stem cell niche the signaling pathways and the essential factors (C). (Adapted from Sato 2013)

All different kinds of differentiated cell types of the small intestinal epithelium originate from the LGR5^{+} stem cells at the crypt base. The born progeny undergoes rapid expansions with a high proliferation rate by the synthetized factors from the stem cell niche. The progenitor cells continue upwards migration along the crypt axis and they differentiate into specialized cell types at the crypt-villus-junction. Terminally differentiated cells lose their proliferative ability. Only the Paneth cells escape this upwards migration and move downwards to the crypt base to reside there as crypt base columnar cells (van der Flier 2009). This unifying theory was proven by a lineage tracing experiment, in which CBCs which had incorporated 3H-thmidine died and were taken up via phagocytosis by other CBCs. This process resulted in radioactive phagosomes, which offered to track the cells. Importantly, these phagosomes were found within more differentiated cells, suggesting that the stem cells of progenitor cells had undergone differentiation. (Cheng 1974, Barker 2012, Clever 2013). The epithelial homeostasis and the specification of different cells is sustained through some signaling pathways like Wnt, Notch, BMP and EGF (Leushacke 2012, Middendorp 2014) ***Figure6***.

Wnt signalling is the main regulator of crypt proliferation, which is driven by the key effector protein β-catenin. LGR5 and LGR4 are found in Wnt expressed compartments as a R-Spondin-1 receptor, which can enhance the Wnt signalling through the interconnection with Frizzled/Lrp, act as Wnt co-receptor. (de Lau 2011, Peng 2013, Kazanskaya 2004, Koo 2014). After binding of Wnt protein to the Frizzled/LRP receptors of, β-catenin is stabilized and released from the APC complex. The activated β-catenin translocates to the nucleus, where it activates by binding Tcf ”transcription factors”, which is a nuclear effector for expression of Wnt target genes. Normally free cytoplasmic β-catenin is degraded from the destruction complex APC and Axin by phosphorylating of Ser and Thr residues of β-catenin, which makes it a target for ubiquitin E3 ligase Rnf43/Znrf3, but the Wnt binding inactivate this destruction complex, which make able the accumulation of β-catenin in cytoplasm and subsequently in nucleus. (Clevers 2013, de Lau 2014). LGRs in interaction to R-Spondin-1 can control the Wnt-Frizzled initiating signaling pathways. The Wnt agonist R-spondin-1 with Wnt3a can increase the Wnt signaling by providing a strong connection to the extracellular domain of LGR4/5 and a specific binding to Rnf43/Znrf3 with Furin domains of R-spondin-1, which results the membrane clearance and neutralization of Rnf43/Znrf3. After the inactivation of the negative controller of Wnt signaling E3 ligase Rnf43/Znrf3 is the expression of Wnt target genes are enhanced (de Lau 2011). Interestingly, Wnt3a deficient crypts can show a normal growth *in vivo* but it is impaired *in vitro*, because the Wnts are not only secreted from Paneth cells, but also from the environmental mesenchyme. The same was also shown for R-spondins and BMP inhibitors (Farin 2012). Many mutant forms of APC tumor suppressor genes are found in colorectal cancer. Nonfunctional APC leads to the accumulation of β-catenin and transcriptional activation of Wnt target genes; e.g. proliferation initiating genes like cMyc and cyclin D1. Studies using knock-out mice for these genes could demonstrate a blockage of the self-renewal of intestinal adult stem cells (Groden 1991, Kinzler 1991, Muncan 2006).

Wnt receptor antagonist Dll1 and Dll4 are Notch ligands expressed on Paneth cells and contribute the Notch signaling in neighboring cells, which is important for maintenance of an undifferentiated state of the stem cells. $Dll1^{+}$ secretory

progenitor cells are able to convert into LGR5 stem cells (Van Es 2012, Clevers 2013).In case of the inhibition of Notch signaling, differentiation of stem cells into secretory lineage cells is favored, showing that Notch signaling is important for the balance of the enterocyte-secretory fate. (Pinto 2003, Pellegrinet 2011). The transcription factors Hes1 (a classical notch-induced gene) and Match1 (or Atoh1) can regulate each other for the switching into enterocyte-secretory lineage. Hes1 represses Match1 in proliferative crypt stem cells, whereas inhibition of Hes1 reveals increased secretory cells and decreased enterocytes as a result of active Match1. In contrast, the ablation of Match1 results in depletion of all secretory cells (Jensen 2000, Yang 2001, and Shroyer 2007).

Besides Wnt3 and Dll1 there is also another essential factor, which is produced by Paneth cells; the epidermal growth factor (EGF). Upon binding of EGF to the EGF receptor (EGFR) many important signaling cascades are activated, e.g. MAPK signaling (Wong 2012), which is known to result in important survival and proliferation signals.

BMP signaling is most dominantly found to be active in the differentiation zone and in the villi, where it ensures the maintance of proper differentiation. The ligands are provided from the mesenchyme of the villi (Haramis 2004), whereas the BMP inhibitors are provided from the mesenchyme of crypt (Kosinski 2007). In case of the inhibition of BMP through the BMP inhibitor Noggin, crypt-like structures occur in the villi (Sato 2013).

The Wnt target genes EphrinB and the transcription factor Sox9 are important for **Paneth cell** formation, their downwards migration and for location in the crypt bottom (Battle 2002, Bastide 2007, Sato 2013, Potten 2009). SPDEF (SAM pointed domain-containing Ets transcription factor) is the transcription factor for the **goblet cells**. (Gregorieff 2009, Noah 2010). Neurogenin3 expression is important for the maturation of **enteroendocrine cells** (Jenny 2002). **Tuft cells** are derived from the Dll-positive progenitors (Bjerknes 2012). The transcription factor SpiB plays a role for the **M cell** formation and RANKL cytokine induces their development (de Lau 2012).

1.1.3.3.1.2 Development of the small intestine

The gut tube is derived from endoderm. At embryonic day (E) 7.5 of the mouse embryo, the epithelium is squamous. At E8.5, the gut tube epithelium expands along the anterior-posterior axis. The anterior endoderm builds the foregut tube, the middle part forms the midgut tube and the posterior endoderm makes up the hindgut tube. At this time point the epithelium becomes a cuboidal-like structure. The emergence of the gut tube is concluded at E9.5, which consist of a pseudo-stratified epithelium and surrounded mesenchyme, which is specified from mesoderm (Wells 2014, Tan 2014) ***Figure7.***

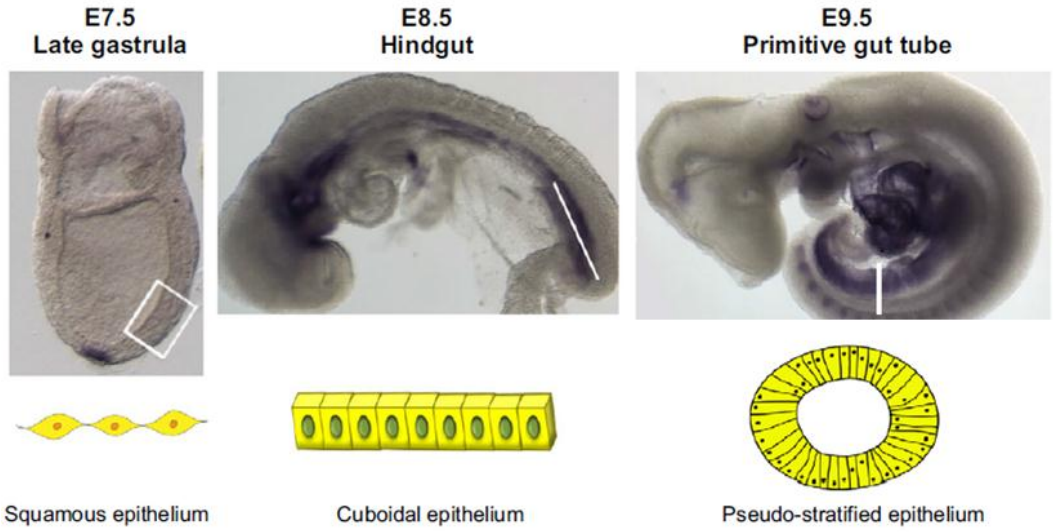

Figure 7: The emergence of the gut tube in mouse embryo. (Modified from Wells 2014)

The inner surface epithelium begins to form about E9.5 and from E13.5 to E18.5 it begins to enlarge and expand the thickness of the epithelium. Between E16.5 and postnatal day 7 the gut gains its self-renewing ability (Grosse 2011, Gregorieff 2005, Korinek 1998). In a mouse the gut development is accomplished three weeks after birth (Barker 2013) ***Figure8.***

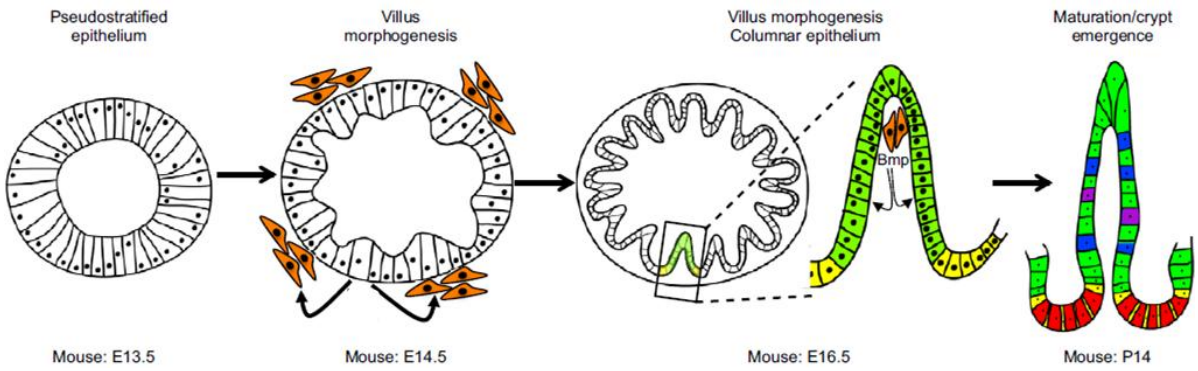

Figure 8: The scheme of the murine gut development. (Modified from Wells 2014)

1.2 The large intestine; colon

The architecture of the colon differs from that of the small intestine. Instead of carrying villi, the colon has a flat surface containing only crypts ***Figure9***, which at the bottom also harbor stem cells, but lack Paneth cells. Colon crypts are carrying the absorptive colonocytes and high numbers of the goblet cells that are specialized for the compaction and excretion of useless materials (Gregorieff 2005, Barker 2008, and Middendrop 2014).

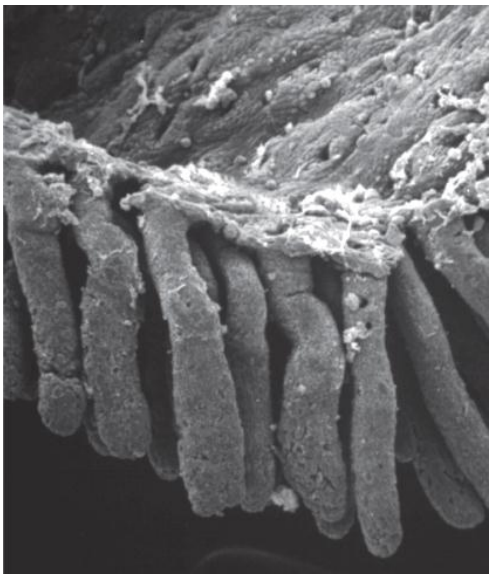

Figure 9: The electron microscopy image of colon. (Adapted from Barker 2013)

1.2.1 Intestinal stem cell and cancer

Despite the development of therapeutic technologies, colorectal cancer (CRC) is still a one of the major death causing health threats (Fujii 2014). It is the fourth most common human cancer type worldwide (Siegel 2012, Ferlay 2012, and Cunningham 2010) and results from a series of mutations which affect the cell cycle. Since terminally differentiated cells have a short lifespan and lost their proliferative potential, it is suggested that the long lived crypt base cells can give rise to cancer (Clevers 2011). Abundant crypt proliferation can cause hyperplasia and adenoma, which can develop to carcinoma. The depletion of the tumor suppressor gene APC in the stem cell compartment leads to adenoma formation in the small intestine and colon via hyperactive Wnt/β-catenin signaling. Moreover, it results in a reduction of $LGR5^+$ stem cell numbers (Powell 1992, Leushacke 2012, Barker 2009). However, the loss of APC in non-stem cell compartments does not cause adenoma growth (Schepers 2012). Therefore, intestinal adult stem cells are believed to be the potential candidates as origin of cancer stem cells (Merlos-Suarez 2011, Ong 2014).

Since the stem cell niche was discovered, the $LGR5^+$ stem cells can be cultivated *in vitro* on matrigel (which is a basement membrane substitute) upon addition of essential factors like R-spondin-1, Noggin and EGF for small intestinal cultures and Wnt for colonic cultures from rodents. The stem cells then proliferate, differentiate and build “mini guts”, so called orgonoids. Additionally Wnt3a, p38 inhibitor and ALK 4/5/7 inhibitor need to be included for human colorectal stem cell (Carmon 2011, Sachs 2014).

This *in vitro* culturing system of adult stem cells or cancer stem cells can offer some opportunities for research of disease models, gene therapy and for drug development (Koo 2014). The CRISPR/Cas9 system represents an example for therapeutic genome targeting in organoid, which is established via homologous recombination to correct the mutant cyctic fibriosis transmembrane conductor receptor (CFTR) gene from patients (Dekkers 2013). The organoid cultures from tumors with colorectal cancer and the knockdown of target gene expression using viral vectors give a chance to analyze and to understand the mechanisms of tumor development and progression and functional analysis of cancer

associated genes (Tan 2014, Fujii 2014), as well as functional testing of anticancer therapies.

1.3 Epidermal Growth Factor Receptor (EGFR)

The Epidermal Growth Factor (EGF) Receptor family, also known as ErbB family, consists of four structurally related tyrosine kinase receptors; EGFR (ErbB1), HER2 (ErbB2), HER3 (ErbB3), and HER4 (ErbB4), which can trigger an internal signaling pathway via binding of an external peptide ligand like EGF or EGF-like growth factors (Sibilia 2007, Schneider 2008, Schleissinger 2002).

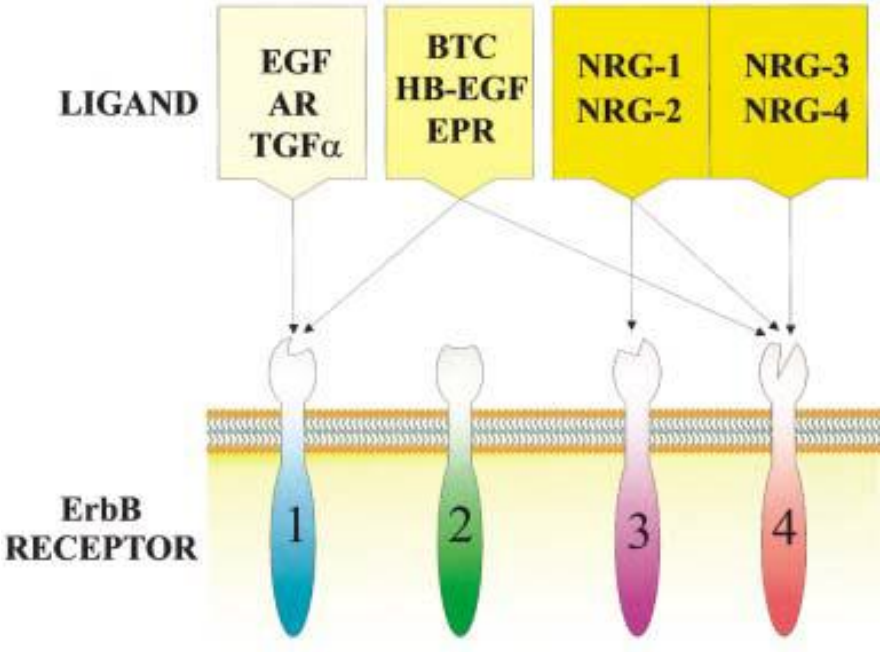

Figure 10: A scheme of the ErbB family receptors and their ligands. (Adapted from Olayioye 2000)

EGF, amphiregulin (AR), and transforming growth factor-α (TGF-α) bind to ErbB1, while betacellulin (BTC), heparin-binding EGF (HB-EGF) and epiregulin (EPR) show dual binding action to ErbB1 and ErbB4. ErbB4 can recognize additionally neuregulin 3 (NRG-3) and neuregulin 4 (NRG-4), while ErbB3 has a binding specificity to neuregulin 1 (NRG-1) and neuregulin 2 (NRG-2). The receptor ErbB3 does not have kinase activity, because it lacks some important amino acids on the intracellular domain (Guy 1994). ErbB2 acts as a coreceptor and heterodimerization partner for the other members of the ErbB family, but it

does not have known direct ligands, as it does not have a functional ligand-binding domain (Riese 1995, Chang 1997, Zhang 1997, Thazar 1996) ***Figure10.***

The EGFR consists of three units: the ligand binding extracellular domain, the hydrophobic transmembrane domain and the intracellular protein kinase domain. Ligand binding causes the formation of homo- and heterodimers on which contribute to autophosphorylation of the intracellular domain of the receptor (Hunter 1981, Yarden 2012). Although it was believed for a long time, that the EGFR is expressed on all types of cells except hematopoietic cells (Salomon 1995), our group was recently able to demonstrate that EGFR expression is inducible on immune cells upon their activation (Lanaya 2014). The EGF-like factors can be expressed and act in an autocrine and in a paracrine manner (Olayioye 2000).

The auto- or transphosphorylation of ErbB receptors can initiate many important signaling processes from proliferation to differentiation and organogenesis like activation of PI3K/AKT (angiogenesis, survival, tumorigenesis), ras/raf/MEK/MAPK (mitogen activated protein kinase)/ ERK (cell cycle, gene expression), Jun/Fos (cell growth/differentiation, chemotaxis, cell shape) and JAK/SRC/STAT (cell proliferation and evasion of apoptosis) pathways, phospholipid metabolism phospholipase C-γ (PLC-γ), phospholipase D (PLD), phosphatidylinositol-3-kinase (PI3-K) mediated by cofactors PKC, Rho, and phosphatidylinositol biphosphate (PIP2). EGFR can activate $Ca2^{+}$ mediated pathways like RaI and NFkB. EGF is important for motility in a Rho-dependent manner, a protein which is responsible for cell rounding and cortical actin polymerization, as well as for Rac-dependent membrane ruffling and lamellipodia formation (Jorrisen 2003).

EGFR and their subsequently signaling activation is controlled in early steps by protein modifications and in late stages through the transcription regulation. There are Tyr-specific phosphates like DEP1 (density enchanced phosphatase), which can dephosphorylate the EGFR. In this scenario, EGFR remains at the plasma membrane, but gets inactivated. Another regulatory mechanism is internalization of the receptor. The ubiquitin-ligase CBL, together with AIP4 (activation induced phosphatase 4), can target phosphorylated

receptors to endosomes (clathrin coated vesicles) upon ubiquitylation. This can lead to lysosomal degradation unless deubiquitylating enzymes (DUBs) target them for recycling. The vesicle, which contains ligand bound receptor as targeted for lysosomal degradation, is called multivescular body (MVB). Lrig1 can interact with all four members of RTKs and recruit the enchanced ubiquitylation (Gur 2004, Mellman 2014).

Although the adaptor protein Grb2 can recruit Ras and SOS and thereby activate kinase cascades like RAF/MEK/ERK/MAPK and PI3-K/PDK/AKT pathways, they are controlled by intrinsic and extrinsic negative feedback. ERK can negatively regulate RAF, moreover it has been shown that AKT, activated by another kinase cascade, can suppress RAF activation downstream of EGFR (Avraham 2011).

Besides the ligand binding activation of EGFR, the receptor can also be transactivated by cytokines like growth hormone and prolactin. This transactivation is achieved by phosphorylation of tyrosine residues by Jak2 (Janus tyrosine kinase 2) and by G-protein coupled receptor stimulation such as endothelin-1, bombesin, thrombin and lysophosphatidic acid. All these kinds of transactivation can occur in an autocrine, paracrine or juxtacrine manner.

Moreover, ADAM (a disintegrin and metalloprotease domain) proteins, which are anchored at membrane, are serving as metalloproteinases. This means, that they are responsible for the release of the membrane-anchored ligand-precursors by shedding them from the membrane (Carpenter 2000, Yamauchi 1997, Normanno 2006).

1.3.1 EGFR and cancer

The initiation of the signaling pathways play a role on tumor pathogenesis, angiogenesis and on cancer progression by providing the interaction of tumor cells with surrounding microenvironment to form metastasis (de Luca 2008).As EGFR is very crucial for cellular processes like proliferation, differentiation and survival during the different organ development and epithelial cells and tissue homeostasis, the overexpression or hyperactivation of EGFR results in malignancy involving different organs like breast, lung, pancres, colon, stomach,

and skin (Olayioye 2000). Many of these organs are strongly affected, upon deletion of EGFR, showing developmental defects.

Loss of EGFR leads to growth retardation and various organ abnormalities in mice (Miettinen 1995, Sibilia and Wagner 1995), resulting in death at different time points during development in different genetic backgrounds (Sibilia and Wagner 1995). EGFR-/- mice in a 129/Sv background already die *in utero* at E11.5, while in a C57BL/6 background mutant mice can survive until birth. The longest survival can be seen in a MF1/C3H background, where EGFR-/- mice survive up to postnatal day 20. If the mutants die in utero, they mainly die due to placental defects. In case they survive until birth, death is mainly due to lung immaturity. However, all mutants have several organ defects and abnormalities in brain, heart, skin, bone and eyes (Miettinen 1995, Sibilia and Wagner 1995).

The overexpression of EGFR was observed in 100% of human head and neck cancers, and was also detected in other cancer types such as pancreatic, colorectal, breast, ovarian, prostate, bladder, non-small-cell lung cancer and glioblastomas (Salomon 1995). 50% to 70% of colon carcinoma show an EGFR or ErbB3 overexpression, whereas 30% of human breast carcinomas have ErbB2 aberrations (Normanno 2003). 22% of human primary colon carcinomas demonstrate ErbB4 expression. The research group of Spano (2005) investigated EGFR expression in 143 patients colon carcinoma samples from 148 patients and found overexpression in 143 of them (97%). Moreover, they describe highest EGFR expression in stage 3, but not in stage 4 (according to the International Union against cancer TNM staging system), which can mean that there is a correlation between EGFR overexpression and tumor invasion (Spano 2005a). Interestingly, the expression of the EGFR was not found to be homogeneous within the tumor, as the group also postulated that the EGFR expression is highest in the deepest regions of tumors (Spano 2005b).

Several EGFR inhibitors were invented for therapeutic purposes, like tyrosine kinase inhibitors “gefitinib” and “erlotinib”, monoclonal antibodies (C225) and antisense approaches (Baselga 2002).

C225 associates with the ligand-binding domain of EGFR and thereby competes with the natural EGFR ligands, leading to reduced intracellular signaling. This

can subsequently reduce CDK2, 4 and 6 expression resulting in cell growth arrest in G1 phase (Huang 1999).

It has been shown that gefitinib can inhibit the cell growth of the TGF-α and EGFR expressing colon cancer cell line GEO. Gefitinib interacts with the intracellular domain and inhibits the tyrosine kinase, thereby also blocking intracellular signaling. Moreover, at high doses, gefitinib can also induce apoptosis (Ciardello 2000).

Since EGFR is important for tumor proliferation in colon carcinoma, application of an EGFR inhibitor can reduce the tumor progression, and can even be more effective in combination with chemotherapy and radiation (Spano 2005b)

1.4 Mouse models

In my studies, I made use of two different knock-out mouse models to investigate the effect of EGFR deletion on intestinal stem cells.

1) $EGFR^{fl/fl}$ $LGR5Cre^{ERT2}EGFP$ mice

Transgenic mice, in which the promoter and exon1 of the EGFR are flanked by loxP sites, were crossed to $LGR5Cre^{ERT2}EGFP$ knock-in mice ***Figure11***. Hereby, expression of Cre recombinase is driven by the LGR5 promoter, which in the intestine is exclusively expressed by the stem cells. Importantly, Cre^{ERT2} is a Cre recombinase fused to the ligand binding domain of the estrogen receptor. In order to achieve Cre translocation to the nucleus, an estrogen receptor homolog needs to be applied, which in my case was done by intraperitoneal injection of tamoxifen. This results in EGFR-deleted $LGR5^{+}$ stem cells ($EGFR^{\Delta LGR5}$). In addition, the knock-in allele also encodes for enhanced green fluorescence protein (EGFP) as a tracing marker. In the intestine, this construct shows a mosaic expression (Koo 2014).

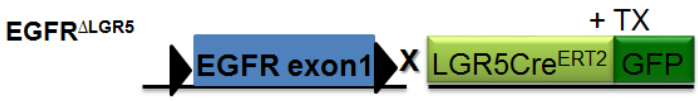

Figure 11: The scheme of the EGFR floxed allele crossed to the $LGR5Cre^{ERT2}EGFP$ allele. $EGFR^{\Delta LGR5}$

The mosaic expression is traceable with GFP immunofluorescence staining on prefixed frozen sections ***Figure12*A.** Since the villi are surrounded by multiple crypts and up to 10 crypts supply new cells for one single villus epithelium, the villi will always be supplied by some crypts, which still express EGFR. This can also be visualized by a GFP staining of an intestinal whole mount ***Figure12*B.**

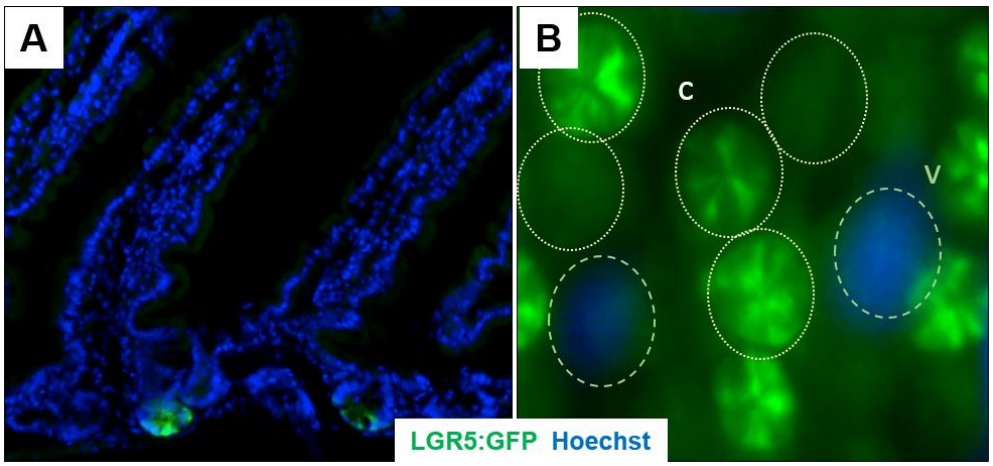

Figure 12: (A) The GFP immunofluorescence staining of on 6µm thick prefixed frozen small intestinal sections of EGFR$^{fl/fl}$LGR5Cre^{ERT2}EGFP mice. (B) The whole mount staining of GFP; circles with c indicate crypts and dotted circles with v indicate villi. Green=GFP; blue=Hoechst

2) EGFR$^{fl/fl}$ VillinCre mice

In this constitutively active mouse model, Cre is expressed under the control of a 9 kb regulatory region of the murine villin gene. The Villin-Promotor is active at E9.5 but the activation of Villin-Cre in the whole intestinal epithelium (including the stem cells) occurs first at E12.5. The deletion of EGFR by this strategy is termed as delta intestinal epithelial cells (EGFR$^{\Delta IEC}$) (El Marjou 2004) ***Figure13.***

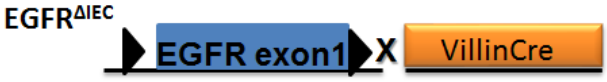

Figure 13: The scheme of the EGFR floxed allele crossed to the VillinCre allele. EGFR$^{\Delta IEC}$

1.5 The Aim

Since it is mentioned in many studies that EGF is one of the important essential factors for the stem cell niche *in vitro*, my study aimed in investigating the role of the EGFR in intestinal stem cells.

For this purpose, I employed mice lacking EGFR in different intestinal epithelial cells and in vitro organoid cultures derived thereof.

I investigated all three compartments of the small intestine, as well as the colon, by performing histological analysis of differentiation and proliferation. Moreover, I performed organoid culture *ex vivo* with isolated crypts from both mouse models, $EGFR^{\Delta LGR5}$ and $EGFR^{\Delta IEC}$ mice, respectively.

2 Results

2.1 Establishment of a EGFR deletion protocol in EGFR$^{fl/fl}$ LGR5Cre^{ERT2}EGFP mice

6-8 weeks old mice were intraperitoneally injected with 50 µl of tamoxifen (20 mg/ml) for five consecutive days, followed with a tamoxifen injection once a week ***Figure14***. As the EGFR is a very stable protein (Yarden 2001) and usually several cell divisions are necessary in order to dilute out residual EGFR protein, I performed analysis of the intestine for successful deletion at 4 weeks and 1 week after the first 5 day treatment with Tamoxifen.

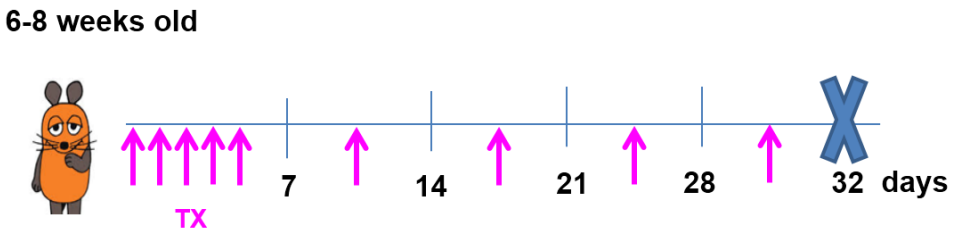

Figure 14: Time scale of tamoxifen injection (4 weeks) to EGFR$^{fl/fl}$LGR5Cre^{ERT2}EGFP mice.

Analysis of EGFR deletion after 4 weeks of tamoxifen injection was performed by an EGFR immunohistochemistry (IHC) staining on 4µm thin paraffin sections of the intestine ***Figure15.***

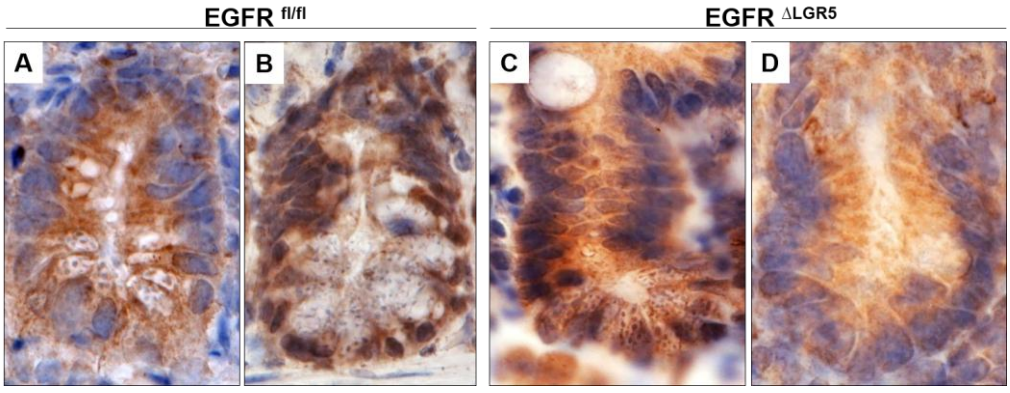

Figure 15: (A) & (B) The microscopic image of EGFR IHC staining after4 weeks of tamoxifen injection in crypts of EGFR$^{fl/fl}$ (control) mice, where the EGFR is detectable. (C) EGFR is still present in the crypt of the EGFR$^{\Delta LGR5}$ mice, (D) EGFR protein is absent in some crypts of EGFR$^{\Delta LGR5}$ mice. Blue=Hematoxylin; brown=EGFR

EGFR IHC staining shows, that the EGFR can be deleted in LGR5^{+} stem cells 4 weeks after tamoxifen injection. However, the deletion cannot be observed in every crypt, as the Lgr5-Cre transgene has a mosaic expression (Wong 2000, Kim 2011, Tian 2011).

Moreover, staining for EGFR 1 week after tamoxifen treatment ***Figure16*** showed, that the EGFR was absent in several crypts even within this short time period. As expected, the deletion was detectable only partially and not in every crypt due to the mosaic expression Lgr5-Cre transgene ***Figure17.***

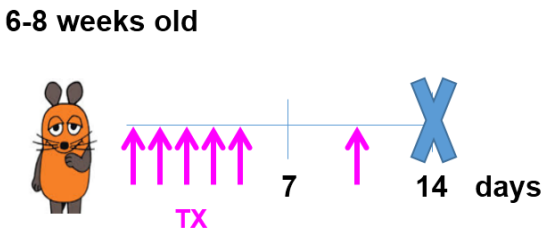

Figure 16: Time scale of tamoxifen injection (1 week) to EGFR$^{fl/fl}$LGR5Cre^{ERT2}EGFP mice.

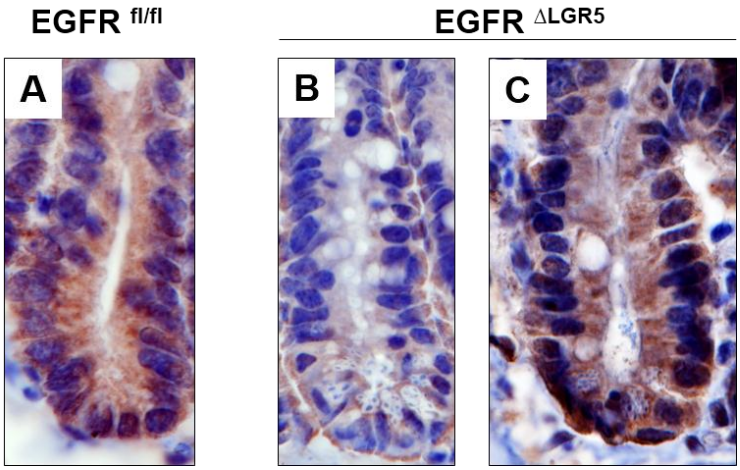

Figure 17: The EGFR IHC staining of small intestinal samples after one week of tamoxifen injection. (A) Control mice contain EGFR. (B) Tamoxifen treated EGFR$^{fl/fl}$LGR5CRE^{ERT2}EGFP mice do not exhibit EGFR in the crypt. (C) Tamoxifen treated EGFR$^{fl/fl}$LGR5CRE^{ERT2}EGFP mice are still showing EGFR protein in the crypt. Blue= Hematoxylin; brown=EGFR

The colon, which also harbors LGR5^{+} stem cells, showed a similar deletion pattern as the small intestine ***Figure18***.

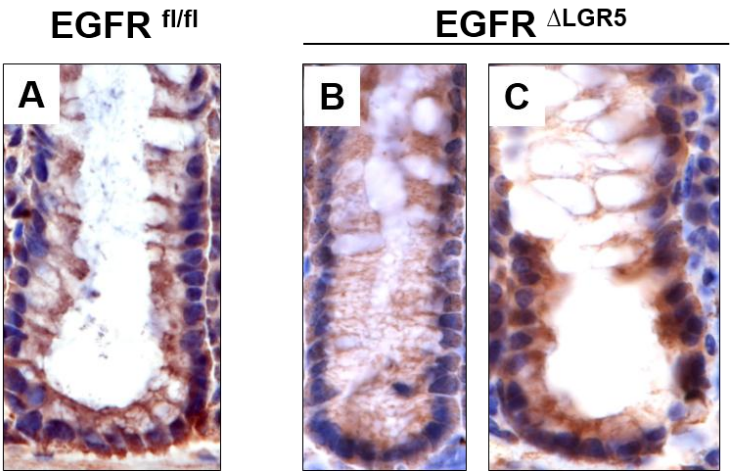

Figure 18: EGFR IHC after one week of tamoxifen injection on colon sections. (A) Control mice have normal EGFR expression. (B) Tamoxifen injected mice do not show EGFR expression in some crypts of colon. (C) Some crypts in colon of tamoxifen injected mice still show a positive EGFR staining. Blue=Hematoxylin; brown=EGFR

2.2 Analysis of EGFR mutant Gastrointestinaltract

2.2.1 The morphology of small intestine from control and EGFR$^{\Delta LGR5}$

To characterize EGFR$^{\Delta LGR5}$ intestines, I first evaluated the basic morphology by a Hematoxylin & Eosin (H&E) staining and measured the length and the width of the villi from control and EGFR$^{\Delta LGR5}$ mice within the three small intestinal compartments duodenum, jejenum and ileum. There were no morphological differences detectable between control and EGFR$^{\Delta LGR5}$ mice. Both, villus length and width showed similar results ***Figure19***.

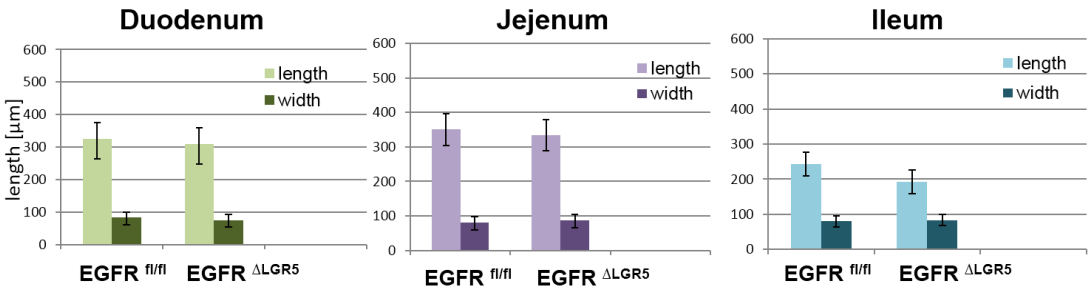

Figure 19: Length and width of villi from control and EGFR$^{\Delta LGR5}$ mice. Each diagram shows another compartment of small intestine; duodenum, jejenum and ileum. The light bars are for the length and the dark bars are for the width of villi. Control n=4; KO n= 6

2.2.2 The effect of the EGFR deletion on the differentiation of EGFR$^{\Delta LGR5}$ intestines

I next investigated the capacity of EGFR deficient stem cells to give rise to the different terminally differentiated cell types, by staining for all different post mitotic cells: enterocytes, goblet cells, tuft cells, paneth cells, which are originated from LGR5^{+} stem cell at the crypt base. The mucosa secreting "goblet cells" were visualized by a combined PAS & Alcian blue staining, which also identifies the different pH value between the goblet cells. According to the PAS & Alcian blue staining, the blue color shows the acidic goblet cells, pink is for neutral, magenta for slightly acidic and deep purple represents the mixture of neutral and acidic goblet cells ***Figure20***.

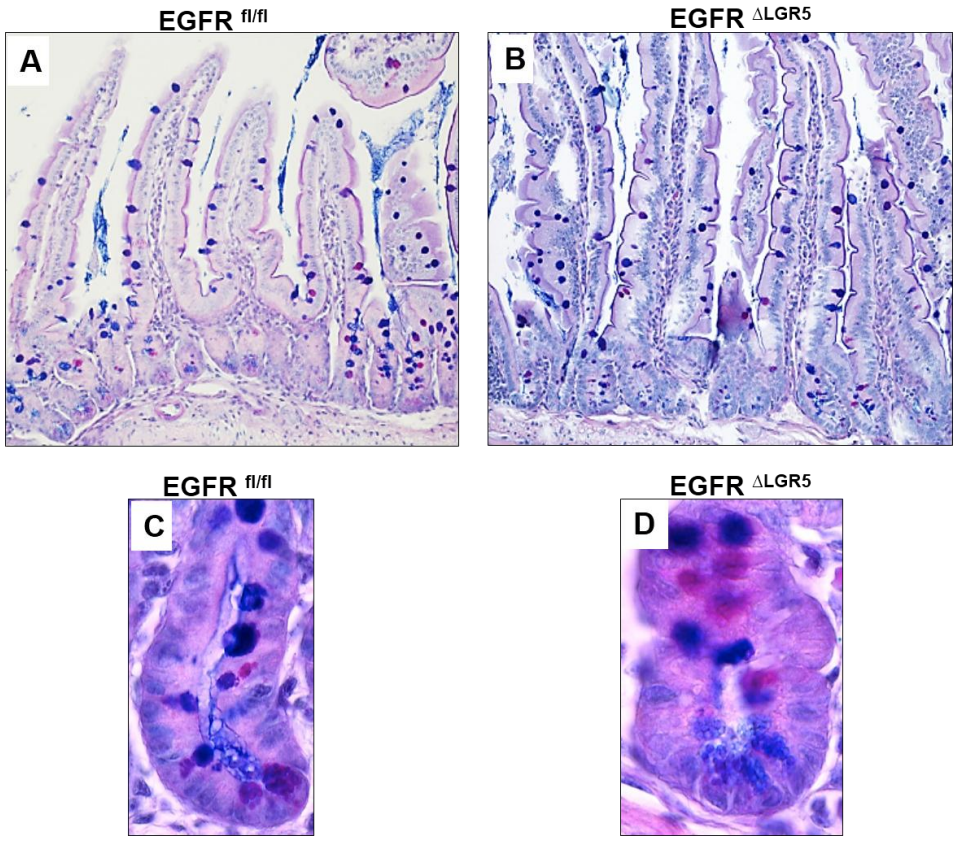

Figure 20: The microscopic image of Pas & Alcian blue staining of small intestinal samples from (A) control mice, (B) EGFR$^{\Delta LGR5}$ mice (C) crypt of control mice (D) crypt of EGFR$^{\Delta LGR5}$. Blue=acidic; pink=neutral; lila=lightly acidic; deep purple=the mixture of neutral and acidic. (Magnification of A,B 20x and C,D 60x)

The PAS & Alcian blue staining did not differ between control and EGFR$^{\Delta LGR5}$ mice and it is quantified by counting the numbers of different pH value goblet cells on villi in a microscopic field of a 20x objective. Again, I separated the quantification into the three compartments duodenum, jejenum and the ileum. The graphical representation can be seen in ***Figure21***. The number of mucosa secreting cells in each compartment is similar in control and EGFR$^{\Delta LGR5}$ mice.

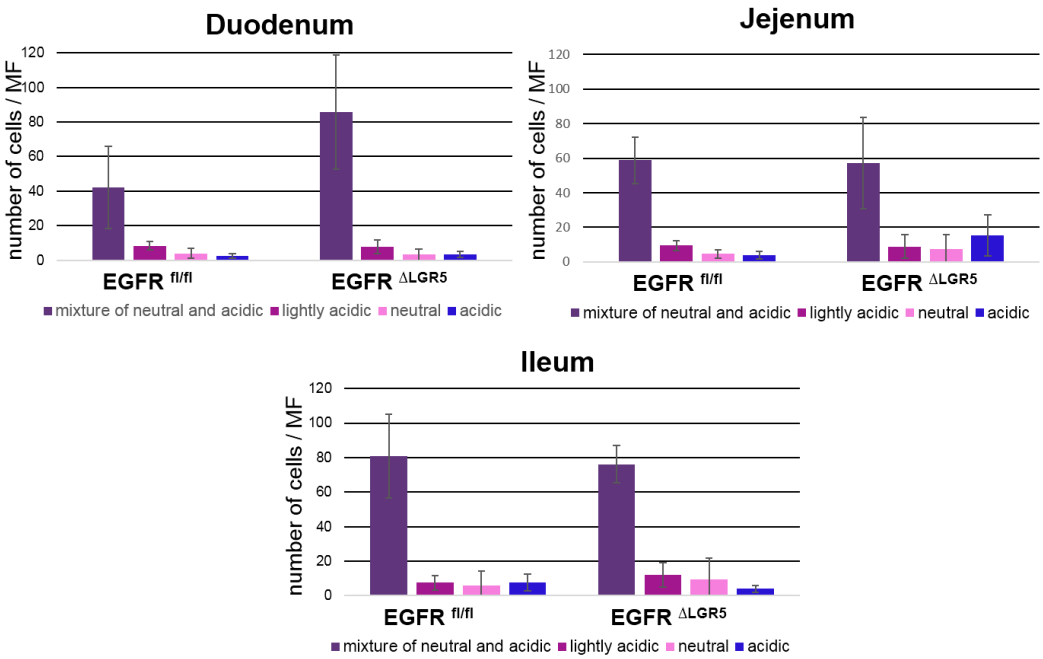

Figure 21: Average numbers of different pH value goblet cells on villi from the intestinal compartments; duodenum, jejunum and ileum. Each diagram shows the results in different compartment. The y-axis gives the numbers of the cells for each microscopic field of 20x magnification. Each color represent a different pH value; blue=acidic; pink=neutral; lila=lightly acidic; deep purple=the mixture of neutral and acidic. Control n=4; KO n=6

2.2.3 The effect of the EGFR on the proliferation of ΔLGR5 mice

Since EGFR deletion seems not to be important for the normal morphological appearance of the small intestine and for the differentiation of the intestinal epithelial cells, I next wanted to investigate, whether the stem cell proliferation was normal. Therefore, I chose the 1 week deletion time point and pulsed the mice with 70µl Bromodeoxyuridine (BrdU) (12.5 mg/ml), which can detect the proliferating cell *in vivo* by incorporating into the newly synthetizing DNA strand in S-phase via replacing thymidine during replication, either 24h or 4h prior to sacrificing the mice. Paraffin sections were stained with α-BrdU to detect cells which incorporated BrdU (red) and with α-β4Integrin (green) to see the epithelial cell borders ***Figure22***.

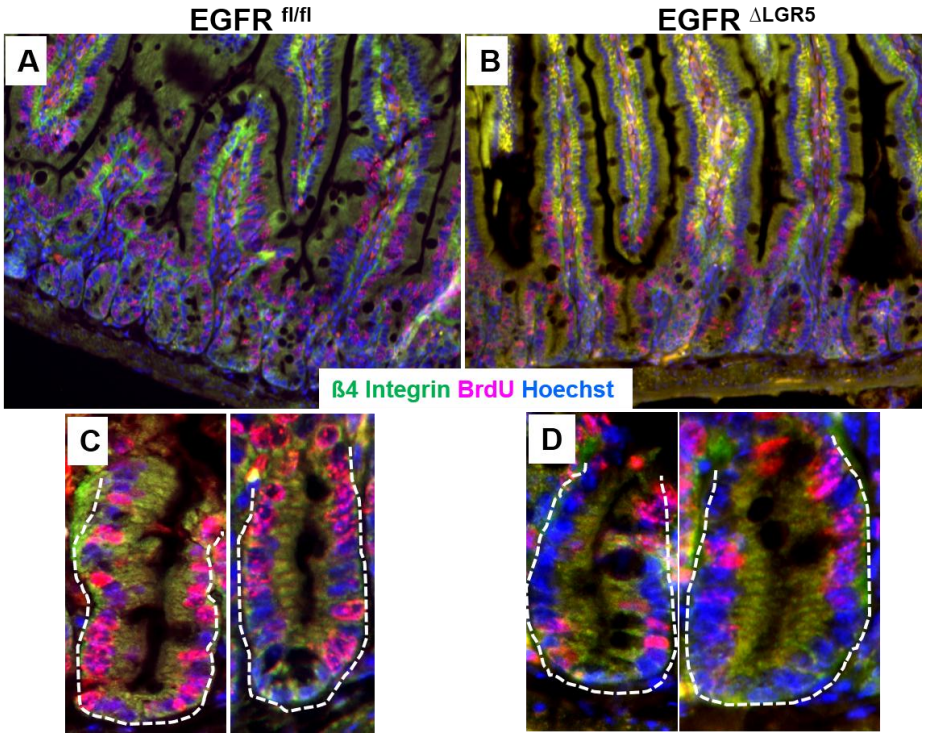

Figure 22: Microscopic images of BrdU staining on small intestinal samples from (A) control mice and (B) EGFR$^{\Delta LGR5}$ mice, the BrdU staining in crypts of (C) control mice and (D) EGFR$^{\Delta LGR5}$ mice. Magnification of A, B 20x and C, D 40x.

The quantification of BrdU positive epithelial cells 24h after pulsing shows, that the number of BrdU^{+} cells is significantly reduced in each crypt of EGFR$^{\Delta LGR5}$ mice (***Figure 23B***) and also reduced in each villus (***Figure 23A***) of these animals ***Figure23.***

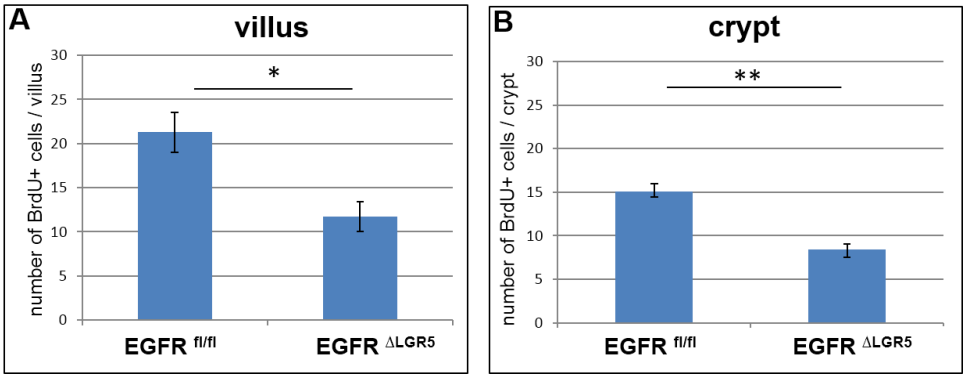

Figure 23: BrdU^{+} cells (A) per villus from control and EGFR$^{\Delta LGR5}$ mice and (B) per crypt from control and EGFR$^{\Delta LGR5}$ mice. Control n=5; KO n=3, based on TTEST * < 0.05; ** < 0.01; *<0.001**

Reduced BrdU incorporation was also observed in colon epithelial cells of EGFR$^{\Delta LGR5}$ mice at the 24h time point. The number of BrdU^{+} cells in colon crypts of EGFR$^{\Delta LGR5}$ mice were significantly reduced in comparison to the control mice ***Figure 24.***

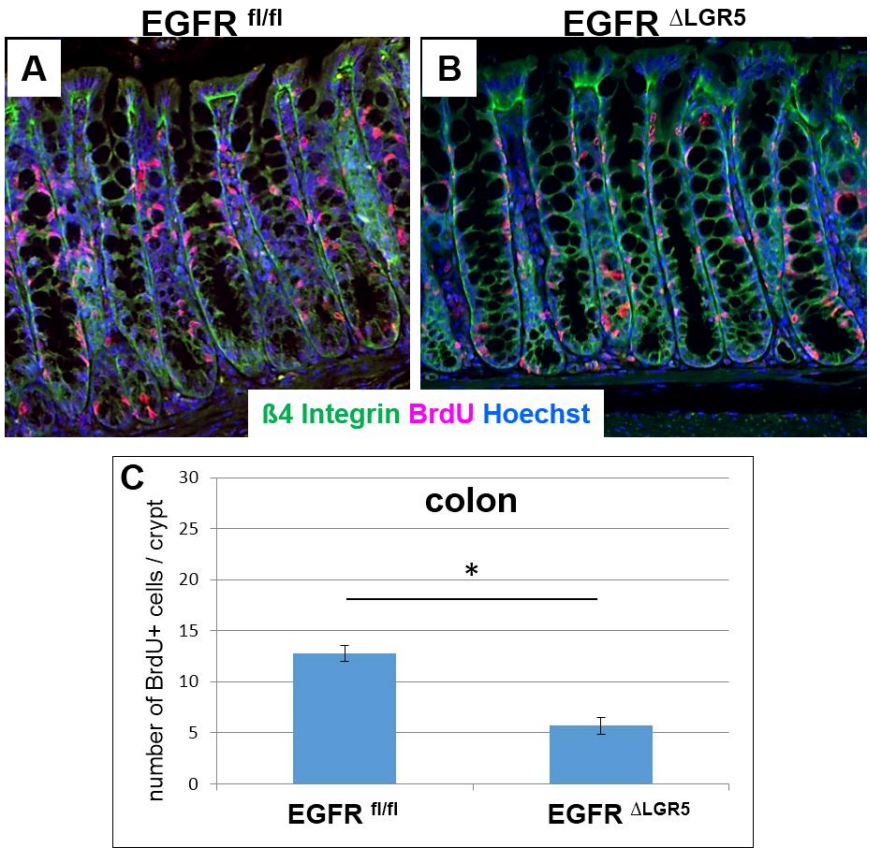

Figure 24: The microscopic image of the BrdU staining on colon sections (A) from control mice, (B) from EGFR$^{\Delta LGR5}$ mice. (C) The statistical analysis of the BrdU^{+} cell numbers average per colon crypt between control and EGFR$^{\Delta LGR5}$ mice. Green=β4 Integrin; red=BrdU; blue=Hoechst, control n=5; KO n=3; based on TTEST * < 0.05; **<0.01; *<0.001**

Reduced BrdU labeling in the villus could also mean, that the cells are not perfectly migrating after deletion of EGFR. By pulsing 4h with BrdU I checked the early proliferation before the cells exit the crypt. The number of BrdU^{+} cells was significantly decreased in small intestinal crypts of EGFR$^{\Delta LGR5}$ mice as compared to control mice 4h after BrdU pulsing. However, in the colon comparable numbers of BrdU+ cells were observed 4h after pulsing ***Figure25*** .

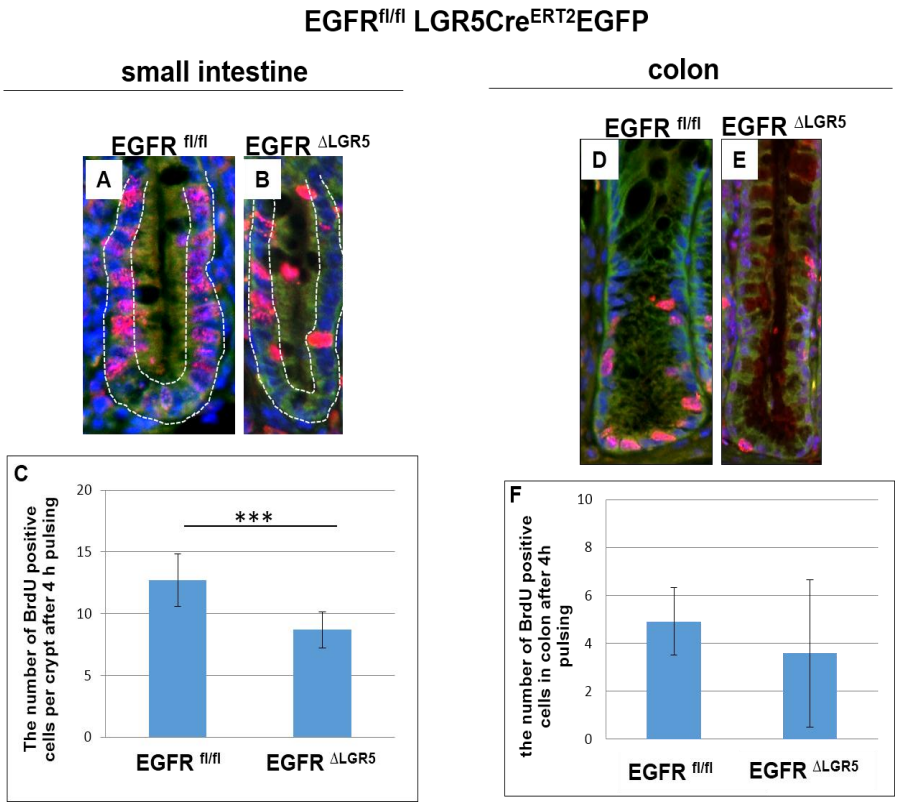

Figure 25: Microscopic images of the BrdU staining at 4h (A) in crypts from control mice, (B) from EGFR$^{\Delta LGR5}$ mice. (C) Average of BrdU^{+} cell numbers per crypt between control and EGFR$^{\Delta LGR5}$ mice. (D) Microscopic images of the BrdU staining at 4h in colon from control mice (E) from EGFR$^{\Delta LGR5}$ mice. (F) Average BrdU^{+} cell numbers per colon crypt between control and EGFR$^{\Delta LGR5}$ mice. Green=β4 Integrin; red=BrdU; blue=Hoechst, control n=5; KO n=3; based on TTEST * < 0.05; **<0.01; *<0.001**

This data indicate that the EGFR deletion has an effect on the proliferation of intestinal cells despite of the mosaic expression of Lgr5-Cre transgene, suggesting that the BrdU^{+} cell numbers would be more reduced, if EGFR could be deleted in every crypts.

2.2.4 Constitutive deletion of EGFR; EGFR$^{fl/fl}$ VillinCre

Because of the mosaic deletion pattern of Lgr5-Cre, I employed an additional mouse model (Villin-Cre) to investigate the effect of the EGFR on differentiation and proliferation of the intestinal epithelium.

In Vil-Cre, Cre is active from E12.5 in every gut epithelial cell (El Marjou 2004) resulting in EGFR deletion in the whole intestinal epithelium. Therefore I analyzed the small intestine and colon of 6-8 week old mice in order to have an age-matched comparison to my previous experiments with the EGFR$^{\Delta LGR5}$ mice.

Complete deletion of EGFR was confirmed in small intestine and colon samples of EGFR of EGFR$^{\Delta IEC}$ mice by EGFR IHC stainings ***Figure26***.

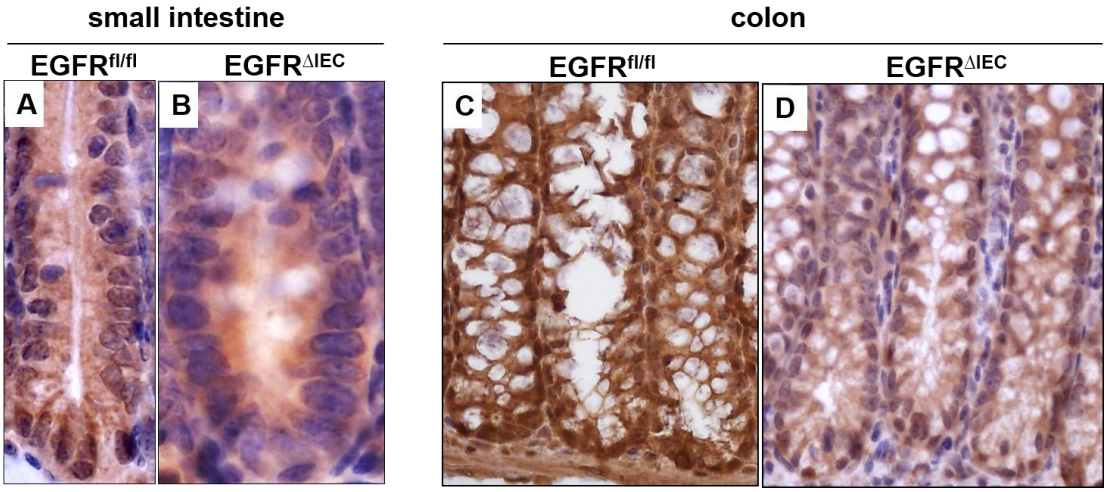

Figure 26: EGFR IHC (A) in the crypt compartment of small intestine from control mice, (B) from EGFR$^{\Delta IEC}$, (C) in the colon from control mice and (D) from EGFR$^{\Delta IEC}$ mice. Blue=Hematoxylin; brown=EGFR

Furthermore I performed the same morphological analysis as before by measuring the length and width of the villi on H&E stained paraffin sections of the small intestine. Surprisingly, the gut showed no gross morphological alterations and villus length and width were comparable between control and EGFR$^{\Delta IEC}$ mice within the different small intestinal compartments ***Figure27***.

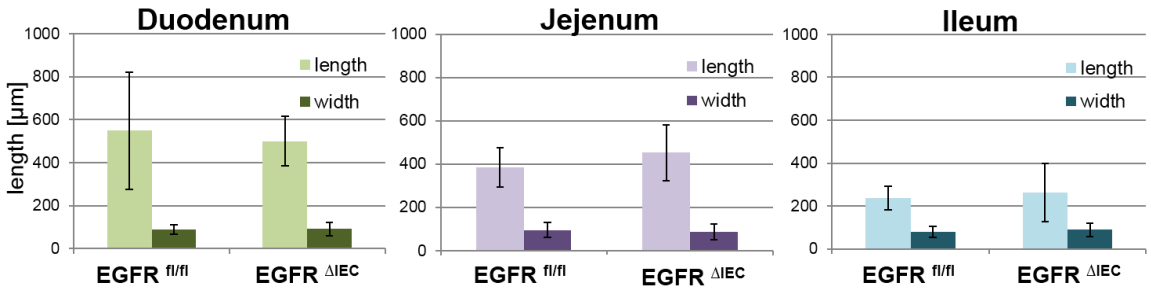

Figure 27: Length and width of villi from control and EGFR$^{\Delta IEC}$ mice. Each diagram shows another compartment of small intestine; duodenum, jejenum and ileum. The light bars are for the length and the dark bars are for the width of villi. Control n=2; KO n=6

2.2.5 The effect of the EGFR deletion on the differentiation of EGFR$^{\Delta IEC}$ intestine

2.2.5.1 Mucosa secreting goblet cells

The combined PAS & Alcian blue staining shows mucosa secreting goblet cells, which are a differentiated cell type of small intestinal epithelium. Comparable goblet cell numbers were detected between control and EGFR$^{\Delta IEC}$ mice ***Figure28***.

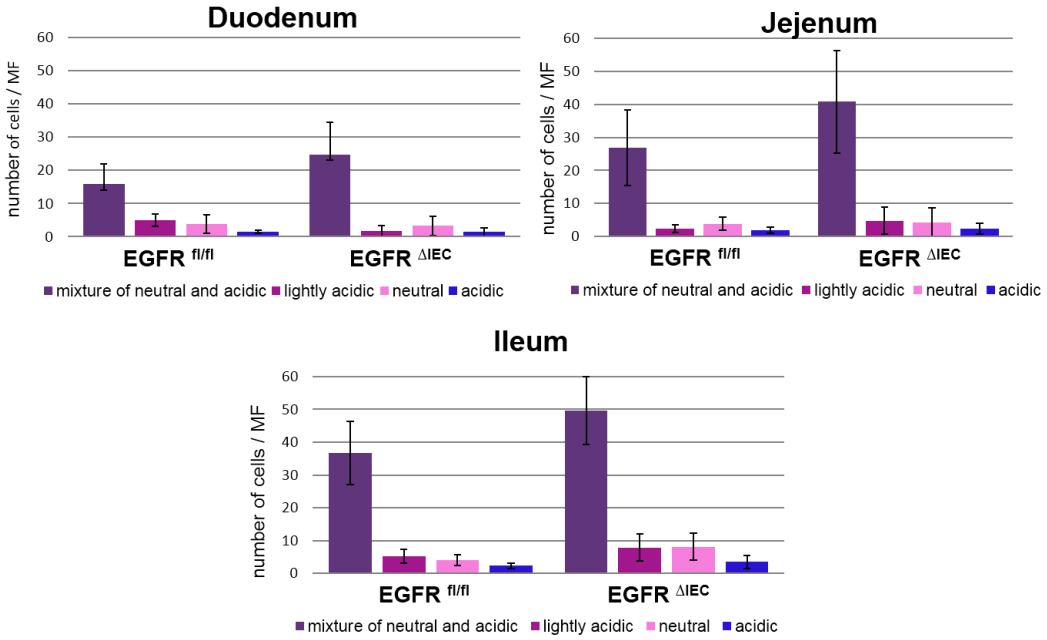

Figure 28: Average numbers of different pH value goblet cells on villi from the intestinal compartments; duodenum, jejunum and ileum. Each diagram shows the results in different compartment. The y-axis gives the numbers of cells on a microscopic field of 20x objective. Each color represent a different pH value; blue=acidic; pink=neutral; lila=lightly acidic; deep purple=the mixture of neutral and acidic. Control n=6; KO n=2

2.2.5.2 Enteroendocrine cells & Paneth cells

For further analysis of the effect of EGFR deletion on differentiation in small intestinal epithelium, other differentiated cell types were visualized like enteroendocrine cells and paneth cells, which are the essential cells of the stem cell niche by providing important factors for the maintance of proliferation and differentiation while secreting antimicrobial substances. Hormone producing enteroendocrine cells are observable with a synaptophysin IHC staining and the

paneth cells were detected with a lysozyme IHC staining. For the quantification of the Enteroendocrine cell staining, the numbers of the synaptophysin positive cells were counted from 80 villi for each mouse. Also, the average of Paneth cells per crypt from 30 crypts for each mouse were calculated. The analysis revealed that the numbers of both cell types, enteroendocrine and Paneth cells, are comparable between the control and EGFR$^{\Delta IEC}$ mice ***Figure29.***

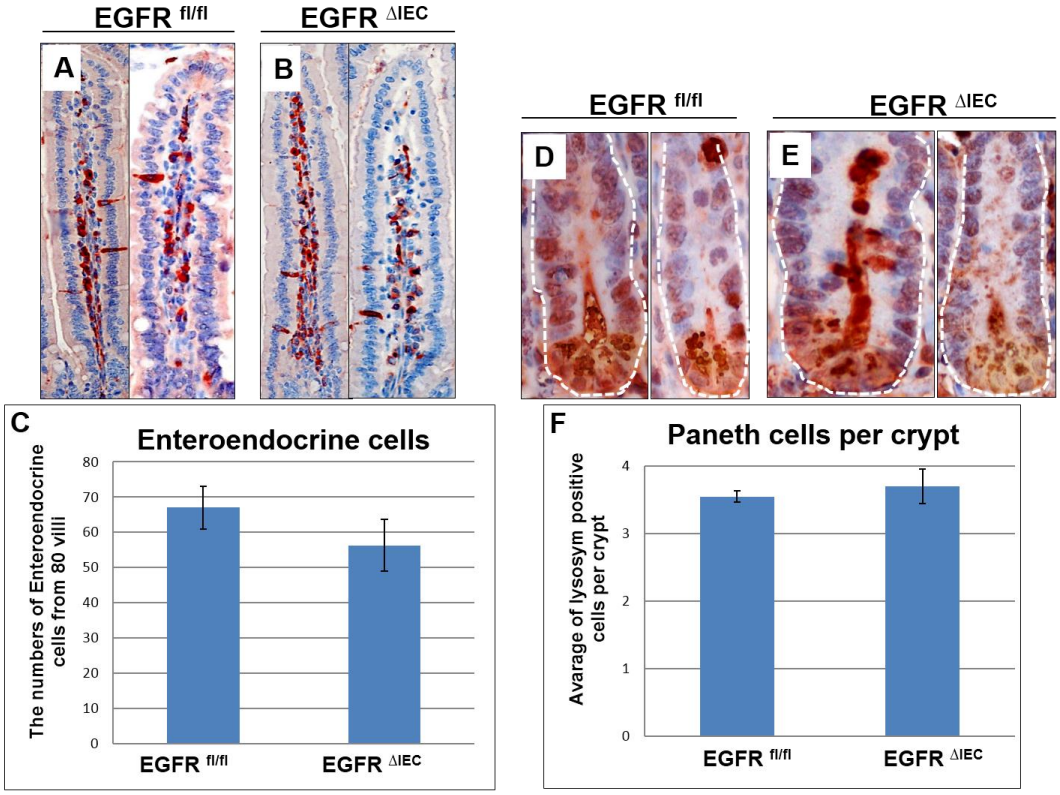

Figure 29: Microscopic images of the synaptophysin staining on villi (A) from control mice, (B) from EGFR$^{\Delta IEC}$ mice. (C) Graphical representation of enteroendocrine cell numbers from control and EGFR$^{\Delta IEC}$ mice. (D) Microscopic images of the lysozyme staining on crypts of control mice and (E) of EGFR$^{\Delta IEC}$ mice. (F) Graphical representation of Paneth cell analysis from control and EGFR$^{\Delta IEC}$ mice. Control n=2; KO n=6

2.2.5.3 Crypt characterization

As I have a constitutive deletion of EGFR, I performed some additional experiment to determine the crypt size and to check the Lrig1 expression, which is predicted as a marker for +4cells.

2.2.5.3.1 Crypt size

The Ki67 protein marks cycling cells, which in the case of the small intestine marks the whole crypt compartment (the stem cells and the rapidly proliferating progenitor cells from the TA compartment). Therefore the number of Ki67 positive cells is a measure for the crypt size. According to this, sections of the small intestine were stained with Ki67 and the crypt length was measured. The results show comparable crypt sizes between control and EGFR$^{\Delta IEC}$ mice ***Figure30.***

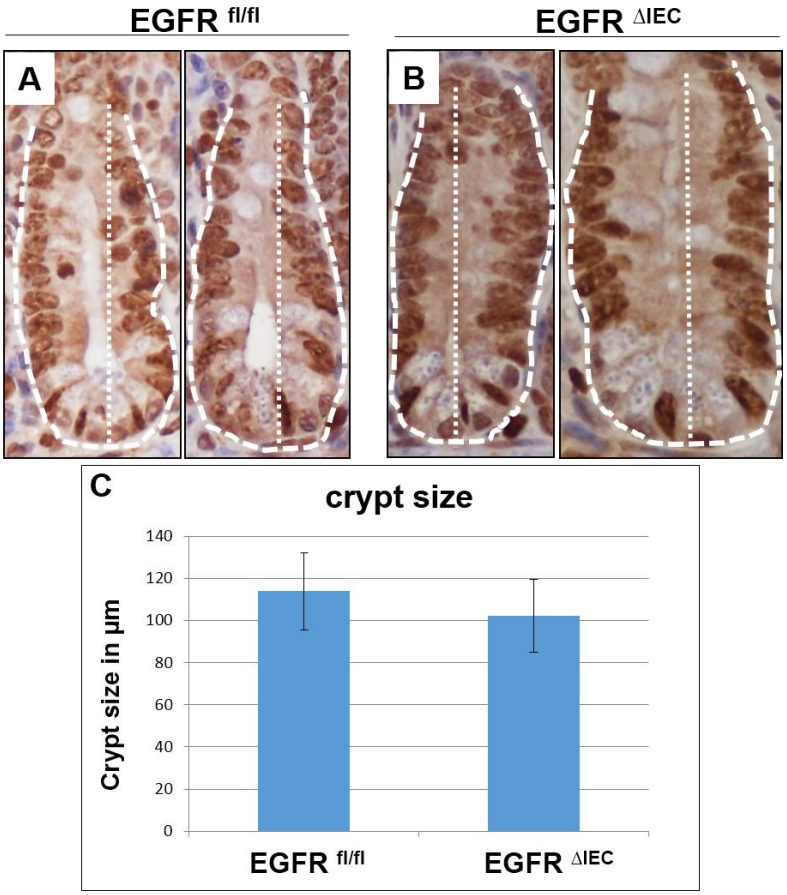

Figure 30: Microscopic images of Ki67 staining in crypt compartment (A) from control mice, (B) from EGFR$^{\Delta IEC}$ mice. (C) Diagram of the crypt length in µm between control and EGFR$^{\Delta IEC}$ mice. Control n=2; KO n=6, blue=Hematoxylin; brown=Ki67

2.2.5.3.2 Lrig1 expression

Leucine rich repeats and immunoglobin like domain 1(Lrig1), which is a negative regulator of ErbB signaling by forming complexes with all ErbB proteins on the surface and inducing their degradation (Wong 2012, Barker 2012), is predicted as a marker for +4 cells. However, its expression can also be found in $LGR5^{+}$ stem cells at the crypt base and in the whole crypt compartment. Lrig1 expression appeared normal and comparable in crypts of control and $EGFR^{\Delta IEC}$ ***Figure31***.

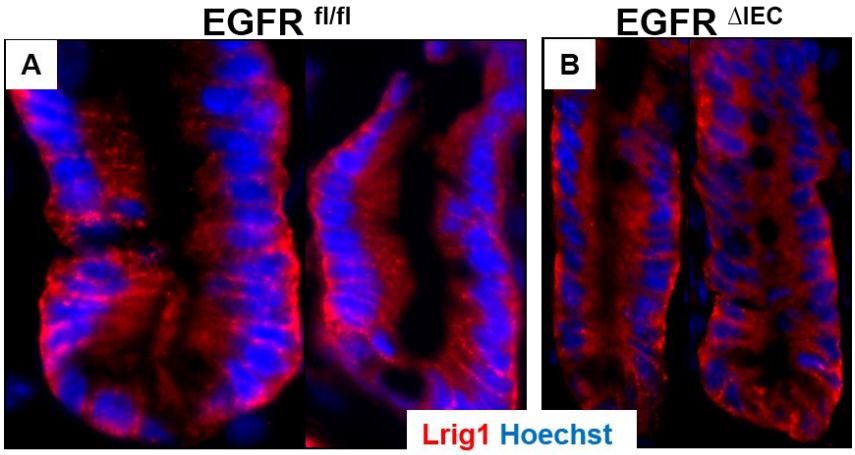

Figure 31: Microscopic images of immunofluorescence staining Lrig1 antibody from (A) control and (B) $EGFR^{\Delta IEC}$ mice. Red=Lrig1; blue=Hoechst

2.2.6 The effect of EGFR on the proliferation of ΔIEC mice

As the gut morphology, crypt size and quantification of distinct differentiated cell types showed comparable results between $EGFR^{\Delta IEC}$ and control mice, I conclude that the presence of EGFR on intestinal epithelial cells does not seem to be important for the differentiation of the gut epithelium.

Analysis of cell proliferation was performed analogous to $EGFR^{fl/fl}LGR5Cre^{ERT2}$ mice: BrdU incorporation was quantified 4h and 24h after pulsing, respectively. I injected 70µl BrdU (12mg/ml) 4h or 24h before sacrifice to 6-8 week old $EGFR^{fl/fl}$ VillinCre mice. Again, in the small intestine, $BrdU^{+}$ cells were counted separately on villi and crypts, or for the whole colon. Surprisingly, analysis of the 24h time point showed, that there were comparable numbers of BrdU+ cells in the villi of control and $EGFR^{\Delta IEC}$ mice. In the crypts of the small intestine as well

as in the colon there was a trend towards reduced numbers of BrdU incorporation in EGFR$^{\Delta IEC}$ mice ***Figure32&33***. However, as the sample number of control mice was too low, statistical analysis could not be performed.

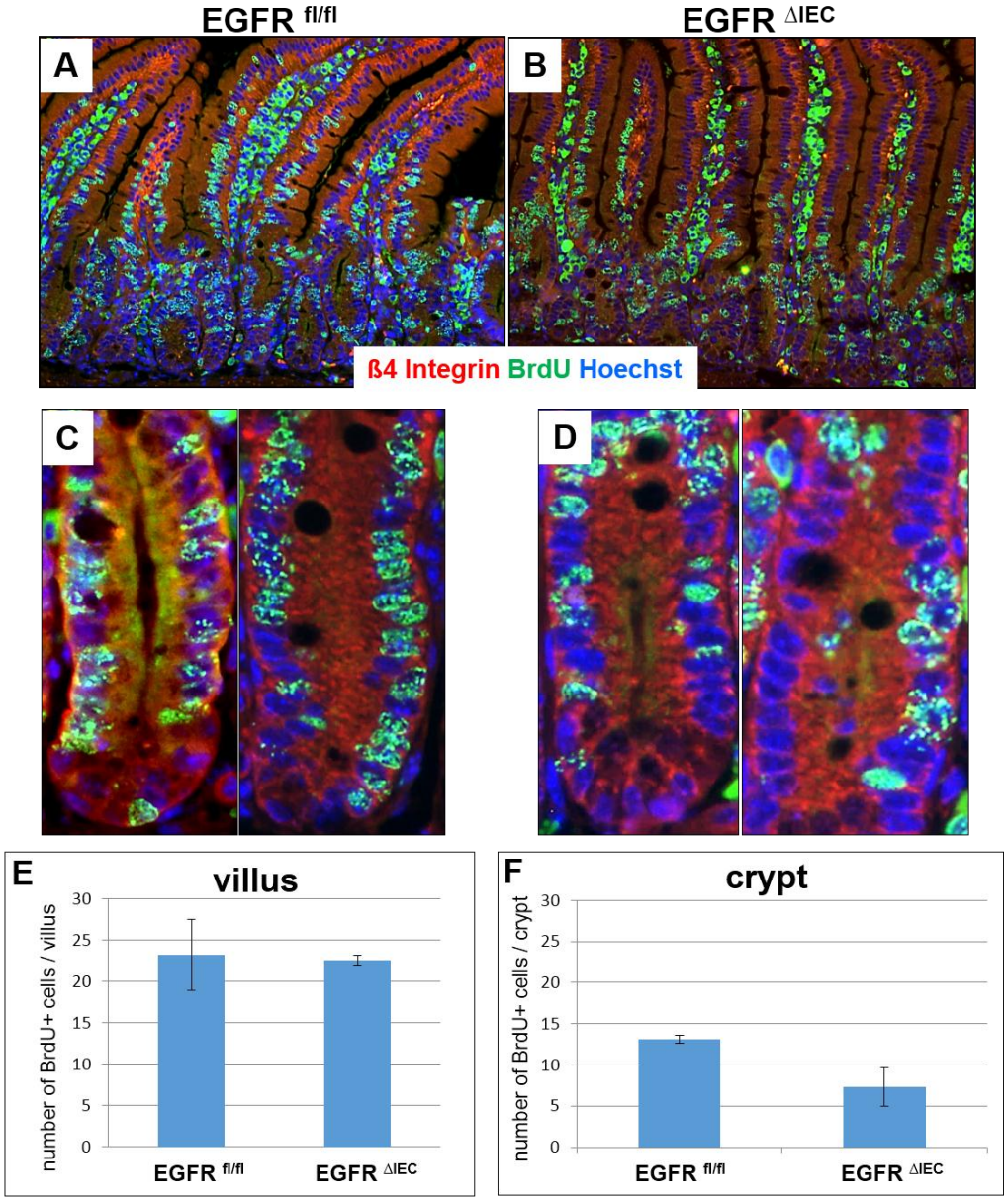

Figure 32: Microscopic images of BrdU staining of small intestinal samples (A) from control mice (B) from EGFR$^{\Delta IEC}$ mice. BrdU staining on crypts of (C) control mice, (D) EGFR$^{\Delta IEC}$ mice. (E) The diagram shows the average of BrdU^{+} cell numbers per villus and (F) per crypt between control and EGFR$^{\Delta IEC}$ mice. Control n=2; KO n=6; green=BrdU, red=β4 Integrin; blue=Hoechst

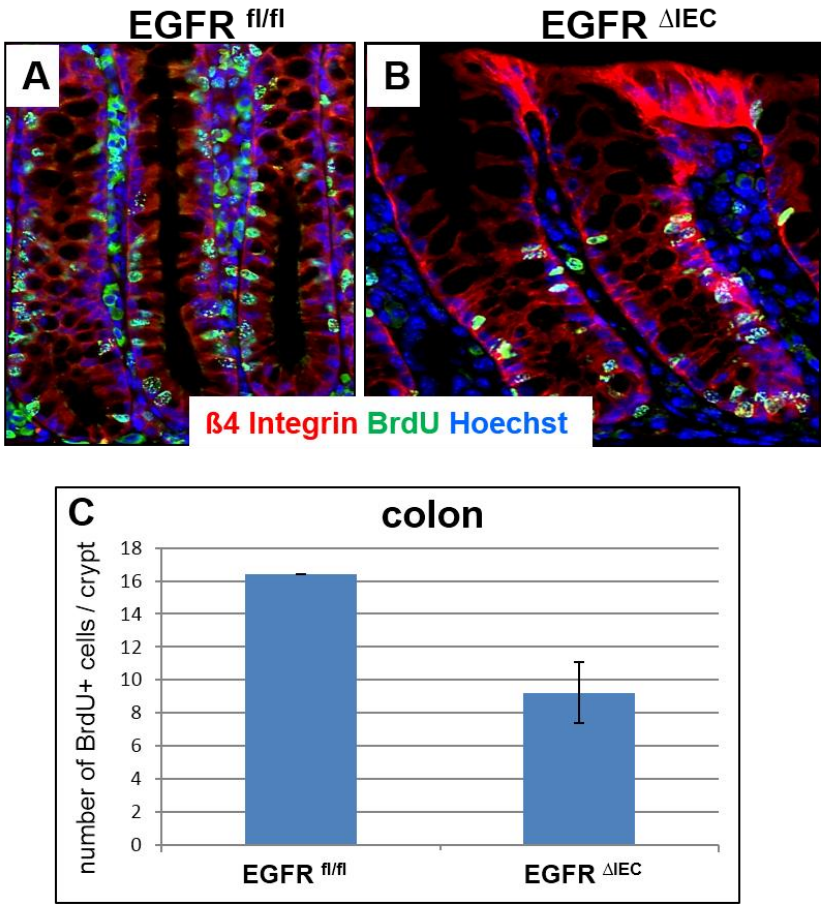

Figure 33: Microscopic images of BrdU staining on colon samples from (A) control and (B) EGFR$^{\Delta IEC}$ mice. (C) The diagram of the BrdU positive cell numbers in colon crypt from control and EGFR$^{\Delta IEC}$ mice. Control n=2; KO n=6; green=BrdU, red=β4 Integrin; blue=Hoechst

I next checked the early proliferation before the cells exit the crypt by pulsing with BrdU 4h prior to analysis. The number of BrdU^{+} cells was comparable in small intestinal crypts and in the colon of EGFR$^{\Delta IEC}$ mice 4h after BrdU pulsing ***Figure34***.

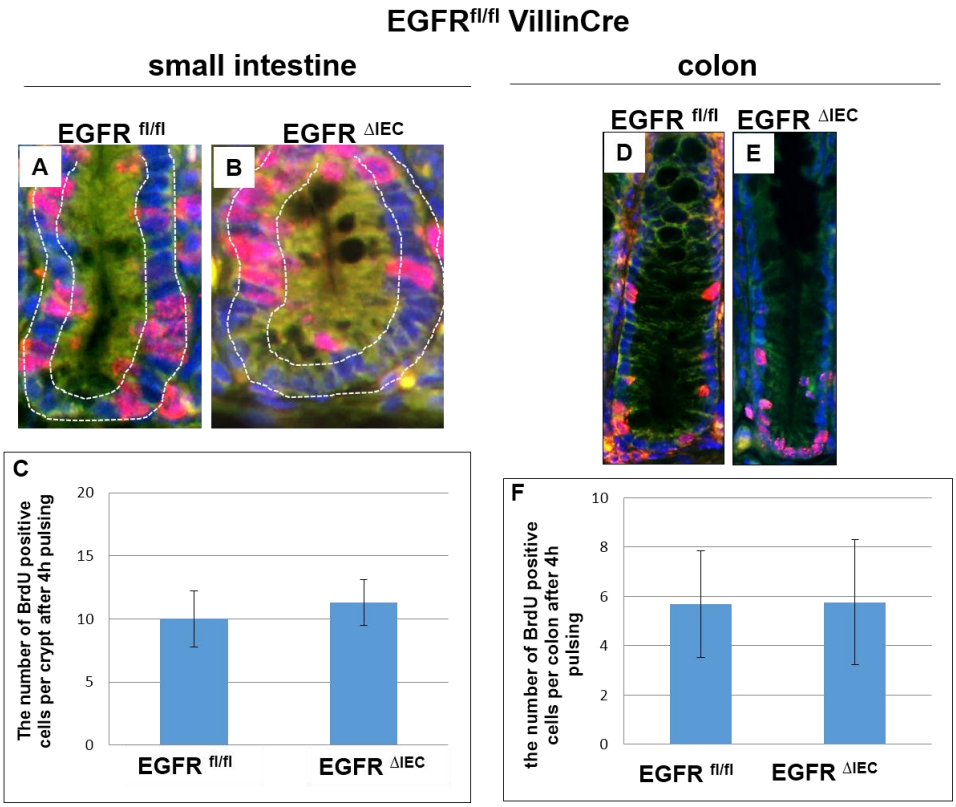

Figure 34: Microscopic images of BrdU (4h) staining (A) in crypts from control mice, (B) from EGFR$^{\Delta IEC}$ mice. (C) Quantificaiton of BrdU^{+} cell numbers per crypt in control and EGFR$^{\Delta IEC}$ mice. (D) The microscopic image of the BrdU (4h) staining in colon from control mice (E) from EGFR$^{\Delta IEC}$ mice. (F) Quantification of BrdU^{+} cell numbers per colon crypt in control and EGFR$^{\Delta IEC}$ mice. Green=β4 Integrin; red=BrdU; blue=Hoechst, control n=5; KO n=3; based on TTEST * < 0.05; **<0.01; *<0.001**

These data show that EGFR$^{\Delta IEC}$ mice have comparable proliferation levels with control mice. EGFR$^{\Delta IEC}$ mice, whose EGFR is deleted from E.12.5 in every gut epithelial cells, should have figured out a compensatory mechanism for EGFR deletion, which could be the main reason, why EGFR$^{\Delta IEC}$ mice have unimpaired proliferation, while EGFR$^{\Delta LGR5}$ mice show reduced proliferation despite of the mosaic expression of Lgr5-Cre transgene.

Although several studies showed that EGFR signaling is very important for development and growth of the intestine and has a direct effect on stem cell proliferation and crypt size (Miettinen 1995, Barker 2013, Wong 2012) my studies using conditional knock-out mice were able to show that EGFR-deficient intestine has an intact morphology and normal differentiation, despite reduced proliferation within the stem cell and TA zone. I therefore speculate, that

compensatory effects are responsible for my observations. Thus, I aimed to investigate the abundance of the second population of intestinal stem cells, the +4 cells, and the potential alteration of the expression levels of other ErbB family members.

2.2.6.1 +4 cells expression

As "+4 cells" are damage responsive reserve stem cells, they were first addressed as a possible compensation source. According to the publication of Umar 2012, the slow cycling +4 cell were stained with DCAMKL-1 antibody and the staining was quantified through counting the DCAMKL-1 positive cells from 150 crypts for each mouse. +4 cell distribution is not homogeneous and cannot to be found in every crypt, however some crypts have more than one. Therefore, the average of the DCAMKL-1 positive cells per crypt was calculated. Comparison of the number of +4 cells between control and EGFR$^{\Delta IEC}$ mice showed comparable results, suggesting that EGFR-deficient intestine does not increase the number of reserve stem cells in order to ensure proper differentiation and function ***Figure35***.

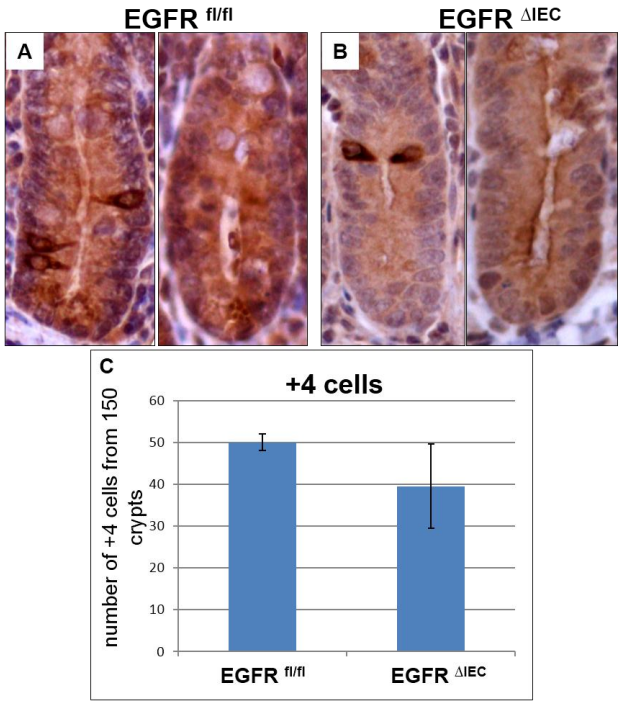

Figure 35: Microscopic images of the DCAMKL-1 staining showing the +4 cells in (A) control and (B) EGFR$^{\Delta IEC}$ mice. (C) The diagram of the average +4 cell numbers per crypt from 150 crypts between control and EGFR$^{\Delta IEC}$ mice. Control n=2; KO n=6, blue=Hematoxylin; brown=DCAMKL-1

It is of note, that a publication of Gerbe et al 2009, showed that DCAMKL-1 is not an exclusive marker to identify +4 cells, as the protein is also postulated as a marker for early progenitors of Tuft cells. Moreover, DCAMKL-1 positive cells are irradiation resistant but they do not show an increase in number in response to damage (Itzkovitz 2012, Westphalen 2014). In either case, it can be concluded that there is no compensatory overrepresentation of +4 cells or no effect on Tuft cell differentiation in the absence of EGFR in the intestine.

2.2.6.2 Expression of EGFR ligands and ErbB family members

To investigate potential compensatory upregulation of ligand expression as a consequence of EGFR deletion, crypts were isolated with 2mM EDTA and RNA was extracted. mRNA levels of ErbB receptors and EGFR ligands EPR, HB-EGF and BTC, which can bind to the ErbB receptor HER4, were quantified by quantitative real-time PCR (qRT-PCR). Thereby I wanted to find out if there are changes in their RNA expression detectable between crypt cells that harbor EGFR and crypt cells that lack EGFR.

As a control, I used RT-PCR for EGFR, demonstrating the deletion of the EGFR and valid integrity of my isolated RNA and cDNA. TBP (TATA Box binding protein) served as housekeeping gene and particular fluorescence intensity of ligands and receptors are related to the house keeping gene TBP. My results show comparable mRNA levels of the ligands EPR, HB-EGF, and BTC, as well as of the ErbB family members HER2 and HER3 between control and $EGFR^{\Delta IEC}$ mice ***Figure36***. As the threshold cycle of HER4, NRG1 and NRG2 immerged after cycle number 30, I considered as undetectable the expression of HER4, NRG1 and NRG2 in isolated crypts (data not shown).

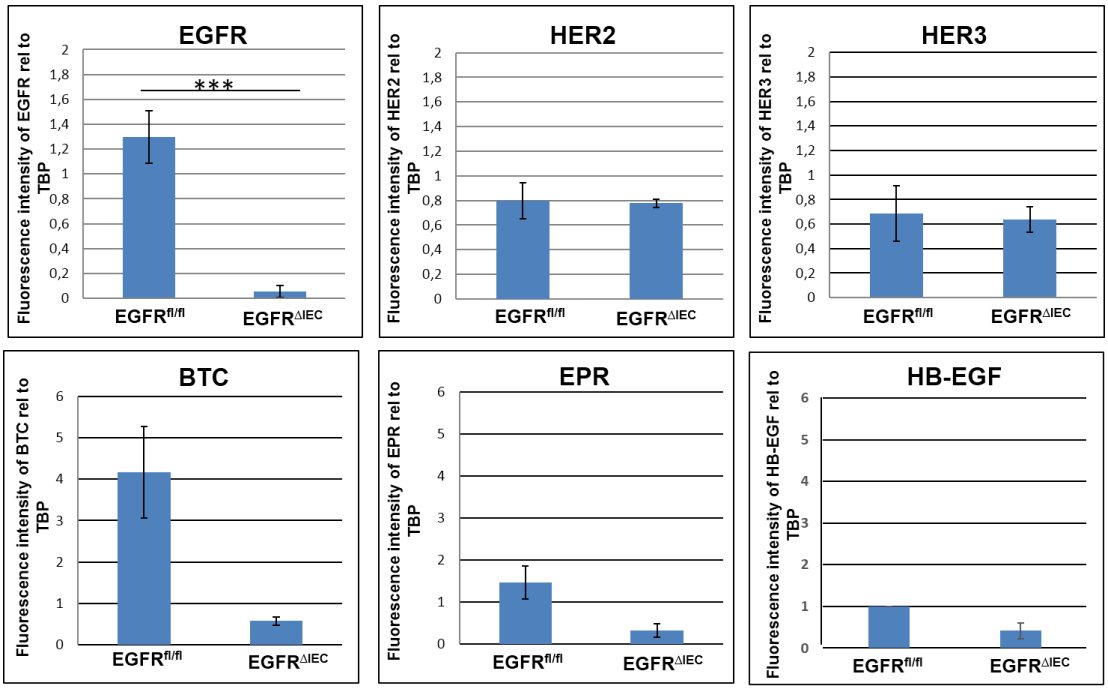

Figure 36: Q-PCR analysis of the ErbB receptors EGFR, HER2, and HER3 and the EGFR ligands BTC, EPR and HB-EGF. Control n=3, KO n=5; except for HB-EGF control n=1 and KO n=2; p-value BTC= 0.189; p-value EPR= 0,191

Although mRNA levels of HER2 and HER3 exhibited comparable levels in my qRT-PCR analysis, I wanted to confirm these results on protein levels by performing IHC stainings. I did so in order to exclude effects by posttranslational regulations. Indeed, it appeared that there were higher protein levels of HER2 and HER3 in the small intestinal crypts of $EGFR^{\Delta IEC}$ mice in comparison to control mice ***Figure37***.

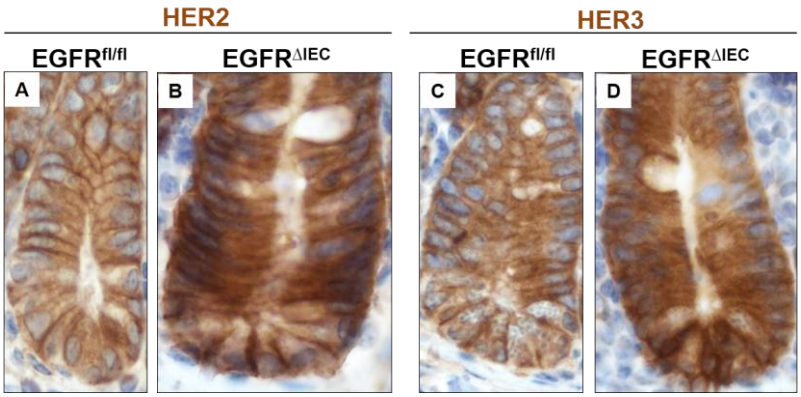

Figure 37: Microscopic images of (A) HER2 staining on control mice and (B) $EGFR^{\Delta IEC}$ mice; (C) HER3 staining on control mice and (D) $EGFR^{\Delta IEC}$ mice.

Interestingly, increased HER2 and HER3 protein levels were not observed in IHC stainings from small intestines from EGFR$^{\Delta LGR5}$ mice ***Figure38***.

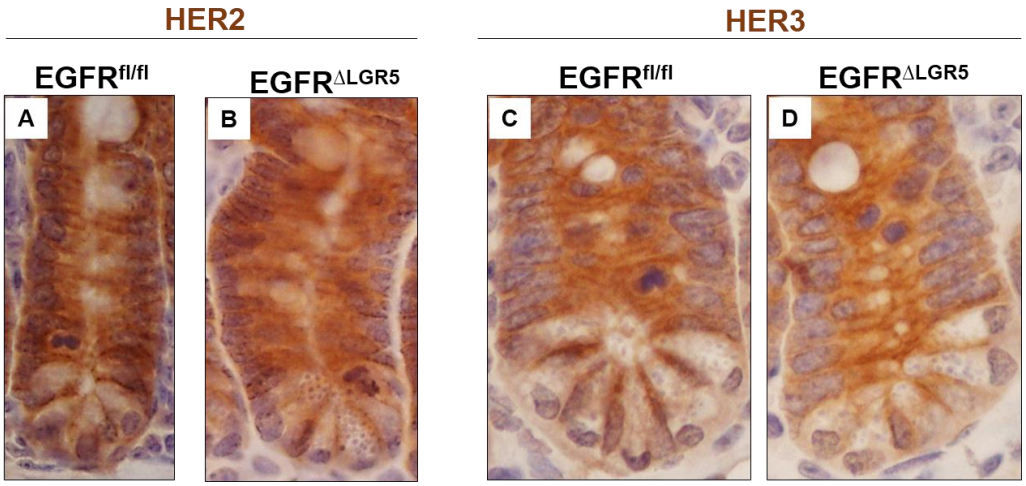

Figure 38: The microscopic image of the (A) HER2 staining on control mice and (B) EGFR$^{\Delta LGR5}$ mice; (C) HER3 staining on control mice and (D) EGFR$^{\Delta LGR5}$ mice.

The transcription factor cMyc, which is a Wnt target and serves as a proliferation initiating gene, is necessary for crypt formation (Bettess 2005), also showed a higher protein expression in EGFR$^{\Delta IEC}$ mice in comparison to control mice as detected by IHC staining ***Figure39.***

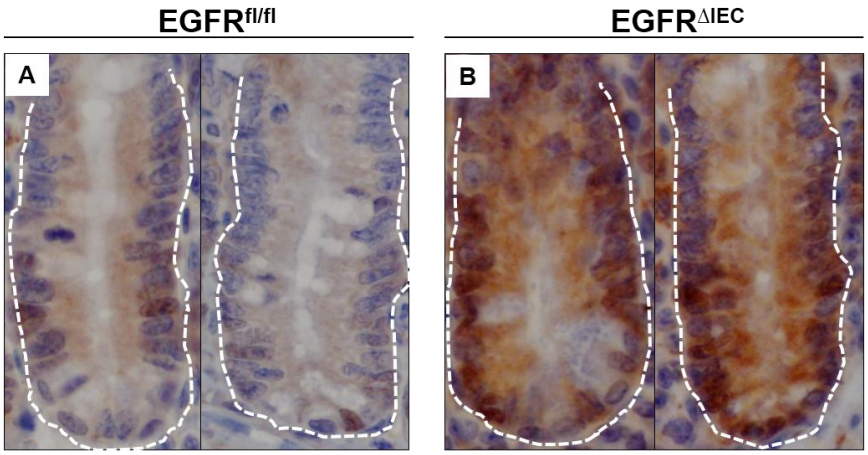

Figure 39: The microscopic image of cMyc IHC staining (A) on control and (B) EGFR$^{\Delta IEC}$ mice. Blue=Hematoxylin; brown= cMyc

However, it was difficult to determine HER2 and HER3 protein levels on IHC staining that is why I next performed western blot analysis from protein lysates

of isolated crypts to see the expression levels of HER2 and HER3 in crypts of EGFR$^{\Delta IEC}$ mice. ***Figure40***.

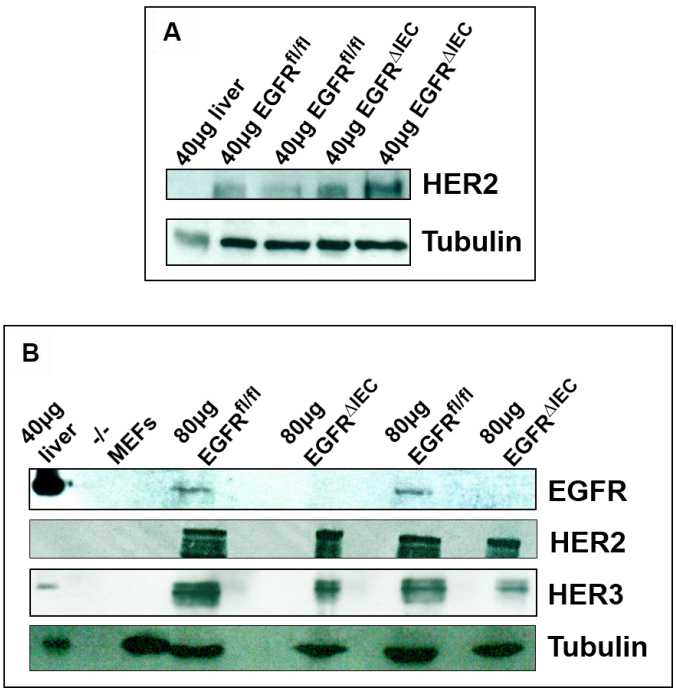

Figure 40: Western blot analysis of EGFR, HER2, HER3 and Tubulin. (A) As the liver does not express HER2, the liver lysate was a negative control for HER2. (B) As a positive control for EGFR 40µg liver and for a negative control EGFR knock out MEFs (-/-) were loaded.

The quantification of Western Blot analysis were performed at Image Studio lite (version 4.0): ***Figure41***

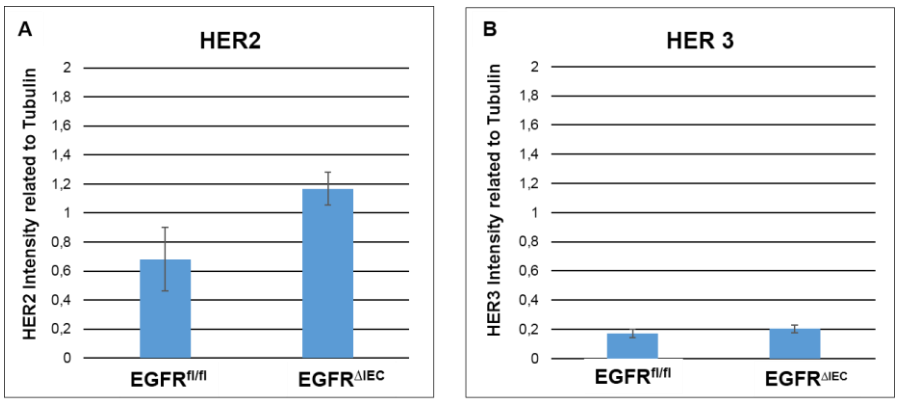

Figure 41: (A) HER2 intensity related to the Tubulin between control and EGFR$^{\Delta IEC}$ mice. (B) HER3 intensity related to the Tubulin between control and EGFR$^{\Delta IEC}$ mice.

In spite of on IHC showing trend for increased HER2 expression in EGFR-deleted intestine, it couldn't confirmed with Western Blot analysis. These results show no upregulation of other receptors.

2.2.6.3 In *vitro* organoid cultures

I also performed *in vitro* experiments using organoid cultures. Therefore, I isolated small intestinal crypts from control, $EGFR^{\Delta LGR5}$ and $EGFR^{\Delta IEC}$ mice with 2mM EDTA and cultured them on matrigel (basement membrane substitute) with a growth medium including the essential factors EGF (500 ng/ml) R-spondin-1 (500 ng/ml) and Noggin (100 ng/ml) in a 24 well plate. As a control I used growth medium without EGF. Mice were 6-8 weeks of age and the $EGFR^{\Delta LGR5}$ mice were treated with Tamoxifen 1 week prior to crypt isolation.

The organoid formation was monitored every 2 days and documented by taking images with a cell culture light microscope. At day 3 the crypts isolated from control mice with EGF in their growth medium could maintain the U-shape of the crypt and were already able to expand in the surrounding matrigel environment in order to build a cloud-like structure ***Figure42A***. Crypts isolated from control mice, which were cultured without EGF, stayed a little bit smaller and could not expand as much into their environment as the crypts with EGF, but the crypts still maintained their U-shape ***Figure42B***.

In contrast, the crypts isolated from $EGFR^{\Delta LGR5}$ mice, which were cultured with EGF began to lose the U-shape of the crypt and form circles ***Figure42C***. Living epithelial cells were still detectable around the circle while the crypts isolated from $EGFR^{\Delta LGR5}$ mice cultured without EGF built bigger circles with an apoptotic appearance of the epithelial cells ***Figure42D***. Organoids derived from crypts isolated from $EGFR^{\Delta IEC}$ mice, either cultured with EGF or without EGF mainly contained deformed crypts and apoptotic like structures ***Figure42E&F***.

From day 3 after putting the crypts on matrigel, growth differences between control and both EGFR-deleted genotypes could be observed. At day 5, the organoids from control mice cultured with EGF had built many more crypts arms, while the controls without EGF remained small like at day3, with some of them already showing apoptotic like structures ***Figure42G&H***. Interestingly, organoids from $EGFR^{\Delta LGR5}$ mice cultured with EGF were able to maintain their organoid

growth, however they harbored less crypt arms than organoids from control mice and the possible explanation for this is the mosaic expression of Lgr5-Cre transgene ***Figure42I***. Some of them showed apoptotic circles, while organoids from $EGFR^{\Delta LGR5}$ crypts cultured without EGF showed only big apoptotic structures ***Figure42J***. All organoids from $EGFR^{\Delta IEC}$ crypts, cultured with or without EGF, shrank to a circle and looked like cell debris ***Figure42K&L.***

At day 7, organoids from crypts of control mice cultured with EGF formed big organoids consisting of many surrounding crypts ***Figure42M***, whereas the control crypts cultured without EGF form circles, where the epithelial cells are still viable ***Figure42N***. This appearance is the same in organoids derived from $EGFR^{\Delta LGR5}$ crypts, cultured either with or without EGF. Some of the $EGFR^{\Delta LGR5}$ organoids cultured without EGF built even bigger apoptotic-bodies ***Figure42O&P***. Organoids derived from $EGFR^{\Delta IEC}$ crypts with or without EGF could not show normal growth, as they did not appear to have an intact basement membrane anymore and showed only vesicles ***Figure42R&S.***

Successful organoid formation was only detected in crypts isolated from control mice, which formed “mini-guts” consisting of multiple crypts.

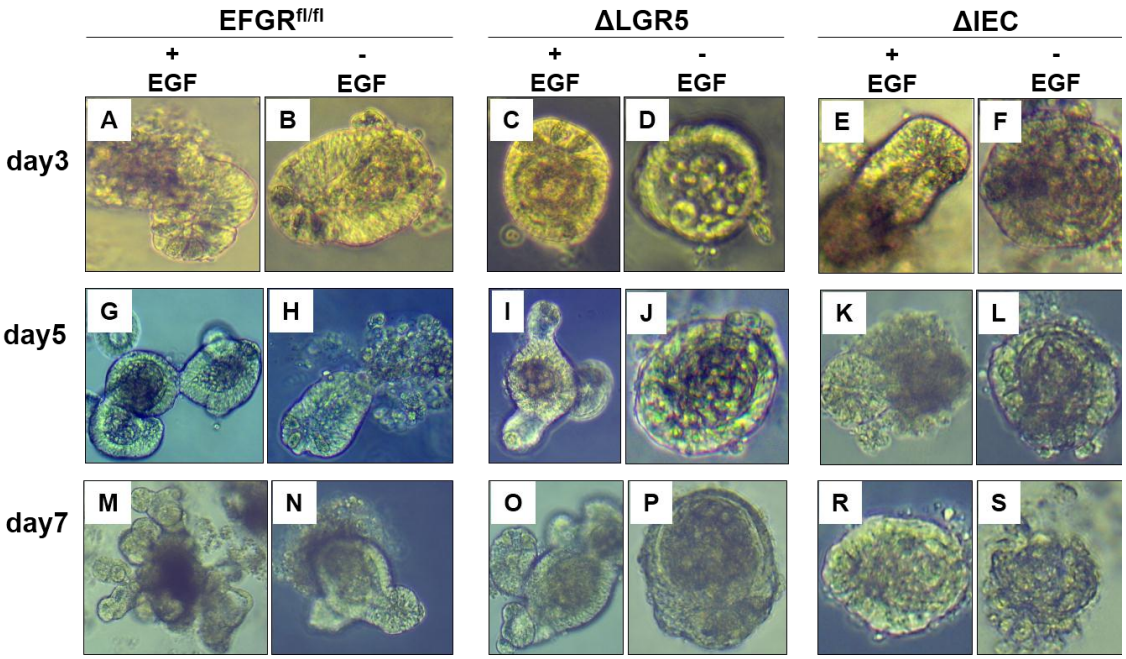

Figure 42: Microscopic images of organoids at day 3 (A-F) from control mice with EGF(A), without EGF (B); from ΔLGR5 mice with EGF (C), without EGF (D); from ΔIEC mice with EGF (E) and without EGF (F). Organoids at day 5 (G-L) from control mice with EGF (G), without EGF (H); from ΔLGR5 mice with EGF (I), without EGF (J); from ΔIEC mice with EGF (K), without EGF (L). Organoids at day 7 (M-S) from control mice with EGF (M), without EGF (N); from ΔLGR5 mice with EGF(O), without EGF (P); from ΔIEC mice with EGF (R), without EGF (S).

With this ex vivo organoid experiment I was able to prove that the EGFR is important for the proliferation of intestinal stem cells and moreover for a normal gut morphology. Only crypts isolated from control mice cultured with EGF were able to form and maintain organoids. Although in early stages $EGFR^{\Delta LGR5}$ crypts were able to survive better than the crypts derived from $EGFR^{\Delta IEC}$ mice, both genotypes were not able to form an organoid *in vitro*.

As mentioned before the Paneth cells have a longer life span than the other differentiated cell types found in the villi. They exit the upwards migration at the crypt-villus-junction and move back down into the crypt base, where they reside 6-8 weeks. This means that one week after tamoxifen treatment isolated crypts of $EGFR^{\Delta LGR5}$ mice still contained Paneth cells harboring EGFR. These Paneth cells could be the answer why the crypts derived from $EGFR^{\Delta LGR5}$ mice can

survive a little bit better than the crypts derived from $EGFR^{\Delta IEC}$ mice. But it should not be forgotten that the Lgr5-Cre transgene has the mosaic expression and in organoid cultures there are EGFR expressing and deleted crypts. In case of $EGFR^{\Delta IEC}$ mice the entire epithelial cells including the Paneth cells do not exhibit EGFR expression. While crypts from $EGFR^{\Delta IEC}$ mice could not succeed in organoid formation *in vitro* but provide normal gut morphology *in vivo*, showing a regular differentiation and proliferation, the mesenchymal niche may be a possible explanation as compensatory element. The mesenchyme is closed to the crypt base and was already described to secrete important factors for stem cells and their proliferation (Barker 2013, Smith 2012).

3 Discussion

The EGFR takes part in many cellular processes from proliferation to survival and differentiation. Therefore it serves very important functions, which need to be tightly regulated and controlled. EGFR expression is found in many cancer types, such as brain and epithelial tumors. Many studies could show, that the receptor homo- and heterodimerization initiates many signaling cascades, which are playing a role on cancer pathogenesis and cancer progression.

It is generally believed, that adult stem cells, which have the capacity to give rise to other differentiated cell types, while they can also renew themselves during the life span, could also be the originating cells for tumors. Cancer stem cells could take over some characteristics of adult stem cells in order to supply the cancerous structure with more cells (Sachs and Clevers 2014).

Neither $EGFR^{\Delta LGR5}$ nor $EGFR^{\Delta IEC}$ showed abnormal gut morphology upon EGFR deletion. EGFR deletion did not affect the differentiation of the distinct intestinal epithelial cells.

However, analysis of proliferation by measuring the incorporation of BrdU 24h after BrdU injection showed significantly reduced numbers of $BrdU^{+}$ cells in both, crypt and villus compartments in $EGFR^{\Delta LGR5}$ mice. Similarly, $EGFR^{\Delta IEC}$ mice, also showed a trend towards reduced BrdU incorporation. Early proliferation is measured 4h after BrdU injection, when the cells are still in the crypt, showed that $EGFR^{\Delta LGR5}$ mice have a significantly reduced proliferation, while the $EGFR^{\Delta IEC}$ mice were comparable to the control.

A possible explanation for the observed results could be provided by the fact, in $EGFR^{\Delta LGR5}$ mice,the EGFR is deleted in adult stage (6-8 weeks old). The mice therefore suffered a sudden loss of EGFR protein in the intestine. In contrast, constitutive deletion of EGFR from VillinCre mice occurs from the E12.5, which means that $EGFR^{\Delta IEC}$ mice might have developed a compensatory mechanism in order to ensure proper gut development (eg. Upregulation of myc). This question should be addressed by analysing intestines of 6-8 week old $EGFR^{fl/fl}$ $VillinCre^{ERT}$ mice, which harbor a Tamoxifen-inducible form of Cre.

Using $EGFR^{fl/fl}$ $VillinCre^{ERT}$ mice could also rule out potential differences of mosaic expression of the $LGR5Cre^{ERT2}EGFP$ construct. Nevertheless, the proliferation of intestinal crypts and also BrdU labeled cells in the villi were significantly decreased in $EGFR^{\Delta LGR5}$ mice. However, one cannot rule out the possibility that the differentiation was normal, because one villus is surrounded by multiple crypts (up to 10). This means, that when the inducible EGFR deletion is not taking place in every crypt (as given by the mosaic expression), each villus always has some “back-up” crypts which still express EGFR.

Sato and colleagues were able to establish a protocol to culture the crypts *ex vivo* on a matrigel, which is a basement membrane substitute, with the minimal requirement of the growth factors EGF, R-spondin-1 and Noggin. The cultured isolated crypts create so called organoids, or mini-guts, *in vitro*.

To analyze the effect of the EGFR deletion in different cell types of the crypt base *in vitro* I isolated crypts from control, $EGFR^{\Delta LGR5}$ and $EGFR^{\Delta IEC}$ mice and cultured them on matrigel with R-spondin-1 and Noggin in the presence or absence of EGF. Without EGF, neither organoids could grow. While the crypts isolated from control mice, cultured with EGF, formed large organoids with several surrounding crypt arms, the crypts from $EGFR^{\Delta IEC}$ mice presented only apoptotic structures, characterized by encircled crypts and disaggregated vesicles. Crypts derived from $EGFR^{\Delta LGR5}$ mice only formed very small organoids with few crypts, which were possibly those crypts, where the EGFR was not deleted due to the mosaic expression of the Cre construct.

These *in vitro* experiments revealed that the EGFR is important for the proliferation and survival of intestinal epithelial cells. Although $EGFR^{\Delta IEC}$ mice show a normal gut differentiation and slightly reduced proliferation *in vivo*, they are absolutely not able to survive and form a mini-gut *in vitro*. A possible explanation for this could be that the stromal cells of the sub-epithelial tissue, which constitute the mesenchymal niche close to the crypt compartment, secrete factors, which help the EGFR-deficient stem cells niche to maintain the gut morphology *in vivo*. It was shown, that the pericryptal stromal cells also secrete Wnt, EGF, Noggin and Notch ligand Dll4 (Barker 2013). These stromal cells could be the compensatory solution as response to the lack of EGFR. As

these cells are not present within the organoid culture, this could explain why crypts from $EGFR^{\Delta IEC}$ mice could not grow *ex vivo*. Moreover, this could also give an answer to the question, why $EGFR^{-/-}$ mice show defects in the intestinal epithelium, since there also stromal cells lack the EGFR, which might prevent them from the initiation of compensatory signaling (Miettinen 1995).

4 Materials and Methods

4.1 Materials

4.1.1 Buffers

Tail buffer:

50 mM Tris-HCl pH 8

100 mM EDTA

100 mM NaCl

1% SDS

TE buffer:

1 M Tris pH 8

0.5 M EDTA pH 8

Alcian blue solution:

1% Alcian blue

In 3% aq. Acedic acid

PBS 10X 1L:

80g NaCl

2g KCl

18.05g $Na_2HPO_4.2H_2O$

2.4g KH_2PO_4

in dH2O

pH 7.4

Blocking solution:

5% Horse Serum

0.1% Triton

1% BSA in PBS

TBS 10X 1L:

100ml 2M Tris pH 7.5

300ml 5M Nacl

in dH2O

TBS-T 1X 1L:

100ml 10X TBS

899ml H_2O

1ml Tween-20

PAGE buffer 5X:

75g Tris base

360g Glycine

pH 8.3 (HCl)

add H_2O to 1000ml

Running buffer 1X:

200ml 5X page buffer

5ml 20%SDS

795ml H_2O

Transfer buffer 1X:

200ml 5X page buffer

200ml methanol

600ml H_2O

Stripping buffer 500mL:

31.5ml 1M Tris pH 6.8

50ml 20% SDS, Add 360µl β-mercaptoethanol prior to use

Bradford solution:

10mg Coomassie BBG 250

5ml abs. EtOH

10ml 85% Orthophosphıracid

Add to 100ml H_2O

Basal culture medium:

2mM GlutaMax 100

10mM HEPES

100U/ml penicillin/100mg/ml streptomycin

In Advanced DMEM/F12

Growth medium:

1X N2 supplement

1X B27 supplement

1mM N-acetylcysteine

50ng/ml EGF

100ng/ml mNoggin

500ng/ml R-spondin-1

In basal culture medium

4.1.2 Reagents and solutions

Phospahte Buffered Saline w/o Ca&Mg	D8537-24X500ML	Sigma Aldrich
Proteinase K	3115852001	Roche
dNTPs	U1240	Promega Freezer
DreamTaq DNA Polymerase	EP0704	Fermentas Thermo Fisher Scientific
Dimethyl sulfoxide DMSO	1.096.780.100	Merck
Taq-Polymerase	11435094001	Roche
GeneRuler 1kb DNA Ladder	SM0311	Fermentas Freezer 707
Serva DNA Stain Clear G, 5ml	39804.02	AL-Labortechnik Serva
Dako Target Retrieval Solution (10x)	S1699	Dako
Tri Reagent	T9424-200ML	Sigma Aldrich
Trichlormethan/Chloroform	3313,4	Carl Roth
ProtoScript® II Reverse Transcriptase	M0368L	NEB
Power SYBR® Green PCR Master Mix	4368708	Applied Biosystems Life Technologies
cellculture water	W3500-24X500ML	Sigma Aldrich
Rotiphorese® Gel 30 Acrylamid - und Bisacrylamid-stammlösung	3029.1	Roth
2-mercaptoethanol	M3148-25ML	Sigma Aldrich
SDS ultra pure	2326.2	Roth
PageRuler Prestained Protein Ladder	26616	Fermentas Freezer

Amersham Hyperfilm ECL triple pack	28-9068-37BOM3P	VWR
SuperSignal West PICO Chemiluminescent Substrate-Trial Kit, 50 mL	10445685	Thermo Scientific/Pierce
Albumin from bovine serum	A3059	Sigma Aldrich
Isopropanol	1.096.341.011	VWR
Sucrose BioXtra, ≥99.5%	S7903-1KG	Sigma Aldrich
Acetone,	34850-2.5L	Sigma Aldrich
Alcianblau 8 GS (C.I. 74240)	3082.3	Roth
Schiff's Reagent	3952016-500ML	Sigma Aldrich
Periodic acid	P7875-25G	Sigma Aldrich
Hydrogen peroxide contains inhibitor	216763-100ML	Sigma Aldrich
Endogenous Biotin-Blocking Kit	E21390	life technologies/Invitrogen / Fisher Scientific
EGF biotinylated	E3477	Life Technologies
SignalStain Boost IHC Detection Reagent HRP, Rabbit	8114 P	NEB
ImmPACT DAB substrate kit	SK-4105	SZABO-SCANDIC
Idetect Universal Mouse KIT,HRP	31101	Labs Biotechnology
Target Antigen Retrieval Solution 10x	S1699	Dako
Antigen Retrieval Solution pH6	S2369	Dako
Antigen Retrieval Solution pH9	S2367	Dako
AEC Substrate Buffer	28719	Idlabs
AEC Chromogen	28935	Idlabs
Horse Serum	16050-122	Gibco
Goat Serum	16210-064	Gibco

Hoechst 33258	861405-500MG	Sigma Aldrich
M.O.M. Blocking Kit	FKM-2201	Szabo Scandic / Vectorlaboratories
Tween 20	4859.1	Carl Roth
Cover glass 24x50mm	631-1574	VWR
Mounting medium	S3025	Dako
Aquatex	1.085.620.050	Merck
2-Propanol ≥99,5	9866,1	Carl Roth
Ethanol absolute EMPLURA	8.187.602.500	VWR
HCl 32 %	X896.2	Roth
Corning® Matrigel® Growth Factor Reduced (GFR) Basement Membrane Matrix, Phenol Red-Free, 10mL	356231	Corning
Human Recombinant - Spondin1	4645-RS-025	R&D
Recombinant murine Noggin	250-38	Peprotech
EGF	E4127	Sigma Aldrich
N2 Supplement	17502-048	Life Technologies
B27 Supplement	17504-044	Life Technologies
2mM GlutaMax	35050-038	Life Technologies
DMEM/F12	12634-010	Life Technologies
Hepes buffered HBSS	14175-053	Fisher/Invitrogen
Foetal Bovine(Calf) Serum	7.01LES	Source BioScience
Cell Strainer,70 µm	BDL352350	Szabo-Scandic-Corning
BD Falcon™ Petri dish, steril	391-2002	Falcon/BD Becton Dickinson CDC/ VWR

Sunflower Seed Oil	S5007-250	Sigma Aldrich
Tamoxifen citrate salt	T9262-5G	Sigma Aldrich
5-Bromo-2'-deoxyuridine	10280879001	Roche
Trizma® base, ≥99.9%	T1503-5KG	Sigma Aldrich
EDTA	34103	Calbiochem
Sodium Chloride	31434-1KG-R	Sigma Aldrich
Paraformaldehyd	0335.3	Roth
Triton X 100	3051.3	Roth
Glycine for electrophoresis, ≥99%	G8898-1KG	Sigma Aldrich
Kaliumchlorid	P017.2	Roth
Glucose	HN06.0	Roth
Ortho-Phosphosäure	6366.1	Roth
peqGOLD Universal Agarose	35-1020	Peqlab
di-Sodiumhydrogenphospate dihydrate	4984.1	Roth
Potassium dihydrogen phosphate	3904.2	Roth
Tetramethyl-ethylenediamine	T9281-50ML	Sigma Aldrich

4.2 Methods

4.2.1 Optimization of sample embedding for histology

To interpret the experiment results efficiently the whole intestine should have been observed on a one staining. Therefore an alternative swiss rolls like Clevers is established by using the basic lab tools like pipet tip. The small intestine is cut longitudinally and wrapped carefully around a pipet tip. After fixation of the tissue in 4%PFA over the night the rolls can be corrected easily, because the tissue is not slippery any more. During the embedding it is important that all layers are placed on a one plane to have the optimal cutting angle. After the fixation and the dehydration the samples are ready for paraffin embedding **Supplementary figure 1**.

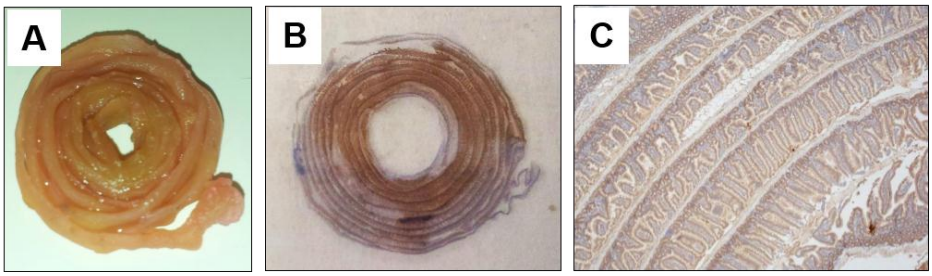

Supplementary figure *1*: (A) Macroscopic picture of for paraffin embedding prepared small intestinal sample. (B) Microscopical image of the immunohistochemistry staining using a 1x objective and. (C) a 10x objective.

4.2.2 PCR

4.2.2.1 DNA isolation

According to the mouse number the tip of the adequate finger of 5-10 day old mice was cut off with a scissor and put into 500µl of tail buffer. For the digestion 0.5mg/ml Proteinase K. was added and the tubes were incubated at 55°C over night. 200µl of saturated 6M NaCl were added and tubes were shook 5 min with 1050 rpm at RT on Eppendorf Shaker and centrifuged for 10 min at 13,000 rpm at RT. Supernatants without top phase and pellet were transferred to a new tube and 500µl of isopropanol were added. And mixed by inverting with hand 2 min. After centrifugation for 10 min at full speed, the supernatant was removed and pellet was washed with 1ml 70% EtOH and spined 15 min with full speed and the pellets were air-dried. Finally the pellet were resuspended in 500µl TE buffer and shook 2 h at 37°C.

4.2.2.2 PCR protocols

Villin CRE PCR

One sample (24µL)

2.5µl 10X Dream Taq Buffer (Roche)

0.5µl dNTP (10mM)

5µl primer VillinCre_for (1.2 µM)

5µl primer VillinCre_rev (1.2 µM)

0.1µl Taq polymerase (5U/µl)

10.9µl H2O

Thermal cycling conditions

94°C – 2 min.

94°C – 30 sec.

59.6°C – 1 min.

72°C – 45 sec. _39x

72°C – 3

4°C – ∞

LGR5 PCR

One sample (24µL)

2.5µl GB Buffer

2.5µl DMSO

2.5µl dNTP (10mM)

2.5µl primer Lgr5_ for (1.25 µM)

2.5µl primer Lgr5_rev (1.25 µM)

0.3µl Taq polymerase (5U/µl)

12.5µl H2O

Thermal cycling conditions

94°C – 2 min

94°C – 30 sec

53°C – 45 sec

65°C – 1 min ___ 35x

65°C – 5 min

4°C – ∞

EGFR PCR

One sample (24 µl)

2.5 µl 10x Dream Taq buffer

0, 25 µl dNTP's (10 mM)

5 µl primer R4 (1.2 µM)

5 µl primer R6 (1.2 µM)

0.15 µl Taq polymerase

11, 1 µl H_2O

Thermal cycler conditions

95 °C – 2 min.

95 °C – 30 sec.

54 °C – 40 sec.

72 °C – 1 min. 30 sec. _39x

72°C – 5 min.

15 °C - ∞

4.2.2.2.1 PCR primers

VillinCre_ for: CAAGCCTGGCTCGACGGCC

VillinCre_rev: CGCGAACATCTTCAGGTTCT

EGFR_for_R4: GCCTGTGTCCGGGTCTCGTCG

EGFR_rev_R6: CAACCAGTGCACCTAGCCTGGC

LGR5_for: CACTGCATTCTAGTTGTG

LGR5_rev: CGGTGCCCGCAGCGAG

4.2.3 Histological stainings

Paraffin embedded samples were cut 4µm thick at a microtome (with Feather microtome blades type A35) and applied to DAKO IHC glass slides.

4.2.3.1 H&E staining

The glass slides were incubated minimum 30min at 55°C. The sections were deparaffinized in Xylol for 2 x 1min, and rehydrated with alcohol serial 100%; 70% EtOH 2 times for 1min for each cases and washed 2x with distilled water for 1 min each. Slides were incubated in freshly filtrated Hematoxylin for 7min and washed in 3 cuvette tap water, followed the incubation in SOTT solution for 45 sec. After incubation in warm tap water for 5min, slides were differentiated with flowing tap water for 3min and then in distilled water. Afterwards the slides were incubated in Eosin for 1min, and washed in 2 cuvettes of distilled water, followed by a dehydration alcohol series: 70%; 2x96% and 2x 100% EtOH, 1min for each and put finally in n-Butyl acetate (EBE) until mounting with the mounting medium Entellan.

4.2.3.2 PAS & Alcian blue staining

The glass slides were incubated minimum 30min at 55°C. The sections were deparaffinized in Xylol for 2 x 1min, and rehydrated with alcohol serial 100%; 70% EtOH 2 times for 1min for each cases and washed 2x with distilled water for 1 min each. Deparaffinized and rehydrated sections were stained 15min in Alcian blue solution (1% Alcian blue in 3% aq. acetic acid), followed washing in running tap water for 2min and rinsed in distilled water. After treating with 0.5% aq. Periodic acid for 5min, the slides were washed in distilled water and stained in Schiff's reagent for 10min. and washed well in running tap water for 5min. Nuclei were stained with Hematoxylin and washed in tap water for 2min. The slides were differentiated with acid alcohol and washed in SOTT solution and in water, followed by a dehydration alcohol series: 70%; 80%; 2x96% and 2x 100% EtOH, 1min for each and put finally in n-Butyl acetate (EBE) until mounting with the mounting medium Entellan.

4.2.3.3 Immunohistochemistry (IHC) staining

The glass slides were incubated minimum 30min at 55°C. The sections were deparaffinized in Xylol for 2 x 1min, and rehydrated with alcohol serial 100%; 70% EtOH 2 times for 1min for each cases and washed 2x with distilled water for 1 min each. The deparaffinized and rehydrated slides were cooked for 2 hours with the proper antigen retrieval solution in an antigen retrieval pressure machine and afterwards washed 3x 5min with 1X PBS at RT. For the inhibition of endogenous peroxidase the slides were incubated 10min in 3% H_2O_2 in methanol. After washing the slides 3x 5min with 1X PBS, the staining area was delineated using a hydrophobic pen (Dako pen). The slides were incubated 20min in reactive A from endogenous blocking kit and after washing 3x 5min with 1X PBS, 20min in reactive B from the endogenous blocking kit. The slides were blocked for 1h with 100µl blocking solution and stained with 100µl first antibody over night at 4°C. Next day the slides washed 3x 5min and incubated 1h with 100µl second biotinylated antibody. After washing 3x 5min with TBS-T (1% Tween in 1X TBS) slides were incubated 30 min in solution A+B in TBS-T (1 drop of each reactive of KIT in 2.5 ml 1X TBS-T), followed after washing DAB reaction (ImmPACT DAB 1 drop for 1 ml diluent). The reaction should be observed under the light microscope for the detection of optimal reaction time. The reaction was stopped by putting slides in tap water and rinsed in distilled water. After the nuclei were stained with Hematoxylin for 30 sec. and washed in distilled water, the slides were dehydrated with alcohol series: 70%; 80%; 2x96% and 2x100% EtOH, 1min for each and put finally in n-Butyl acetate (EBE) until mounting with the mounting medium Entellan.

Please find at the table the antibodies with proper antigen retrieval solution and DAB reaction times:

Antibody	Firma	Clone number	Antigen Retrieval	Blocking Solution	Dilution	DAB reaction time
EGFR	Cell Signalling 4267	D38B1	1mM EDTA; pH 8.0	5%HS, 0,1% Triton, 1% BSA PBS	1:50 in BS	1.5 - 2 min
cMyc	Cell Signalling 5605	D84C12	1X Green Magic Buffer	5%HS, 0,1% Triton, 1% BSA PBS	1:100 in BS	1,5 min
DCAMKL1	Abcam	ab37994	1X DAKO AR	5% milk in PBS	1:200 in BS	1,5 min
HER2	Cell Signalling 4290	D8F12	1mM EDTA; pH 8.0	5%HS, 0,1% Triton, 1% BSA PBS	1:100 / 1:200 in BS	1 - 1,5 min
HER3	Cell Signalling 12708	D22C5	1mM EDTA; pH 8.0	5%HS, 0,1% Triton, 1% BSA PBS	1:100 / 1:200 in BS	1 - 1,5 min
Ki67	Abcam	15580	1X DAKO AR	5%HS, 0,1% Triton, 1% BSA PBS	1:100 / 1:200 in BS	1 min
Lysozyme	Dako A0099	EC 3.2.1.17	1X DAKO AR; pH 6.0	Universal Mouse KIT HRP, AEC	1:200 in 1%BSA PBS	1,5 - 2 min
Synaptophysin	Eubio	GTX100865	1X DAKO AR; pH 9.0	Universal Mouse KIT HRP, AEC	1:1000 in 1%BSA PBS	2 min

4.2.3.4 Immunofluorescence staining (IF)

In OCT tissue tek embedded and on dry ice frozen samples were stored at -20°C or -80°C until sectioned at -20°C in a cryo-microtome. 6µm thick sections were cut and stored at -20 or -80°C until further usage for staining.

The sections were dried at RT for 15min and fixed in 4% PFA for 10min. After washing 3x 5min in 1x PBS the staining area was delineated with a hydrophobic pen and incubated for 1h in 100µl Blocking Solution, followed by incubation with primary antibody over night at 4°C. Next day the slides were washed with 1X PBS 3x 5min and incubated with 100µl of secondary antibody (1:500 dilution) with Hoechst for 1h at RT. After washing 3x 5min with 1X PBS, the slides were embedded using DAKO mounting medium.

Please find at the table the fluorescence antibodies and the proper dilutions:

Antibody	Firma	Number	Dilution	Isotypes
goat pAB GFP-FITC	Abcam	ab6662	1:200	goat
purified anti-CD104 beta4 Integrin	BD Biosciences	553745	1:200	rat
Hoechst 33258	Sigma	861405-500MG	1: 1000	
Anti-BrdU antibody [BU1/75 (ICR1)]	Abcam	ab6326	1:50	mouse
Goat anti mouse LRIG 1 Affinity	R&D Systems / Biomedica	RD-AF3688	1:20	goat
Alexa Fluor® 594 Donkey Anti-Goat IgG (H+L) Antibody	Life technologies/ Invitrogen / Fisher Scientific	A-11058	1:500	donkey
Alexa Fluor® 594 Donkey Anti-Rat IgG	Molecular Probes / Life technologies	A-21209	1:500	donkey
Alexa Fluor® 488 Goat Anti-Rat IgG (H+L) Antibody	Molecular Probes (Invitrogen)	A-11006	1:500	goat
Alexa Fluor anti mouse A488	Invitrogen Fisher	A11011	1:500	goat
Alexa Fluor anti mouse A594	Invitrogen Fisher	A11005	1:500	goat

4.2.3.4.1 Prefixation

The samples were put into the plastic histo cassette and incubated 4h at 4 ^{0}C in 4% PFA. They were washed 3x5min with 1X PBS and incubated over night at 4 ^{0}C in 30 % Sucrose (in 1x PBS with 0.1% NaN_3). After washing with 1X PBS the samples were taken out of the histo cassette, dried quickly on a sheet of kitchen roll and embedded in O.C.T tissue tek on dry ice.

4.2.3.4.2 Whole mount staining

The biopsies were fixed at 4% PFA for 30min at RT and washed 3x 5min with 1X PBS. After they were incubated in 0.5% Triton X-100 in PBS, were continued like in the IF staining (IF staining).

4.2.3.5 BrdU staining

Each mouse was injected in 15 min. interval, which is the estimated required time for one mouse preparation. After 4/24 hours of first injection the first mouse small intestine & colon were prepared and followed in correct injection order.

The 5µm thick paraffin sections on glass slides were incubated minimum 30min at 55°C. The sections were deparaffinized in Xylol for 2 x 1min, and rehydrated with alcohol serial 100%; 70% EtOH 2 times for 1min for each cases and washed 2x with distilled water for 1 min each. The deparaffinized and rehydrated slides were cooked with 1x Dako Antigen Retrieval Solution in the pressure machine. Then they were washed 3x 5min 1X PBS at RT. and the staining area were definite using the fatty pen (Dakopen). After the 1h blocking in 100µl Blocking solution the primary antibody (ß4 Integrin 1:100 in blocking solution) was incubated overnight at 4^0 C. Next day the slides were washed 3x 5min with 1X PBS and secondary antibody were incubated for 1h at RT. After washing 3x 5min with PBS the slides were incubated in 1N HCL for 1h at 37^0 C followed washing 3x 5min with PBS. The slides were blocked with M.O.M. KIT blocking solution and α – BrdU antibody (1:50) in M.O.M Diluent was stained at 4^0 C overnight. Next day washed slides were incubated with secondary antibody and Hoechst for 1h at RT and the slides were embedded.

4.2.4 qRT-PCR

4.2.4.1 RNA extraction

100µl isolated crypts were resuspended in 1ml Trizol and centrifuged 5 min at 13000 rpm at 4°C. 1ml of the Trizol phase was taken into 2ml Eppendorf tube and 240µl ddH_2O (DECP water) and 200µl chloroform were added, mixed by vortexing and incubated 10min at RT and mixed again before centrifuged 15 min at 13000 rpm at 4°C.The aqueous phase was transferred to fresh tube and 1µl Glycoblue and 560µl cold isopropanol were added, followed the incubation on ice for 30min. The supernatant was removed after centrifugation for 30min at 13000rpm. They were washed 2x with 75%EtOH and centrifuged 5 min with full speed. The supernatant was removed and the pellet was dried and dissolved in 19µl ddH_2O (DECP water).

4.2.4.2 cDNA

For the cDNA synthesis 1µg RNA in 10µl (in DECP water) was required. The PCR tubes were incubated at 65°C for min after pipetting 2µl 60µM Hexamer and 2µl 10mM dNTPs. The tubes were put on ice and spined. Additionally 4µl 5X Buffer and 2µl dTT with 0.50µl SS-polymerase were added and put in PCR machine for following program:

25°C 12min

42°C 50min

70°C 15min

Finally the cDNA was diluted 1:4 in nuclease free water and frozen at -20°C.

4.2.4.3 qRT-PCR

Primer Mix:

5µl for Primer

5µl rev Primer

90µl dH_2O

For PCR reaction:

1µl Primer Mix

5µl SYBR Green

3µl dH_2O

1µl cDNA

4.2.4.3.1 Q-PCR primers

ErbB2_for: ATCAACTGCACCCACTCATGT

ErbB2_rev: ATCAGGAACAACAGGACGCC

ErbB3_for: CCCAAGGGTGTAAGGGACCA

ErbB3_rev: CGCTCCAAGTAGCGTCTCAT

ErbB4_for: GCCAGACCTTGACCAGAACT

ErbB4_rev TTGAGTAACGCAGGCTCCAC

BTC_for: GCTGTCATCCTCTTCGGAAACA

BTC_rev: ATGTCCTGTCCATCTGGGAA

EPR_for: CACCGAGAAAGAAGGATGGA

EPR_rev: TCACGGTTGTGCTGATAACTG

HB-EGF_for: ACCAGTGGAGAATCCCCTATAC

HB-EGF_rev: GCCAAGACTGTAGTGTGGTCA

NRG1_for: ACAGAAACTAATCTGCAAACTGCTC

NRG1_rev: ATCCCAAGATGCTTGTAGAAGCTGG

NRG2_for: ACATCGAGGGCATCAACCAG

NRG2_rev: TCAGCCTTTTGCTTAGGATCTG

TBP_for: GGGGAGCTGTGATGTGAAGT

TBP_rev: CCAGGAAATAATTCTGGCTCAT

4.2.5 Western Blot

The isolated crypts were lysed in 1X lysis buffer (1X RIPA) and the protein concentration was measured with Bradford (1ml Bradford, 5µl of sample, at 595nm). At least 40µg protein with 6X Loading buffer were loaded in 10% SDS PAGE and the gel was let to run very slowly in running buffer at 10mA and the blot was transferred to the membrane at 100mA over night (16h) at 4°C. The membrane was washed with TBS-T and blocked with 5%BSA in TBS-T, followed the incubation of primary antibody at 4°C over night and on next day the membrane was incubated in secondary antibodies with HRP in 5% milk TBS-T. After washing the blot was developed with the developing agents ECL.

Please find at the table the Western Blot antibodies and their isotypes:

Antibody	Firma	Clone number	Dilution	kDa	+Na Acid (5%)	Isotypes
EGFR	Cell Signalling 4267	D38B1	1:500 in 5% BSA TBS-T	175	1:250	Rabbit
HER2	Cell Signalling 4290	D8F12	1:1000 in 5% BSA TBS-T	185	1:250	Rabbit
HER3	Cell Signalling 12708	D22C5	1:1000 in 5% BSA TBS-T	185	1:250	Rabbit
Hsp90	Cell Signalling 4894		1:1000 in 5% BSA TBS-T	90	1:250	Rabbit
Tubulin	Sigma	T9026	1:5000 in 5% BSA TBS-T	55	1:250	Mouse
Actin	Sigma	A2066	1:1000 in 5% BSA TBS-T	42	1:250	Rabbit

4.2.6 In vitro culture

4.2.6.1 Crypt isolation

The collected mouse small intestine was cut longitudinally and cleaned and scraped from the villi using a scissor. After washing with PBS it was cut in to small 2-4mm pieces and transferred to a 50ml tube. 25ml ice-cold PBS was added and pipetted up and down a few time with 10ml pipette, removed the supernatant after settling down and added ice-cold PBSO. This was repeated until the supernatant is almost clear. After adding 25ml 2mM EDTA they were incubated for 30min on a roller in icebox. After the incubation they were centrifuged at 800 rpm for 5min at 4°C and removed the supernatant. 10ml PBSO with 10%FBS (FBS is only for the *in vitro* cultivation, not for protein isolation) was added and pipetted up and down 3 times with 10ml pipette. The supernatant was collected passing the 70µm strainer and it was repeated 3

times using new strainers. The crypts were collected by centrifuging at 800rpm for 5min.

4.2.6.2 Organoid culture

After the isolating crypts, they were resuspended with 10ml cold basal culture medium. 20µl of the suspension was placed in an empty 24 well plate to count the crypt numbers. 100-1000 crypts were needed for 1 well and 1 ml at 4°C thawed Matrigel was used for 20 wells, which means 1 well was filled with 50µl Matrigel. Desired number of crypts were spinned at 800rpm for 5min and mixed with Matrigel using a pre-cooled 1000µl pipet tip. 50µl of resuspended Matrigel was applied without bubbles into the center of a well from a pre-warmed 24-well plate. After incubation 1-2min at RT the 24 well plate was transferred to a 37°C incubator for 5min and subsequently 500µl growth medium was added to each well. The crypt culture was incubated at 37°C and the growth medium was changed every 2-3 days. After 7-10 days the organoids have grown so dense that they need be passaged.

4.2.6.3 Paraffin embedding of organoids

Organoids were washed with PBS and fixed in Matrigel for 4h with 10% neutral buffered formalin. Matrigel was resuspended in PBS using mechanical disruption of pipetting. They were centrifuged at 311g for 5min. The lower third of the 1.5 ml conical tubes was cut using a hot scissors and organoids pellet was mixed with 1% hot agarose. The agarose/organoid slurry was immediately added to the cut 1.5 ml tubes and finally agarose plugs were fixed in 10% neutral buffered formalin overnight at 4°C and embedded in paraffin blocks. The EGFR expression on organoid-sections can be checked with an IHC staining ***Supplemantary Figure2.***

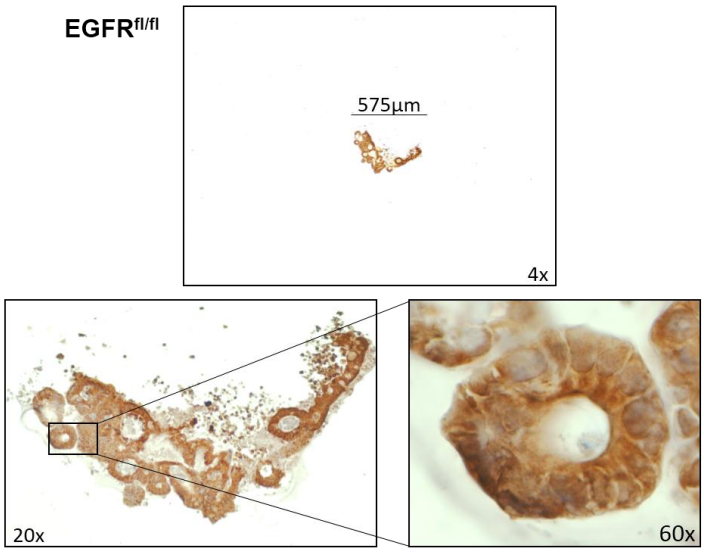

Supplementary figure 2: The microscopic image of EGFR IHC of paraffin embedded control organoids with 4x, 20x and 60x Magnifications. Blue=Hematoxylin; brown=EGFR

4.2.7 Tamoxifen preparation

For 20X TX was weighed 0.7g of tamoxifen stock and filled into a 50ml Falcon, added 3.5ml of 100% pure EtOH and filled up to 35 ml with sun flower seed oil. The Falcon was put in a beaker, which was filled with ice. The Falcon (inside the beaker) was put under the sonication for 20min full power. Meanwhile liquid nitrogen and Eppendorf tubes were prepared. After sonication immediately (1ml) aliquots of the 20X tamoxifen were froze it in the liquid nitrogen and stored at -20°C.

5 List of Abbreviations

ADAM: A disintegrin and metalloprotease domain

APC: Adenomatosis polyposis coli

AR: Amphiregulin

Bmi1: Bone morphogenic protein inhibitor

BrdU: Bromodeoxyuridine

BTC: Betacellulin

CBCc: Crypt base columnar cells

DCAMKL-1: Double cortin calcium / calmodulin kinase-like 1

EGF: Epidermal growth factor

EGFR: Epidermal growth factor receptor

EPR: Epiregulin

EtOH: Ethanol

FBS: Fetal Bovine Serum

HB-EGF: Heparin binding EGF like growth factor

Hsp90: Heat shock protein 90

IEC: Intestinal epithelial cells

IF: Immunofluorescence

IHC: Immunohistochemistry

ISC: Intestinal stem cell

LGR5: Leucine-rich-repeat-containing G-protein-coupled receptor 5

Lrig1: Leucine rich repeats and immunoglobin like domain 1

LRP: Lipoprotein receptor-related protein

MEFs: Mouse embryonic fibroblasts

NRG: Neuregulin

PAS: Periodic Acid Schiff

PBS: Phosphate buffered saline

PBSO: Phosphate buffered saline without calcium and magnesium

PFA: Paraformaldehyde

RT: Room temperature

Tcf4: T-cell factor 4

TGF: Transforming growth factor

TX: Tamoxifen

6 References

Ashok R. Gunawardene, Bernard M. Corfe and Carolyn A. Staton Classification and functions of enteroendocrine cells of the lower gastrointestinal tract. Int. J. Exp. Path. 2011 92, 219–231

Avraham R, Yarden Y. Feedback regulation of EGFR signalling: decision making by early and delayed loops. Nat Rev Mol Cell Biol. 2011 (2):104-17

Barker N, Tan S, Clevers H. Lgr proteins in epithelial stem cell biology. Development. 2013 (12):2484-94

Barker N, van Oudenaarden A, Clevers H. Identifying the stem cell of the intestinal crypt: strategies and pitfalls. Cell Stem Cell. 2012 (4):452-60

Barker N. , Rachel A. Ridgway, Johan H. van Es, Marc van de Wetering, Harry Begthel, Maaike van den Born, Esther Danenberg, Alan R. Clarke, Owen J. Sansom & Hans Clevers. Crypt stem cells as the cells-of-origin of intestinal cancer. Nature 2009 457, 608-611

Barker N. Adult intestinal stem cells: critical drivers of epithelial homeostasis and regeneration. Nature Reviews Molecular Cell Biology 2013 15, 19–33

Barker N., Johan H. van Es, Jeroen Kuipers, Pekka Kujala, Maaike van den Born, Miranda Cozijnsen, Andrea Haegebarth, Jeroen Korving, Harry Begthel, Peter J. Peters & Hans Clevers. Identification of stem cells in small intestine and colon by marker gene Lgr5 Nature 2007, 1003-1007

Baselga J. Targeting the epidermal growth factor receptor with tyrosine kinase inhibitors: small molecules, big hopes. J Clin Oncol 2002 20: 2217–2219

Bastide P, Darido C, Pannequin J, Kist R, Robine S, Marty-Double C, Bibeau F, Scherer G, Joubert D, Hollande F, Blache P, Jay P. Sox9 regulates cell proliferation and is required for Paneth cell differentiation in the intestinal epithelium. J Cell Biol. 2007 (4):635-48

Batlle E, Henderson JT, Beghtel H, van den Born MM, Sancho E, Huls G, Meeldijk J, Robertson J, van de Wetering M, Pawson T, Clevers H. Beta-catenin and TCF mediate cell positioning in the intestinal epithelium by controlling the expression of EphB/ephrinB. Cell. 2002 (2):251-63..

Bettess Michael D., Nicole Dubois, Mark J. Murphy, Christelle Dubey, Catherine Roger, Sylvie Robine, and Andreas Trumpp. c-Myc Is required for the formation of intestinal crypts but dispensable for homeostasis of the adult intestinal epithelium. Mol Cell Biol. 2005 (17): 7868–7878

Bezençon C, Fürholz A, Raymond F, Mansourian R, Métairon S, Le Coutre J, Damak S. Murine intestinal cells expressing Trpm5 are mostly brush cells and express markers of neuronal and inflammatory cells. J Comp Neurol. 2008 (5):514-25

Bjerknes M, Cheng H. Re-examination of P-PTEN staining patterns in the intestinal crypt. Nat Genet. 2005 (10):1016-7

Bjerknes M, Khandanpour C, Möröy T, Fujiyama T, Hoshino M, Klisch TJ, Ding Q, Gan L, Wang J, Martín MG, Cheng H. Origin of the brush cell lineage in the mouse intestinal epithelium. Dev Biol. 2012 (2):194-218

Bjerknes M, Cheng H. Clonal analysis of mouse intestinal epithelial progenitors. Gastroenterology. 1999 (1):7-14.

Bryan A Ong, Kenneth J Vega, and Courtney W Houchen. Intestinal stem cells and the colorectal cancer microenvironment. World J Gastroenterol. 2014 (8): 1898–1909

Cairnie A.B., L.F. Lamerton, G.G. Steel Cell proliferation studies in the intestinal epithelium of the rat: I. Determination of the kinetic parameters. Experimental Cell Research 1965 (39) 528–538

Carmon Kendra S., Xing Gong, Qiushi Lin, Anthony Thomas, and Qingyun Liu. R-spondins function as ligands of the orphan receptors LGR4 and LGR5 to regulate Wnt/β-catenin signaling. PNAS 2011 vol. 108 no. 28

Carpenter G. EGF receptor transactivation mediated by the proteolytic production of EGF-like agonists. Sci STKE. 2000(15):pe1

Chang Han, David J. Ries, Walter Gilbert, David F. Stern & U. J. Mc Mahan. Ligands for ErbB-family receptors encoded by a neuregulin-like gene. Nature 1997 387, 509 - 512

Cheng H, Leblond CP. Origin, differentiation and renewal of the four main epithelial cell types in the mouse small intestine. I. Columnar cell. Am J Anat. 1974 (4):461-79

Ciardello F, Caputo R, Bianco R et al. Antitumor effect and potentiation of cytotoxic drugs activity in human cancer cells by ZD-1839 (Iressa), an epidermal growth factor receptor-selective tyrosine kinase inhibitor. Clin Cancer Res 2000; 6: 2053–2063

Clevers H, Batlle E. SnapShot: the intestinal crypt. Cell. 2013 (5):1198-1198

Clevers H. Stem Cell: A unifying theory for the crypt Nature. 2013 (7439):53-4

Clevers H.Stem Cells: The intestinal crypt, a prototype stem cell compartment Cell. 2013 (2):274-84

Clevers Hans, Roel Nusse. Wnt/β-Catenin Signaling and Disease. Cell 2012 149, 1192-1205

Clevers Hans. The cancer stem cell: premises, promises and challenges. Nature Medicine 2011 313–319

Clevers HC, Bevins CL.Paneth cells: maestros of the small intestinal crypts. Annu Rev Physiol. 2013 75: 289-311

Cunningham D, Atkin W, Lenz HJ, Lynch HT, Minsky B, Nordlinger B, Starling N. Colorectal cancer. Lancet. 2010 (9719):1030-47

Cynthia Kosinski, Vivian S. W. Li, Annie S. Y. Chan, Ji Zhang, Coral Ho, Wai Yin Tsui, Tsun Leung Chan, Randy C. Mifflin, Don W. Powell, Siu Tsan Yuen, Suet Yi Leung and Xin Chen. Gene expression patterns of human colon tops and basal crypts and BMP antagonists as intestinal stem cell niche factors. Proc Natl Acad Sci U S A., 2007; 104(39): 15418–15423

de Lau W, Barker N, Low TY, Koo BK, Li VS, Teunissen H, Kujala P, Haegebarth A, Peters PJ, van de Wetering M, Stange DE, van Es JE, Guardavaccaro D, Schasfoort RB, Mohri Y, Nishimori K, Mohammed S, Heck AJ, Clevers H. Lgr5 homologues associate with Wnt receptors and mediate R-spondin signaling. Nature. 2011 (7360):293-7

de Lau W1, Kujala P, Schneeberger K, Middendorp S, Li VS, Barker N, Martens A, Hofhuis F, DeKoter RP, Peters PJ, Nieuwenhuis E, Clevers H. Peyer's patch M cells derived from Lgr5(+) stem cells require SpiB and are induced by RankL in cultured "miniguts". Mol Cell Biol. 2012 (18):3639-47

de Lau Wim, Weng Chuan Peng, Piet Gros, and Hans Clevers. The R-spondin/Lgr5/Rnf43 module: regulator of Wnt signal strength. Genes Dev. 2014 (4): 305–316

De Luca A, Carotenuto A, Rachiglio A, Gallo M, Maiello MR, Aldinucci D, Pinto A, Normanno N. The role of the EGFR signaling in tumor microenvironment. J Cell Physiol. 2008 (3):559-67

Dekkers JF, Wiegerinck CL, de Jonge HR, Bronsveld I, Janssens HM, de Winter-de Groot KM, Brandsma AM, de Jong NW, Bijvelds MJ, Scholte BJ, Nieuwenhuis EE, van den Brink S, Clevers H, van der Ent CK, Middendorp S, Beekman JM. A functional CFTR assay using primary cystic fibrosis intestinal organoids. Nat Med. 2013 (7):939-45

el Marjou F, Janssen KP, Chang BH, Li M, Hindie V, Chan L, Louvard D, Chambon P, Metzger D, Robine S. Tissue-specific and inducible Cre-mediated recombination in the gut epithelium. Genesis. 2004 (3):186-93.

Farin HF1, Van Es JH, Clevers H. Redundant sources of Wnt regulate intestinal stem cells and promote formation of Paneth cells. Gastroenterology. 2012 (6):1518-1529.e7

Ferlay J, Soerjomataram I, Dikshit R, Eser S, Mathers C, Rebelo M, Parkin DM, Forman D, Bray F. Cancer incidence and mortality worldwide: Sources, methods and major patterns in GLOBOCAN 2012. Int J Cancer. 2014 10.1002/ijc.29210

Francois Gerbe, Catherine Legraverend, Philippe Jay. The intestinal epithelium tuft cells: specification and function. Cell. Mol. Life Sci. 2012 69:2907–2917

Fujii M, Sato T. Culturing intestinal stem cells: applications for colorectal cancer research. Front Genet. 2014 5;5:169

Gal Gur, Chanan Rubin, Menachem Katz, Ido Amit, Ami Citri, Jonas Nilsson, Ninette Amariglio, Roger Henriksson, Gideon Rechavi, Håkan Hedman, Ron Wides, and Yosef Yarden. LRIG1 restricts growth factor signaling by enhancing receptor ubiquitylation and degradation. EMBO J. 2004; 23(16): 3270–3281

Gerbe F, Brulin B, Makrini L, Legraverend C, Jay P. DCAMKL-1 expression identifies Tuft cells rather than stem cells in the adult mouse intestinal epithelium. Gastroenterology. 2009 (6):2179-80

Gordon W. Moran, Fiona C. Leslie, Scott E. Levison and John T. McLaughlin Enteroendocrine cells: Neglected players in gastrointestinal disorders Therapeutic Advances in Gastroenterology 2008 1(1) 51–60

Gregorieff A, Clevers H. Wnt signaling in the intestinal epithelium: from endoderm to cancer. Genes Dev. 2005 (8):877-90.

Gregorieff A, Stange DE, Kujala P, Begthel H, van den Born M, Korving J, Peters PJ, Clevers H. The ets-domain transcription factor Spdef promotes maturation of goblet and paneth cells in the intestinal epithelium. Gastroenterology. 2009 (4):1333-45.e1-3

Groden J, Thliveris A, Samowitz W, Carlson M, Gelbert L, Albertsen H, Joslyn G, Stevens J, Spirio L, Robertson M, et al. Identification and characterization of the familial adenomatous polyposis coli gene. Cell. 1991 (3):589-600

Grootjans J, Hundscheid IH, Buurman WA. Goblet cell compound exocytosis in the defense against bacterial invasion in the colon exposed to ischemia-reperfusion. Gut Microbes. 2013 (3):232-5.

Grosse Ann S., Mark F. Pressprich, Lauren B. Curley, Kara L. Hamilton, Ben Margolis, Jeffrey D. Hildebrand, and Deborah L. Gumucio. Cell dynamics in fetal intestinal epithelium: implications for intestinal growth and morphogenesis. Development. 2011; (20): 4423–4432

Guy PM, Platko JV, Cantley LC, Cerione RA, Carraway KL, III. Insect cell-expressed p180erbB3 possesses an impaired tyrosine kinase activity. Proc Natl Acad Sci U S 1994 91:8132–8136.

Hao HX, Xie Y, Zhang Y, Charlat O, Oster E, Avello M, Lei H, Mickanin C, Liu D, Ruffner H, Mao X, Ma Q, Zamponi R, Bouwmeester T, Finan PM, Kirschner MW, Porter JA, Serluca FC, Cong F. ZNRF3 promotes Wnt receptor turnover in an R-spondin-sensitive manner. Nature. 2012 (7397):195-200

Haramis AP, Begthel H, van den Born M, van Es J, Jonkheer S, Offerhaus GJ, Clevers H. De novo crypt formation and juvenile polyposis on BMP inhibition in mouse intestine. Science. 2004 (5664):1684-6.

He XC, Yin T, Grindley JC, Tian Q, Sato T, Tao WA, Dirisina R, Porter-Westpfahl KS, Hembree M, Johnson T, Wiedemann LM, Barrett TA, Hood L, Wu H, Li L. PTEN-deficient intestinal stem cells initiate intestinal polyposis. Nat Genet. 2007 (2):189-98

Helander HF, Fändriks L. Surface area of the digestive tract - revisited. Scand J Gastroenterol. 2014 (6):681-9

Huang SM, Bock JM, Harari PM. Epidermal growth factor receptor blockade with C225 modulates proliferation, apoptosis, and radiosensitivity in squamous cell carcinomas of the head and neck. Cancer Res 1999; 59: 1935–1940

Hunter T, Cooper JA. Epidermal growth factor induces rapid tyrosine phosphorylation of proteins in A431 human tumor cells. Cell. 1981 (3):741-52.

Ireland H1, Houghton C, Howard L, Winton DJ. Cellular inheritance of a Cre-activated reporter gene to determine Paneth cell longevity in the murine small intestine. Dev Dyn. 2005 (4):1332-6.

Itzkovitz S, Lyubimova A, Blat IC, Maynard M, van Es J, Lees J, Jacks T, Clevers H, van Oudenaarden A. Single-molecule transcript counting of stem-cell markers in the mouse intestine. Nat Cell Biol. 2012 (1):106-14

Janice J. Kim and Waliul I. Khan Goblet Cells and Mucins: Role in Innate Defense in Enteric Infections. Pathogens 2013 (1), 55-70

Jensen J, Pedersen EE, Galante P, Hald J, Heller RS, Ishibashi M, Kageyama R, Guillemot F, Serup P, Madsen OD. Control of endodermal endocrine development by Hes-1. Nat Genet. 2000 (1):36-44

Jorissen RN, Walker F, Pouliot N, Garrett TP, Ward CW, Burgess AW. Epidermal growth factor receptor: mechanisms of activation and signalling. Exp Cell Res. 2003 (1):31-53

Jung Peter, Toshiro Sato, Anna Merlos-Suárez, Francisco M Barriga, Mar Iglesias, David Rossell, Herbert Auer, Mercedes Gallardo, Maria A Blasco, Elena Sancho, Hans Clevers & Eduard Batlle. Isolation and in vitro expansion of human colonic stem cells. Nature Medicine 2011 17, 1225–1227

Kato LM, Kawamoto S, Maruya M, Fagarasan S The role of the adaptive immune system in regulation of gut microbiota Immunol Rev. 2014 (1):67-75

Kazanskaya O, Glinka A, del Barco Barrantes I, Stannek P, Niehrs C, Wu W. R-Spondin2 is a secreted activator of Wnt/beta-catenin signaling and is required for Xenopus myogenesis. Dev Cell. 2004 (4): 525-34

Kim TH, Escudero S, Shivdasani RA. Intact function of Lgr5 receptor-expressing intestinal stem cells in the absence of Paneth cells. Proc Natl Acad Sci U S A. 2012 3932-7

Kinzler KW1, Nilbert MC, Su LK, Vogelstein B, Bryan TM, Levy DB, Smith KJ, Preisinger AC, Hedge P, McKechnie D, et al. Identification of FAP locus genes from chromosome 5q21. Science. 1991 (5020):661-5

Koo BK, Clevers H. Stem cells marked by the R-spondin receptor LGR5. Gastroenterology. 2014 (2):289-302

Korinek V, Barker N, Moerer P, van Donselaar E, Huls G, Peters PJ, Clevers H. Depletion of epithelial stem-cell compartments in the small intestine of mice lacking Tcf-4. Nat Genet. 1998 (4):379-83.

Kucharzik T., N. Lügering, K. Rautenberg, A. Lügering, M.A. Schmidt, R. Stoll, and W. Domschke. Role of M Cells in Intestinal Barrier Function. Ann N Y Acad Sci. 2000; 915:171-83

Lanaya H, Natarajan A, Komposch K, Li L, Amberg N, Chen L, Wculek SK, Hammer M, Zenz R, Peck-Radosavljevic M, Sieghart W, Trauner M, Wang H, Sibilia M. EGFR has a tumour-promoting role in liver macrophages during hepatocellular carcinoma formation. Nat Cell Biol. 2014 (10):972-81

Leushacke M, Barker N. Lgr5 and Lgr6 as markers to study adult stem cell roles in self-renewal and cancer. Oncogene. 2012 (25):3009-22

Leushacke Marc, Nick Barker. Ex vivo culture of the intestinal epithelium: strategies and applications. Gut doi:10.1136/gutjnl-2014-307204

Limbergen Johan Van, Kaoru Geddes, Paul Henderson, Richard K Russell, Hazel E Drummond, Jack Satsangi, Anne M Griffiths, Dana J Philpott, David C Wilson. Paneth cell marker CD24 in NOD2 knockout organoids and in inflammatory bowel disease (IBD) Gut 2013 doi:10.1136/305077

Linheng Li, Hans Clevers. Coexistence of Quiescent and Active Adult Stem Cells in Mammals. Science 2010: Vol. 327 no. 5965 pp. 542-545

Liqin Zhu, Paul Gibson, D. Spencer Currle, Yiai Tong, Robert J. Richardson, Ildar T. Bayazitov, Helen Poppleton, Stanislav Zakharenko, David W. Ellison & Richard J. Gilbertson. Prominin 1 marks intestinal stem cells that are susceptible to neoplastic transformation. Nature 457, 603-607

Luciano L, Real E. Brush cells of the mouse gallbladder. Cell Tissue Res 1990 262, 339–49.

M. W. Smith. Expression of digestive and absorptive function in differentiating enterocytes. Ann. Rev. Physiol. 1985 47:247—60

Mabbott NA, DS Donaldson, H Ohno, IR Williams and A Mahajan, Microfold (M) cells: important immunosurveillance posts in the intestinal epithelium. Mucosal Immunology 2013 6, 666–677

Marjorie Jenny, Céline Uhl, Colette Roche, Isabelle Duluc, Valérie Guillermin, Francois Guillemot, Jan Jensen, Michèle Kedinger, and Gérard Gradwohl. Neurogenin3 is differentially required for endocrine cell fate specification in the intestinal and gastric epithelium. EMBO J. 2002 (23): 6338–6347

Mellman I, Yarden Y. Endocytosis and cancer. Cold Spring Harb Perspect Biol. 2013 (12):a016949

Merlos-Suárez A, Barriga FM, Jung P, Iglesias M, Céspedes MV, Rossell D, Sevillano M, Hernando-Momblona X, da Silva-Diz V, Muñoz P, Clevers H, Sancho E, Mangues R, Batlle E. The intestinal stem cell signature identifies

colorectal cancer stem cells and predicts disease relapse. Cell Stem Cell. 2011 (5):511-24

Metcalfe C, Kljavin NM, Ybarra R, de Sauvage FJ. Lgr5+ stem cells are indispensable for radiation-induced intestinal regeneration. Cell Stem Cell. 2014 (2):149-59

Middendorp S, Schneeberger K, Wiegerinck CL, Mokry M, Akkerman RD, van Wijngaarden S, Clevers H, Nieuwenhuis EE. Adult stem cells in the small intestine are intrinsically programmed with their location-specific function. Stem Cells. 2014 (5):1083-91

Miettinen PJ, Berger JE, Meneses J, Phung Y, Pedersen RA, Werb Z, Derynck R. Epithelial immaturity and multiorgan failure in mice lacking epidermal growth factor receptor. Nature. 1995 (6538):337-41

Miller Harvey, Jianbing Zhang, Rhonda KuoLee, Girishchandra B Patel, Wangxue Chen. Intestinal M cells: The fallible sentinels. World J Gastroenterol 2007 (10): 1477-1486

Muncan V, Sansom OJ, Tertoolen L, Phesse TJ, Begthel H, Sancho E, Cole AM, Gregorieff A, de Alboran IM, Clevers H, Clarke AR. Rapid loss of intestinal crypts upon conditional deletion of the Wnt/Tcf-4 target gene c-Myc. Mol Cell Biol. 2006 (22):8418-26

Muñoz J, Stange DE, Schepers AG, van de Wetering M, Koo BK, Itzkovitz S, Volckmann R, Kung KS, Koster J, Radulescu S, Myant K, Versteeg R, Sansom OJ, van Es JH, Barker N, van Oudenaarden A, Mohammed S, Heck AJ, Clevers H. The Lgr5 intestinal stem cell signature: robust expression of proposed quiescent '+4' cell markers. EMBO J. 2012 (14):3079-91

Nicoletti C. Unsolved mysteries of intestinal M cells Gut 2000 ;47:735-739

Noah TK, Kazanjian A, Whitsett J, Shroyer NF. SAM pointed domain ETS factor (SPDEF) regulates terminal differentiation and maturation of intestinal goblet cells. Exp Cell Res. 2010 (3):452-65

Normanno N, Bianco C, De Luca A, Maiello MR, Salomon DS. Target-based agents against ErbB receptors and their ligands: a novel approach to cancer treatment. Endocr Relat Cancer. 2003 (1):1-21

Normanno N, De Luca A, Bianco C, Strizzi L, Mancino M, Maiello MR, Carotenuto A, De Feo G, Caponigro F, Salomon DS. Epidermal growth factor receptor (EGFR) signaling in cancer. Gene. 2006 (1):2-16

Olayioye MA, Neve RM, Lane HA, Hynes NE. The ErbB signaling network: receptor heterodimerization in development and cancer. EMBO J. 2000 (13):3159-67

Pellegrinet L, Rodilla V, Liu Z, Chen S, Koch U, Espinosa L, Kaestner KH, Kopan R, Lewis J, Radtke F. Dll1- and dll4-mediated notch signaling are required for homeostasis of intestinal stem cells. Gastroenterology. 2011(4):1230-1240.e1-7

Peng WC, de Lau W, Forneris F, Granneman JC, Huch M, Clevers H, Gros P. Structure of stem cell growth factor R-spondin 1 in complex with the ectodomain of its receptor LGR5. Cell Rep. 2013 (6):1885-92

Pinto D, Gregorieff A, Begthel H, Clevers H. Canonical Wnt signals are essential for homeostasis of the intestinal epithelium. Genes Dev. 2003 (14):1709-13

Porter EM,Bevins CL,Ghosh D,Ganz T. The multifaceted Paneth cell. Cell Mol Life Sci. 2002 (1): 156-70

Potten Christopher S. Extreme sensitivity of some intestinal crypt cells to X and γ irradiation. Nature 1977 269, 518 – 521

Potten CS, Gandara R, Mahida YR, Loeffler M, Wright NA. The stem cells of small intestinal crypts: where are they? Cell Prolif. 2009 (6):731-50

Potten CS, Owen G, Booth D. Intestinal stem cells protect their genome by selective segregation of template DNA strands. J Cell Sci. 2002 1;115(Pt 11):2381-8

Powell AE, Wang Y, Li Y, Poulin EJ, Means AL, Washington MK, Higginbotham JN, Juchheim A, Prasad N, Levy SE, Guo Y, Shyr Y, Aronow BJ, Haigis KM,

Franklin JL, Coffey RJ. The pan-ErbB negative regulator Lrig1 is an intestinal stem cell marker that functions as a tumor suppressor. Cell. 2012 (1):146-58

Powell SM, Zilz N, Beazer-Barclay Y, Bryan TM, Hamilton SR, Thibodeau SN, Vogelstein B, Kinzler KW. APC mutations occur early during colorectal tumorigenesis. Nature. 1992 (6392):235-7

Ray D, Ahsan A, Helman A, Chen G, Hegde A, Gurjar SR, Zhao L, Kiyokawa H, Beer DG, Lawrence TS, Nyati MK. Regulation of EGFR protein stability by the HECT-type ubiquitin ligase SMURF2. Neoplasia. 2011 (7):570-8

Riese DJ , van Raaij TM, Plowman GD, Andrews GC, Stern DF. The cellular response to neuregulins is governed by complex interactions of the erbB receptor family. Mol Cell Biol. 1995 (10):5770-6

Sachs N, Clevers H. Organoid cultures for the analysis of cancer phenotypes. Curr Opin Genet Dev. 2014 24:68-73

Salomon DS, Brandt R, Ciardiello F, Normanno N. Epidermal growth factor-relatedbpeptides and their receptors in human malignancies. Crit Rev Oncol Hematol 1995 19:183–232

Sato A, Miyoshi S. Tuft cells in the main excretory duct epithelium of the three major rat salivary glands. Eur J Morphol 1996 34, 225–8.

Sato A. Tuft cells. Anatomical Science International 2007 82, 187 –199

Sato T, Clevers H. Growing self-organizing mini-guts from a single intestinal stem cell: mechanism and applications. Science. 2013 (6137):1190-4.

Sato T,van Es JH,Snippert HJ,Stange DE,Vries RG,van den Born M,Barker N,Shroyer NF, van de Wetering M, Clevers H. Paneth cells constitute the niche for Lgr5 stem cells in intestinal crypts. Nature.2011 (7330):415-8

Sato T,Vries RG,Snippert HJ,van de Wetering M,Barker N,Stange DE,van Es JH,Abo A,Kujala P,Peters PJ,Clevers H. Single Lgr5 stem cells build crypt-villus structures in vitro without a mesenchymal niche. Nature. 2009 (7244):262-5

Schepers AG, Snippert HJ, Stange DE, van den Born M, van Es JH, van de Wetering M, Clevers H. Lineage tracing reveals Lgr5+ stem cell activity in mouse intestinal adenomas. Science. 2012 (6095):730-5

Schlessinger J. Ligand-induced, receptor-mediated dimerization and activation of EGF receptor. Cell. 2002 (6):669-72

Schneider MR1, Wolf E. The epidermal growth factor receptor ligands at a glance. J Cell Physiol. (3):460-6

Shroyer NF, Helmrath MA, Wang VY, Antalffy B, Henning SJ, Zoghbi HY. Intestine-specific ablation of mouse atonal homolog 1 (Math1) reveals a role in cellular homeostasis. Gastroenterology. 2007 (7):2478-88

Sibilia M, Kroismayr R, Lichtenberger BM, Natarajan A, Hecking M, Holcmann M. The epidermal growth factor receptor: from development to tumorigenesis. Differentiation. 2007 (9):770-87

Sibilia M1, Wagner EF. Strain-dependent epithelial defects in mice lacking the EGF receptor. Science. 1995 (5221):234-8

Sibilia Maria and Erwin F. Wagner. Transgenic animals. European Review 1996, pp 371-391

Siegel R, Naishadham D, Jemal A. Cancer statistics, 2012. CA Cancer J Clin. 2012 (1):10-29

Smith Nicholas R., Paige S. Davies, Alain D. Silk, Melissa H. Wongemail. Epithelial and Mesenchymal Contribution to the Niche: A Safeguard for Intestinal Stem Cell Homeostasis. Gastroenterology. 2012 (6): 1426–1430

Spano JP, Lagorce C, Atlan D, Milano G, Domont J, Benamouzig R, Attar A, Benichou J, Martin A, Morere JF, Raphael M, Penault-Llorca F, Breau JL, Fagard R, Khayat D, Wind P. Impact of EGFR expression on colorectal cancer patient prognosis and survival. Ann Oncol. 2005b (1):102-8

Spano JP1, Fagard R, Soria JC, Rixe O, Khayat D, Milano G. Epidermal growth factor receptor signaling in colorectal cancer: preclinical data and therapeutic perspectives. Ann Oncol. 2005a (2):189-94

Specian RD,Oliver MG. The functional biology of intestinal goblet cells. Am. J. Physiol. 1991 260, c183-c193

Sternini Catia, Laura Anselmi, and Enrique Rozengurt. Enteroendocrine cells: a site of ‘taste’ in gastrointestinal chemosensing Curr Opin Endocrinol Diabetes Obes. 2008 15(1): 73–78

Tan Shawna, Nick Barker. Epithelial stem cells and intestinal cancer. Semin Cancer Biol. 2014 (14)00029-7

Tian H, Biehs B, Warming S, Leong KG, Rangell L, Klein OD, de Sauvage FJ. A reserve stem cell population in small intestine renders Lgr5-positive cells dispensable. Nature. 2011 (7368):255-9

Tzahar E, Waterman H, Chen X, Levkowitz G, Karunagaran D, Lavi S, Ratzkin BJ, Yarden Y. A hierarchical network of interreceptor interactions determines signal transduction by Neu differentiation factor/neuregulin and epidermal growth factor. Mol Cell Biol. 1996 (10):5276-87

Umar Shahid. Intestinal Stem Cells. Gastroenterol Rep. Oct 2010 (5): 340–348

van der Flier LG, Sabates-Bellver J, Oving I, Haegebarth A, De Palo M, Anti M, Van Gijn ME, Suijkerbuijk S, Van de Wetering M, Marra G, Clevers H. The Intestinal Wnt/TCF Signature. Gastroenterology. 2007 (2):628-32

van der Flier LG, van Gijn ME, Hatzis P, Kujala P, Haegebarth A, Stange DE, Begthel H, van den Born M, Guryev V, Oving I, van Es JH, Barker N, Peters PJ, van de Wetering M, Clevers H. Transcription factor achaete scute-like 2 controls intestinal stem cell fate. Cell. 2009 (5):903-12

van der Flier LG1, Clevers H. Stem cells, self-renewal, and differentiation in the intestinal epithelium. Annu Rev Physiol. 2009 71:241-60

van Es Johan H., Toshiro Sato, Marc van de Wetering, Anna Lyubimova, Alex Gregorieff, Laura Zeinstra, Maaike van den Born, Jeroen Korving, Anton C.M. Martens, Alexander van den Oudenaarden, and Hans Clevers. Dll1 marks early secretory progenitors in gut crypts that can revert to stem cells upon tissue damage. Nat Cell Biol. 2012; (10): 1099–1104

Veerle Snoeck, Bruno Goddeeris , Eric Cox ,The role of enterocytes in the intestinal barrier function and antigen Uptake. Microbes and Infection 7 2005 997–1004

Walther V1, Graham TA. Location, location, location! The reality of life for an intestinal stem cell in the crypt. J Pathol. 2014 (1):1-4.

Wells JM, Spence JR. How to make an intestine. Development. 2014 (4):752-60

Westphalen Benedikt C., Samuel Asfaha, Yoku Hayakawa, Yoshihiro Takemoto, Dana J. Lukin, Andreas H. Nuber, Anna Brandtner,Wanda Setlik, Helen Remotti, Ashlesha Muley, Xiaowei Chen, Randal May,Courtney W. Houchen, James G. Fox, Michael D. Gershon, Michael Quante and Timothy C. Wang. Long-lived intestinal tuft cells serve as colon cancer–initiating cells. The Journal of Clinical Investigation 2014 124(3):1283-1295

Wong MH, Saam JR, Stappenbeck TS, Rexer CH, Gordon JI. Genetic mosaic analysis based on Cre recombinase and navigated laser capture microdissection. Proc Natl Acad Sci U S A. 2000 12601-6

Wong Vivian W. Y, Daniel E. Stange, Mahalia E. Page, Simon Buczacki,Agnieszka Wabik, Satoshi Itami, Marc van de Wetering, Richard Poulsom, Nicholas A. Wright, Matthew W. B. Trotter, Fiona M. Watt, Doug J. Winton, Hans Clevers & Kim B.. Jensen Lrig1 controls intestinal stem-cell homeostasis by negative regulation of ErbB signalling. Nature Cell Biology 2012 14, 401–408

Yamauchi T, Ueki K, Tobe K, Tamemoto H, Sekine N, Wada M, Honjo M, Takahashi M, Takahashi T, Hirai H, Tushima T, Akanuma Y, Fujita T, Komuro I, Yazaki Y, Kadowaki T. Tyrosine phosphorylation of the EGF receptor by the kinase Jak2 is induced by growth hormone. Nature. 1997 (6655):91-6

Yan KS, Chia LA, Li X, Ootani A, Su J, Lee JY, Su N, Luo Y, Heilshorn SC, Amieva MR, Sangiorgi E, Capecchi MR, Kuo CJ. The intestinal stem cell markers Bmi1 and Lgr5 identify two functionally distinct populations. Proc Natl Acad Sci U S A. 2012 (2):466-71

Yang Q, Bermingham NA, Finegold MJ, Zoghbi HY. Requirement of Math1 for secretory cell lineage commitment in the mouse intestine. Science. 2001 (5549):2155-8

Yarden Y. The EGFR family and its ligands in human cancer. signalling mechanisms and therapeutic opportunities. Eur J Cancer. 2001 Suppl 4:S3-8

Yarden Yosef & Gur Pines. The ERBB network: at last, cancer therapy meets systems biology. Nature Reviews Cancer 2012, 553-563

Zhang D, Sliwkowski MX, Mark M, Frantz G, Akita R, Sun Y, Hillan K, Crowley C, Brush J, Godowski PJ. Neuregulin-3 (NRG3): a novel neural tissue-enriched protein that binds and activates ErbB4. Proc Natl Acad Sci U S A. 1997 (18):9562-7

Curriculum Vitae

Name: Vasfiye Bilge GÖCEN

Birthday: 12.09.1988, Istanbul, Turkey

E-Mail: bilge_goecen@yahoo.de

Education & Qualification:

2008-2012 University of Vienna

Bachelor of Science: "Biology/ Microbiology und Genetic"

2002- 2007 St. Georg Austrian High School in Istanbul,

graduated with the Austrian Matura diploma.

Languages:

Turkish (mother language)

German (Matura level + 6 years academic experience in Vienna)

English (Matura level + 2 years lab experience)

Latin (Matura level)

Research experience:

08/2013- present **Master thesis**; **Medical University of Vienna**

Institute of Cancer Research

Project: The role of EGFR (epidermal growth factor receptor) in intestinal stem cells.

Techniques: isolation of mouse intestine and colon, embedding for cryo and paraffine, cutting of tissues by cryotome and mictome, genotyping PCR, fluorescence activated cell sorting FACS, immunofluorescence, immunohistochemistry, microscope analysis (fluorescence-, light and confocal microscope), western blot, cell culture using primary cells, working with mice (mouse handling and breeding experience)

Supervisor: Univ. Prof. Dr. Maria Sibilia (maria.sibilia@meduniwien.ac.at)

05/2013-06/2013 **Internship**, **Medical University of Vienna**

Institute of Cancer Research

Project: Spontaneous mutations in yeast

Techniques: working with yeast, pouring plates, PCR, cloning cultures, plating

Supervisor:A.o. Univ. Prof. Dr. Erich Heidenreich (erich.heidenreich@meduniwien.ac.at)

04/2013 **Internship, Medical University of Vienna**

Institute of Cancer Research

Project: Telomere maintenance mechanism

Techniques: cell culture (human tumor cell lines), passaging cells, transfection of cells, restriction fragment analysis of plasmid DNA, microscopy, MTT assay, qRT-PCR

Supervisor: A.o. Univ. Prof. Dr. Klaus Holzmann (klaus.holzmann@meduniwien.ac.at)

09/2011-10/2011 **Bachelor Thesis, University of Vienna**

Project: The influence of non coding RNA" DicF" on the translation of "miaA"

Techniques: working with E.coli, cloning plasmids, PCR, gel electrophoresis, SDS PAGE

Supervisor: Armin Resch (armin.resch@univie.ac.at)

Personal skills:

Computer skills: Office software, Photoshop, Flow-Jo, Clone Manager

Social skills: I like to work with people and I am very good at teamwork. After so many years as a trainer I know how to work within a group and how to manage

and motivate them. That is why I am self-confidence to present something in front of people. I am a very organized person.

Personal interests: Dancing, Jogging, Cooking, Self-Defense & Martial Art Sport, Travelling, Acting, Making Movies, Singing, Literature and especially Poetry

Job experience:

2011-2012 – Aerobic trainer in sport centers „John Harris“, „Cumberland“ „Club Danube“, „Selfness Fitness“

2010-2012 – Self-defense trainer for students

2006 – 2007: In Sport club; as assistant trainer

Studentship:

Monthly support for my study is afforded from my alumni high school St. Georg College.

Awards:

2013 I helped with the microbiology part of a project for Moscow Biennale

2008 First place at Iron Lens film let competition (in NÖ)

2007 Two short-stories of mine were published in a Turkish literature book.

2007 Silver medal at karate competition (in Bursa/in turkey)

2006 Bronze medal at karate competition (in Istanbul/in turkey)

2006 First place at poem-competition (in high school)

2004 Second place for a physics project competition

2002 A short story of mine was published in school journal